Double Compression-Expansion Engine Concepts

Experimental and simulation study of a split-cycle concept for improved brake efficiency

Lam, Nhut

2019

Document Version:
Publisher's PDF, also known as Version of record

Double Compression-Expansion Engine Concepts

Double Compression-Expansion Engine Concepts

Experimental and simulation study of a split-cycle concept for improved brake efficiency

by Nhut Lam

LUND
UNIVERSITY

Thesis for the degree of Doctor of Philosophy
Thesis advisor: Professor Per Tunestål, Lund University
Faculty opponent: Professor Robert Morgan, University of Brighton

To be presented, with the permission of the Faculty of Engineering of Lund University, for public criticism in the M:B lecture hall at the Department of Energy Sciences on Friday, the 3rd of May 2019 at 10:15.

Organization
LUND UNIVERSITY

Department of Energy Sciences
Box 188
SE–221 00 LUND
Sweden

Document name
DOCTORAL DISSERTATION

Date of disputation
2019-05-03

Sponsoring organization
Swedish Energy Agency
Volvo Group

Author(s)
Nhut Lam

Title and subtitle
Double Compression-Expansion Engine Concepts: Experimental and simulation study of a split-cycle concept for improved brake efficiency

Abstract
The four-stroke engine was invented by Nikolaus Otto during the second half of the 19th century. Although a lot of technological improvements have been made over the years, the operating principle with four-strokes remains the same. The need and desire of engines with even higher fuel-efficiency is a motivation to study alternative engine concepts.

This thesis presents studies of the Double Compression-Expansion Engine (DCEE) concept. It belongs to the split-cycle engine family because the engine cycle is performed in two or more cylinders. The potential advantages of these concepts are reduced heat transfer loss, while it can be over-expanded which reduces the exhaust loss. These loss reductions provide a potential for higher fuel-efficiency compared to the conventional four-stroke cycle. However, there are also potential drawbacks such as increased gas exchange loss due to multiple gas exchange events to complete the cycle. Another potential drawback is increased engine displacement requirement to obtain the same power as a conventional engine, which means the power density is reduced.

The results of experimental and simulations studies indicates that a brake efficiency of 51.0 % can be achieved with the proposed DCEE concept. With subsystem optimizations and insulation of certain engine components the efficiency can reach 53.7 %. Morevoer, the obtained results indicate a trend for further improved efficiency at even higher loads. But to maintain the same fuel/bulk gas- ratio (dilution rate), a higher inlet pressure is required which also cause higher peak cylinder pressures. The performed engine experiments were limited to 210 bar to preserve the structural integrity and it is expected that the efficiency can improve further with mechanical upgrades.

This thesis also presents simulation studies of other DCEE concepts. They proved to reach even higher efficiencies, but were also operated at much higher peak cylinder pressures compared to the engine experiments. It was also assumed that a low temperature combustion mode could be used, which has the advantage of decreased heat transfer loss, but also pose challenges in controling the combustion process.

Key words
Split-cycle, high efficiency, CO_2 emissions, 1D-modeling, engine experiments, heavy duty engine

Classification system and/or index terms (if any)

Supplementary bibliographical information

Language
English

ISSN and key title
0282-1990

ISBN
978-91-7895-050-8 (print)
978-91-7895-051-5 (pdf)

Recipient's notes

Number of pages
134

Price

Security classification

Double Compression-Expansion Engine Concepts

Experimental and simulation study of a split-cycle concept for improved brake efficiency

by Nhut Lam

LUND
UNIVERSITY

A doctoral thesis at a university in Sweden takes either the form of a single, cohesive research study (monograph) or a summary of research papers (compilation thesis), which the doctoral student has written alone or together with one or several other author(s).

In the latter case the thesis consists of two parts. An introductory text puts the research work into context and summarizes the main points of the papers. Then, the research publications themselves are reproduced, together with a description of the individual contributions of the authors. The research papers may either have been already published or are manuscripts at various stages (in press, submitted, or in draft).

Cover illustration front: The pistons (1 combustion and 5 balancing) used in the experimental test rig of the Double Compression-Expansion Engine.

Funding information: The thesis work was financially supported by Volvo Group and the Swedish Energy Agency (grant numbers P36699-1 and P36699-2).

Faculty of Engineering, Department of Energy Sciences

ISBN: 978-91-7895-050-8 (print)
ISBN: 978-91-7895-051-5 (pdf)
ISRN: LUTMDN/TMHP-19/1146-SE
ISSN: <0282-1990>

Printed in Sweden by Media-Tryck, Lund University, Lund 2019

Cho gia đình tôi

Contents

List of publications

This thesis is based on the following publications, referred to by their Roman numerals:

I **Double Compression Expansion Engine Concepts: A Path to High Efficiency**

N. Lam, M. Tunér, P. Tunestål, A. Andersson, S. Lundgren, B. Johansson
SAE Int. J. Engines 8(4):1562-1578, 2015, 2015-01-1260

II **Double Compression Expansion Engine Concepts: Efficiency Analysis over a Load Range**
N. Lam, A. Andersson, P. Tunestål
SAE Technical Paper 2018-01-0886, 2018

III **Analyzing Factors Affecting Gross Indicated Efficiency When Inlet Temperature Is Changed**
N. Lam, A. Andersson, P. Tunestål
SAE Technical Paper 2018-01-1780, 2018

IV **Simulation of system brake efficiency in a Double Compressions-Expansion Engine-concept (DCEE) based on experimental combustion data**
N. Lam, A. Andersson, P. Tunestål
SAE Technical Paper 2019-01-0073, 2019

V **Double Compression-Expansion Engine Concepts: Study of pathways for efficiency improvements**
N. Lam, A. Andersson, P. Tunestål
Submitted to Applied Energy

Acknowledgments

First of all I want to thank my current supervisor Per Tunestål. He took over the tough responsibility of supervising in a project that he was not involved with at the beginning. During this period, it became clear to me that he has a great ability in understanding complicated matters in very short time. Also the talks we had about Malmö FF and SHL during the coffee brakes were nice moments of the working day. Bengt Johansson, my first supervisor is also greatly thanked. He convinced me of applying for a PhD-position and I've never regretted this decision since. Arne Andersson from AB Volvo also deserves many thanks. He gave me technical feedback and insights that were very useful for my work. He also made sure that there was an experimental engine provided to Lund. My co-supervisor Martin Tunér helped me getting started with the simulation studies in the project, for which I'm very thankful. The anecdotes he shared about cars and vehicles in general during the fika times were nice to hear.

I would also like to thank the other seniors at the division. Öivind Andersson who supervised me during the master thesis project. He is the most skilled person regarding research methodology that I've ever met and is an invaluable asset for a PhD-student. Our newest senior Sebastian Verhelst added a fresh injection of ideas and knowledge to the division and completed the division in many aspects. Besides that it was nice to speak with him regarding two- and four wheeled vehicles during the lunches. Also big thanks to Marcus Thern who contributed with nice insights of doing a PhD and also made this thesis look more professional than it would have.

The technicians at our division, Thomas Lindén, Tommy Petersen, Mats Bengtsson, Anders Olsson, Patrik Johansson and Martin Carlsson deserve many thanks. You all made my engine experiments possible! I would like to especially thank Patrik. He started with basically an empty room and did a very good job transforming it into a well-functioning experimental rig. This probably became the nicest rig of the entire lab. Thanks to head of laboratory Marcus Lundgren for taking care of the time planning for all the ongoing works among other tasks he was responsible for. Many thanks to Catarina, Gity, Elna and Isabelle for taking care of the administrative questions that I had from time to time. Also Robert and Krister are greatly thanked for taking care of the IT-systems.

A nice feature of doing a PhD is the new friends that you meet from all over the world. My officemates Erik Svensson, Kenan Murić and Xinda Zhu all contributed to very nice discussions of everything between earth and heaven. Pablo, Prakash, Mike, Slavey, Changle, Ashish, Stijn, Vikram and Niko are all greeted for the very nice activities we did outside of work. The life as a PhD-student became much more enjoyable during these moments! I also want to thank my other colleagues for the nice discussions we had during lunch and fika times.

I would also like to thank my other friends who understands that life as a PhD-student can be a bit antisocial from time to time. This will be changed now when this thesis is written and defended, I promise!

Last but not least I would like to thank my family for always supporting me. As everybody probably already knows, the unconditional support and love from your parents can never be replaced. Cars and engines have always been an interest for me thanks to my father and is probably a major reason that I committed to do a PhD within the engine field. My mother is also greatly thanked from all my heart for always being there and supporting me regardless of what I decided. And for my two little sisters, I hope that as a big brother I have inspired you in a positive way.

Abstract

The four-stroke engine was invented by Nikolaus Otto during the second half of the 19^{th} century. Although a lot of technological improvements have been made over the years, the operating principle with four-strokes remains the same. The need and desire of engines with even higher fuel-efficiency is a motivation to study alternative engine concepts.

This thesis presents studies of the Double Compression-Expansion Engine (DCEE) concept. It belongs to the split-cycle engine family because the engine cycle is performed in two or more cylinders. The potential advantages of these concepts are reduced heat transfer loss, while it can be over-expanded which reduces the exhaust loss. These loss reductions provide a potential for higher fuel-efficiency compared to the conventional four-stroke cycle. However, there are also potential drawbacks such as increased gas exchange loss due to multiple gas exchange events to complete the cycle. Another potential drawback is increased engine displacement requirement to obtain the same power as a conventional engine, which means the power density is reduced.

The results of experimental and simulations studies indicates that a brake efficiency of 51.0 % can be achieved with the proposed DCEE concept. With subsystem optimizations and insulation of certain engine components the efficiency can reach 53.7 %. Morevoer, the obtained results indicate a trend for further improved efficiency at even higher loads. But to maintain the same fuel/bulk gas- ratio (dilution rate), a higher inlet pressure is required which also cause higher peak cylinder pressures. The performed engine experiments were limited to 210 bar to preserve the structural integrity and it is expected that the efficiency can improve further with mechanical upgrades.

This thesis also presents simulation studies of other DCEE concepts. They proved to reach even higher efficiencies, but were also operated at much higher peak cylinder pressures compared to the engine experiments. It was also assumed that a low temperature combustion mode could be used, which has the advantage of decreased heat transfer loss, but also pose challenges in controling the combustion process.

Populärvetenskaplig sammanfattning

Transport av människor och gods har varit och fyller fortfarande en viktig funktion i vårt moderna samhälle. I vägfordon är förbränningsmotorn den dominerande kraftkällan. Tyvärr innebär detta även problem med lokala luftföroreningar samtidigt som växthusgasen koldioxid släpps ut i stora mängder. Tidigare var myndigheternas huvudfokus att få ner de lokala luftföroreningarna, men på senare tid har det blivit alltmer uppenbart att även koldioxidutsläppen måste minskas drastiskt. Idag står transportsektorn för en betydande andel av dessa utsläpp och har därmed en stor förbättringspotential. Olyckligtvis kan inte den producerade koldioxiden omvandlas till mindre skadliga ämnen i ett efterbehandlingssystem. Det enda sättet är att förbrukningen av fossilt bränsle minskar. Detta kan exempelvis ske med hjälp av motorer med högre verkningsgrad. Verkningsgraden anger utfört arbete per mängd tillförd bränsleenergi. Motorerna som används i dagens person- och lastbilar arbetar enligt den så kallade fyrtakts-principen. Den uppfanns under 1870-talet, och även om mycket har förändrats och förbättrats är arbetsprincipen idag densamma. Fyrtaktsmotorn har några nackdelar som begränsar verkningsgraden. En är att avgaserna inte expanderas fullt ut, vilket innebär att andelen energi som omvandlas till att driva fordonet framåt minskar. En annan är värmeförluster i samband med förbränningen som påverkar verkningsgraden negativt.

Denna doktorsavhandling presenterar studier av ett motorkoncept som kallas för DCEE, vilket är en förkortning för ”Double Compression-Expansion Engine”. DCEE konceptet bygger på att cykeln utförs i flera cylindrar med olika slagvolym. Detta möjliggör full expansion av avgaserna. Konceptet medför även att den värmeöverförande ytan kan reduceras vilket minskar värmeförlusterna. Potentiellt kan därför motorns verkningsgrad förbättras vilket medför lägre förbrukning av bränsle. För att ta reda på möjligheter och begränsningar med detta koncept har experimentella- och simuleringsstudier genomförts.

Två alternativa DCEE konceptförslag har studerats, där det första förslaget har två cylindrar med olika slagvolym. Båda cylindrarna arbetar med fyrtakts-principen och därför har denna variant kallats för ”4-4” konceptet. Simuleringsstudier av detta koncept visade att en bromsad verkningsgrad på 56 % kan uppnås. Det var med antagandet om att konceptet kombinerades med ett avancerat förbränningskoncept där värmeförlusterna kan minskas kraftigt. Men dessa typer av förbränningskoncept är betydligt svårare att styra och därför fortsatte studien med mer konventionella förbränningskoncept. I en följande studie analyserades hur verkningsgraden påverkas över ett lastområde. Den pekade på att högsta verkningsgrad uppnås vid höga laster. Den visade även att vid låga laster bör luftflödet till motorn begränsas med hjälp av sen stängning av insugsventilen. Mindre luftflöde leder till att det maximala trycket under cykeln minskar vilket även minskar friktionsförlusterna. Denna studie pekade även tydligt på att 4-4 konceptet begränsas av

flödesförluster över ventilerna eftersom cylinderhuvudet för den ena cylindern måste ta hand om fyra olika flöden (istället för två som i en vanlig motor). Den tillgängliga ventilarean begränsas därför till hälften och strypförlusterna blir större. En annan nackdel är att kompressions- och expansionsstegen sker i cylindrar med lika stor slagvolym, vilket gör att en naturlig fullständig överexpansion inte kan uppnås. Därför studerades även ett andra konceptförslag, kallat för 2-4-2 konceptet. Detta konceptförslag har 3 olika cylindrar där två av cylindrarna arbetar med tvåtaks-principen och den tredje cylindern arbetar med fyra takter där även förbränningen sker i. Samtliga cylindrar har olika slagvolym. I kombination med att kompressions- och expansions-takten sker i olika cylindrar möjliggörs fullständig naturlig överexpansion. Samtidigt sker inte mer än två olika flöden för varje enskilt cylinderhuvud vilket ökar den tillgängliga ventilarean och reducerar strypförlusterna. I en studie där simulerings- och experimentella verktyg kombinerades visades att detta koncept kan uppnå en bromsad verkningsgrad på 52.8 %. Det krävs dock att avgasportarna görs isolerade för att bevara värmeenergin för expansionen. Med konventionella avgasportar minskar verkningsgraden till 51.0 %. Olika delprocesser i cykeln undersöktes i nästa studie, vilket gav större kännedom om hur cykeln kan optimeras för att ytterligare förbättra verkningsgraden. Den indikerar att verkningsgraden kan förbättras ytterligare till 53.7 %. Samtidigt var de uppmätta kväveoxidutsläppen betydligt lägre än dagens lagkrav på tunga fordon.

Nomenclature & abbreviations

$\dot{m}_f$	Fuel mass flow rate
η_C	Combustion efficiency
γ	Specific heat ratio
λ	Air/fuel-ratio (in relation to stoichiometric)
$\triangle P$	Pressure increase over the combustion process
$BMEP$	Brake mean effective pressure
c_p	Specific heat capacity (isobar)
c_v	Specific heat capacity (isochor)
$c_{p,m}$	Mean piston speed
CA_{50}	Crank angle when 50 % of total heat has been released
$CLMEP$	Combustion loss mean effective pressure
EGR_{rate}	EGR-rate
$EXMEP$	Exhaust loss mean effective pressure
$FMEP$	Friction mean effective pressure
GIE	Gross indicated efficiency
$HTMEP$	Heat transfer mean effective pressure
$IMEP_g$	Gross indicated mean effective pressure
$IMEP_n$	Net indicated mean effective pressure
M	Molar mass
m_f	Injection fuel mass
$P_{exhaust}$	Exhaust back pressure (combustion cylinder)
P_{inj}	Injection pressure

P_{inlet}	Inlet pressure (HP or combustion cylinder)
PCP	Peak cylinder pressure
$PMEP$	Pumping mean effective pressure
Q_{in}	Heat energy input
Q_{LHV}	Lower heating value
$QMEP$	Heat energy
R_{spec}	Specific gas constant
$R_{universal}$	Universal gas constant
SOI	Start of injection
$T_{exhaust}$	Combustion cylinder exhaust temperature
T_{inj}	Injection duration
T_{inlet}	Inlet temperature (HP or combustion cylinder)
V_d	Cylinder displacement
$V_{d,engine}$	Total engine displacement
aRoHR	Apparent rate of heat release
$aTDC_{Fire}$	After top dead center (firing)
$aTDC_{GE}$	After top dead center (gas exchange)
BDC	Bottom dead center
$bTDC_{Fire}$	Before top dead center (firing)
BTE	Brake thermal efficiency
CAC	Charge air cooler
CCI	Compact Compression Ignition
CO	Carbon monoxide
CO_2	Carbon dioxide
DCEE	Double Compression-Expansion Engine

EGR	Exhaust gas recirculation
EIVC	Early inlet valve closing
EVO	Exhaust valve opening
H_2O	Water
HCCI	Homogeneous Charge Compression Ignition
HP cylinder	High pressure cylinder
HP tank	High pressure tank
Induction volume	Swept volume from expansion cylinder TDC until IVC
LIVC	Late inlet valve closing
LN_2	Liquid nitrogen
LP cylinder	Low pressure cylinder
LP tank	Low pressure tank
LTC	Low temperature combustion
MEP	Mean effective pressure
MPRR	Maximum pressure rise rate
NA	Naturally aspirated
NO_x	Nitrogen oxide
NVH	Noise, vibration and harshness
O_2	Oxygen
PPC	Partially Premixed Combustion
RCCI	Reactive Controlled Compression Ignition
Rpm	Revolutions per minute
TDC	Top dead center
TDC_{GE}	Gas exchange TDC
UHC	Unburned hydrocarbons

Chapter 1

Introduction

The four-stroke internal combustion engine has been a great contributor to society over the years since its introduction. It was a direct replacement for the horse and enabled a faster and more efficient transportation of people and goods. As a result the economic growth and standard of living have improved considerably.

However, the combustion engine also emits local air pollutions, which cause health hazards. It also emits carbon dioxide (CO_2) emissions which is a greenhouse gas and contributes to global warming. According to the researchers from Intergovernmental Panel on Climate Change (IPCC), the global warming must be kept below 2 °C above pre-industrial levels to avoid too severe effects [1]. In the same report it is claimed that this target requires 25 % reduction of CO_2 by 2030 compared to 2010 levels and net zero levels around year 2070.

The International Energy Agency (IEA) in 2018 reported that the transport sector in 2016 contributed with 8 Giga tonnes of CO_2 [2]. This amounts to 18 % of the total global CO_2 emissions. Unlike local air pollutions, CO_2 emissions are not possible to eliminate in an exhaust after-treatment system. Instead, more efficient engines with lower fuel consumption are required. Unfortunately, the progress on engine efficiency is not fast. It is noticed in Figure 1.1 that there were periods when the efficiency actually decreased. The reasons for this is more stringent local emission legislations that required compromises on engine efficiency [3].

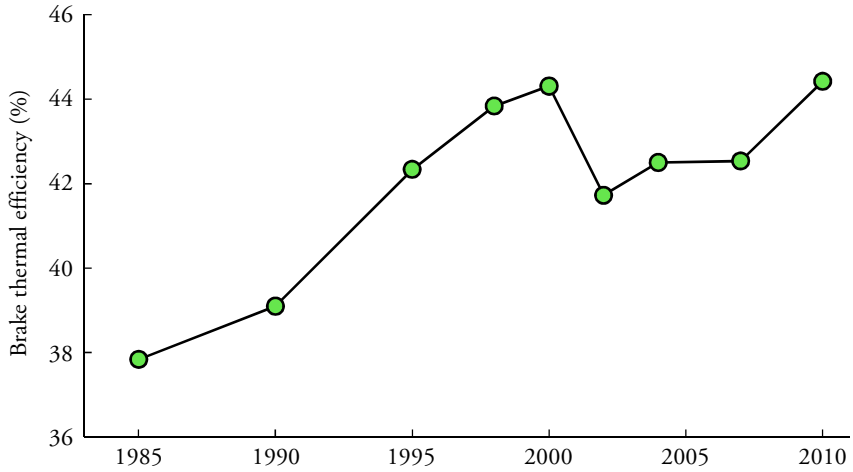

Figure 1.1: Engine brake thermal efficiency over the years at cruise load conditions, adapted from data in [3].

However, since the focus of climate changes has grown over the last years, legislations on CO_2 emissions are starting to be enforced. An example is that passenger cars sold from year 2021 (within the European union) have to emit 95 g/km or less (fleet averaged). If this requirement cannot be reached, fines have to be payed by the vehicle manufacturer.

It is realized that the improvement of engine efficiency alone wont be enough to mitigate the climate changes. More changes need to take place, such as replacing the fossil fuels with biofuels. Even though the issues with CO_2 emissions in this case is eliminated, there are still benefits with improved engine efficiencies since it reduces the operating cost. This is important for commercial vehicles such as trucks since it is used as a tool to earn money for its owner. A vehicle with lower fuel consumption will give a competitive advantage.

Research and development of the four-stroke engine have invented technologies that both improved engine efficiency and reduced harmful emissions. However, the fundamental cycle with four strokes remains the same. This thesis presents studies of a novel engine concept that performs the cycle in several cylinders with differing displacements. It will be referred to as the Double Compression-Expansion Engine (abbreviated DCEE) concept from now on in this thesis.

1.1 Research limitations & objectives

Fuel conversion efficiency of the DCEE concept is the main focus of this work. Local emissions are also considered but is not the main focus. The engine cycle is mainly

studied which means that overall engine layout aspects such as cylinder configuration, engine balancing and specific power density are considered to be outside the scope of this study.

The DCEE concept has mainly been studied in combination with a conventional compression-ignition combustion concept. Simulation studies with a low temperature combustion concept were performed and are presented in Chapter 5. But due to potential combustion control challenges it was decided that the DCEE concept studies will proceed with the conventional compression-ignition combustion concept. As the main focus was on how the novel cycle performs regarding brake efficiency, a well known conventional combustion system is considered a great advantage. The combination of DCEE and advanced combustion concepts is instead suggested as future work.

1.2 Thesis contributions

This thesis presents both experimental and simulation studies of two alternative DCEE concept layouts. The studies have provided a general knowledge about the limitation and potential of these concepts. The main contributions are listed below:

- Simulation study of a DCEE concept with two cylinders at extreme conditions (300 bar peak pressure and 8 bar inlet pressure). The main limitation of this concept is choked flow due to limited flow areas in one of the cylinder heads.
- A study of different load control strategies regarding how load can be varied with highest possible efficiency.
- An experimental and simulation study of a DCEE concept with 3 cylinders. This study provided knowledge about potential efficiency and also knowledge about how optimization of different subsystems can further improve the efficiency of this concept.
- A general study of the inlet temperature effects on the thermodynamic efficiency. This study quantified the effects causing thermodynamic efficiency gains when inlet temperature was reduced and is useful to determine appropriate operating settings for the DCEE cycle.

1.3 Outline

The thesis contains 10 chapters including the present one. A brief presentation of each chapter is provided below.

Chapter 2

This chapter presents a deeper introduction and motivation for the studies of the novel DCEE engine concept. A literature study is presented aiming at learning from past research and finding knowledge gaps regarding this type of engine concepts.

Chapter 3

The two alternative DCEE concepts are introduced, described and discussed in this chapter.

Chapter 4

The experimental hardware facilities, measuring equipment and post processing methods are presented in this chapter.

Chapter 5

The simulation setup, method and results for the first DCEE concept are presented in this chapter.

Related publications

N. Lam, M. Tunér, P. Tunestål, A. Andersson, S. Lundgren, B. Johansson, "Double Compression Expansion Engine Concepts: A Path to High Efficiency", SAE Int. J. Engines 8(4):1562-1578, 2015, 2015-01-1260.

N. Lam, A. Andersson, P. Tunestål, "Double Compression Expansion Engine Concepts: Efficiency Analysis over a Load Range", SAE Technical Paper 2018-01-0886, 2018.

Chapter 6

A study of inlet temperatures effects on the thermodynamic efficiency is presented in this chapter.

Related publication

N. Lam, A. Andersson, P. Tunestål, "Analyzing Factors Affecting Gross Indicated Efficiency When Inlet Temperature Is Changed", SAE Technical Paper 2018-01-1780, 2018.

Chapter 7

This chapter presents the method used for the engine experiments, simulation model and method and finally both the experimental and full system DCEE results.

Related publication

N. Lam, A. Andersson, P. Tunestål, "Simulation of system brake efficiency in a Double Compressions-Expansion Engine-concept (DCEE) based on experimental combustion data ", SAE Technical Paper 2019-01-0073, 2019.

Chapter 8

This chapter presents simulation studies performed to evaluate potential pathways for further improvements of the DCEE system brake efficiency based on the findings in Chapter 7.

Related publication

N. Lam, A. Andersson, P. Tunestål, "Double Compression-Expansion Engine Concepts: Study of pathways for efficiency improvements", Submitted to Applied Energy.

Chapter 9

A summary and conclusions from the findings in this thesis are presented in this chapter.

Chapter 10

Suggestions for future studies based on the findings in this thesis are presented in this chapter.

Chapter 2

Literature review

The four-stroke combustion engine is currently the dominating engine type used in road based vehicles. It is popular because of its high specific power, enabling it to carry a high payload and providing a long operating range. However, with the increasing focus on climate changes its emission of CO_2 is not sustainable. Even after more than a century of research and development the efficiency is still not impressive. Current engines are reported to reach 44-46 % brake efficiency [4] and higher engine efficiencies are always desired. There are ongoing projects aimed at improving the fuel efficiency of transportation vehicles, such as the SuperTruck and SuperTruck II projects coordinated by the US Department of Energy. One of the targets for the SuperTruck II project is to present an engine concept that can achieve a peak brake efficiency of at least 55 % [5]. Exotic technological solutions such as advanced combustion concepts, improved gas exchange system and waste heat recovery will be required to achieve this high efficiency [6].

The engine efficiency is determined by the losses associated with the cycle. Figure 2.1 presents a distribution of the useful work output and the losses occurring during the cycle. Of the energy input as fuel, roughly half is wasted as heat and exhaust losses. Hence, the potential for engine efficiency improvements is the greatest when these losses are considered. The following section will discuss different engine development pathways aiming at improved engine efficiency. But first will the conventional and currently dominating engine cycle be briefly explained.

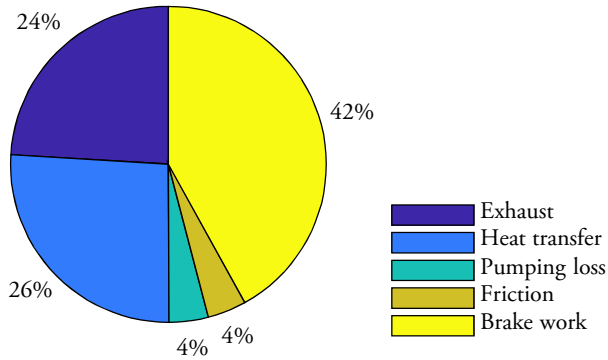

Figure 2.1: Energy distribution of work and losses in a turbocharged, heavy duty diesel engine from 2007 [7].

2.1 The four-stroke cycle

As the name suggests, this cycle completes four strokes per engine cycle. Two complete crankshaft revolutions are required to complete the four strokes. The process is described by the pressure-volume diagram in Figure 2.2 and the four strokes are:

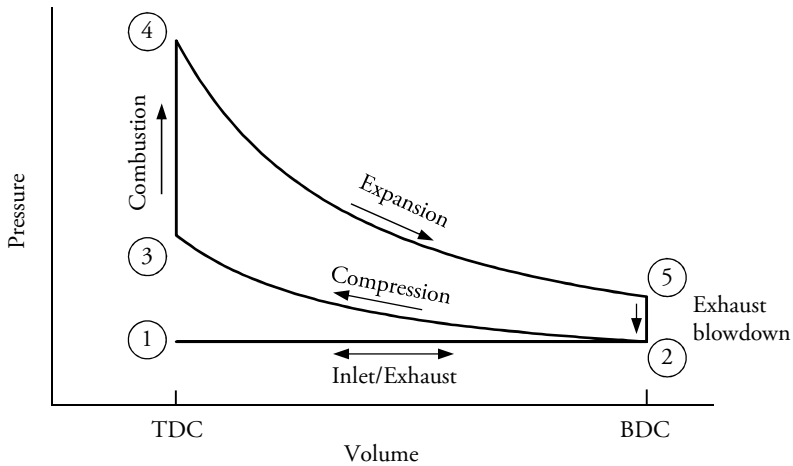

Figure 2.2: Pressure-volume diagram for the four-stroke cycle.

Inlet, $1 \rightarrow 2$
The cycle starts at position 1, with the piston at top dead center (TDC). Air is inducted through an inlet valve when the piston travels towards bottom dead center (BDC).

Compression, $2 \rightarrow 3$
The inlet valve closes and a closed volume is formed. The piston moves from BDC to

TDC which compresses the inducted air. Pressure and temperature increases while the air is compressed.

Combustion/expansion, $3 \rightarrow 4 \rightarrow 5$
At TDC, the combustion is initiated by fuel being injected into the compressed hot air (compression-ignition engines). In a spark-ignition engine a fuel and air mixture is ignited by a spark plug. The release of heat increases the charge temperature and pressure. After combustion the expansion occurs when the piston travels from TDC to BDC. Pressure and temperature of the gas decreases as it expands.

Exhaust, $5 \rightarrow 1$
The piston pushes out the expanded gas through an exhaust valve (note the pressure is above inlet pressure). This completes the cycle and a new cycle can start.

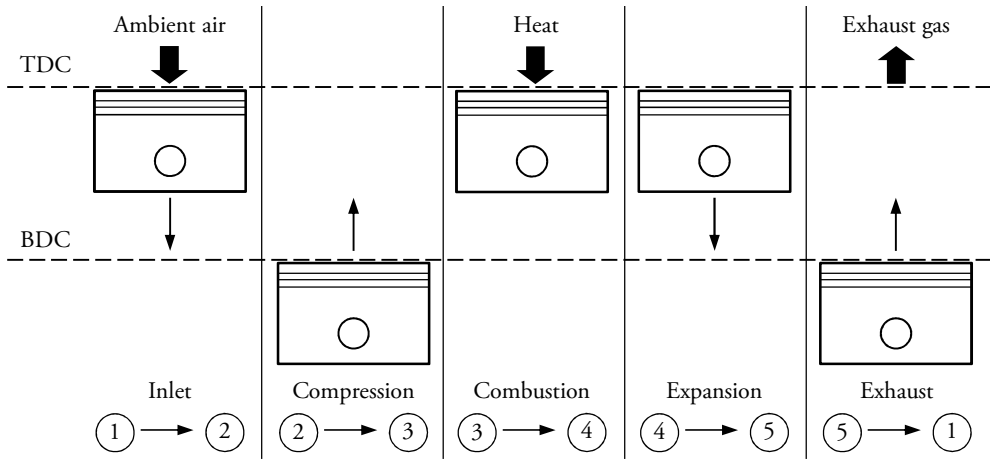

Figure 2.3: Piston motion during the four-stroke cycle. The numbers indicates the position in the pressure-volume diagram in Figure 2.2.

2.2 Improving thermodynamic efficiency through high dilution operation

Highly diluted operation is defined as when the inducted bulk gas quantity is large in relation to the injected fuel mass. The bulk gas can both be pure air or a mixture of air and inert gas (EGR). Highly diluted operation will require a high inlet pressure, especially at high loads where the injected fuel mass is large. By operating the engine highly diluted, the temperature during the combustion event is reduced due to larger mass of bulk gas. The lower temperature reduce heat loss and also maintain a lower specific heat capacity which improves the thermodynamic efficiency [8, 9]. Unfortunately, the requirement of

high inlet pressure can be a challenge for the turbocharger system. The power required to propel the turbocharger compressor increases with inlet pressure [10]. At the same time the higher dilution rate also means that the exhaust temperature decreases, which reduces the potential energy that can be recovered in the turbocharger turbine. At a certain point the extracted turbine power is less than the required power from the compressor and the requested inlet pressure cannot be achieved [11]. Additionally, this discussion only involved an idealized turbocharger. A real turbocharger also has losses that further limits the inlet pressure that is possible to achieve.

There is a potential for further heat loss reduction if advanced combustion concepts are studied, such as Homogeneous Charge Compression Ignition (HCCI) [12, 13], Partially Premixed Combustion (PPC) [14, 15] or Reactive Controlled Compression Ignition (RCCI) [16] concepts. The principal idea of these concepts is that the fuel is more premixed when it is auto-ignited (compared to conventional diffusion combustion). The higher premix level helps avoiding rich zones where high local temperatures are reached and thereby also reduces heat loss [17, 18] and the formation of NO_x. However, these concepts require a high amount of inert gas, which again requires a high inlet pressure to enable high load operation. This means that these concepts also pose challenges for the turbo charging system.

2.3 Engine downsizing

The trend especially noticeable in passenger car engine development is engine downsizing [19, 20]. A combustion engine in general has its highest efficiency when it is operated at high loads. By replacing with a smaller engine the average engine load is increased and the average efficiency is improved [21]. Additionally, a smaller engine with fewer cylinders in general has better mechanical efficiency because of fewer moving parts. The reduced power output due to decreased engine displacement is compensated by the introduction of forced induction or an even higher degree of forced induction. The most common type of forced induction system is the turbocharger system. It consists of a turbocharger compressor and a turbocharger turbine connected on the same shaft. The turbine extracts the residual exhaust energy output from the engine which is used to power the compressor. A systematic layout of the turbocharger forced induction system is presented in Figure 2.4.

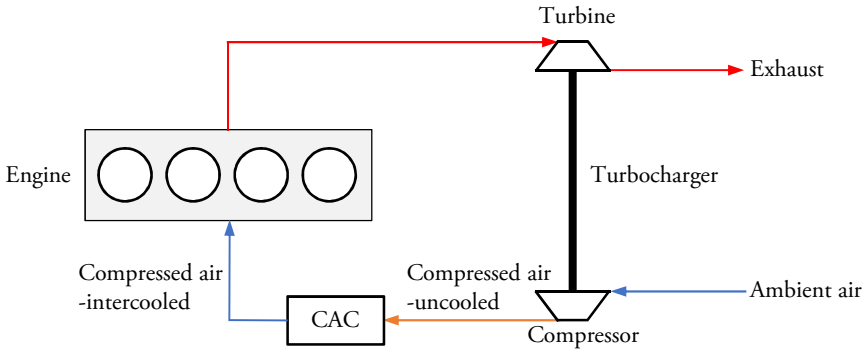

Figure 2.4: The layout of a turbocharged engine.

With the addition of the turbocharger, the engine cycle has effectively become a two stage compression and expansion process. The turbocharger compressor performs the first compression stage and the compressed air is compressed a second time in the engine. The same can be applied for the expansion process, where the first expansion stage occurs inside the cylinder and the second stage occurs in the turbocharger turbine. The increased load capability comes from the higher oxygen concentration of the inlet air due to a higher inlet pressure. But the higher inlet pressure also increases the peak pressure during the combustion phase. A reduction in compression ratio is required to maintain the same peak pressure. If not, the mechanical robustness could be adversely affected. But a reduction in geometrical compression ratio also reduces the effective expansion ratio. This means that less work is extracted, and more energy remains unexploited in the exhaust gases. The turbocharger is unfortunately not able to recover this energy to propel the vehicle, it can only use a fraction of the energy to power the compressor. A large fraction of the exhaust energy is wasted into the ambient air.

The trend of continued engine downsizing requires even higher specific power outputs. The logical solution is to enlarge the turbocharger system with an even higher boost pressure capability. The drawbacks with the turbocharger hence becomes even more apparent when an even larger fraction of the compression and expansion processes occurs outside the cylinder.

Figure 2.5 illustrates a pressure-volume diagram for an imaginary operating point where an inlet pressure (P_{inlet}) of 5 bar is used. Even if the operating point is highly diluted (40 % EGR_{rate} and $\lambda = 1.34$) the cylinder pressure when the exhaust valves open is around 13 bar. There is currently no turbocharger turbine that can efficiently expand from 13 bar to 1 bar in one single stage.

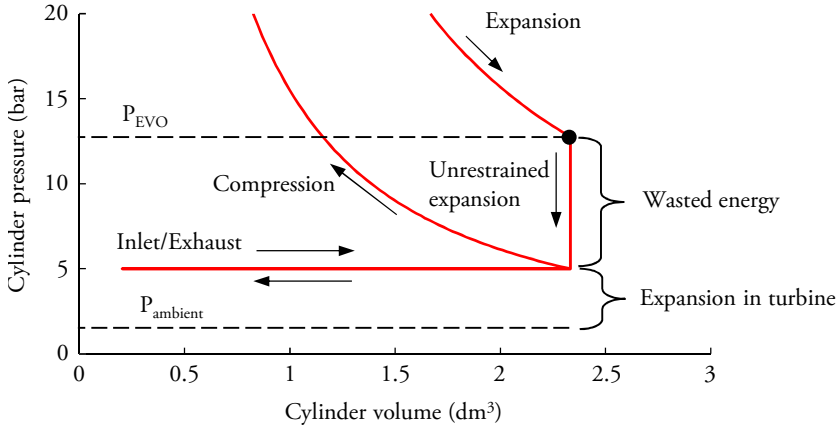

Figure 2.5: PV-diagram illustrating the pressure level at the end of expansion relative to the inlet pressure. 40 % EGR_{rate}, λ = 1.34 and CR = 11.5:1)

2.4 Over-expanded engine cycles

The big drawback with engine downsizing is the high amount of wasted exhaust energy that cannot be efficiently recovered to propel the vehicle. The amount of exhaust loss can be reduced by utilizing cycles which are over-expanded. A cycle is defined as over-expanded when the effective expansion ratio is greater than the compression ratio. An example of such a cycle is the Atkinson "Cycle engine" invented and patented by James Atkinson in 1887 [22]. This concept uses a complicated crank mechanism where the four strokes are performed every engine crank revolution. More interesting is that the inlet and compression strokes were significantly shorter than the expansion and exhaust strokes, enabling a greater expansion ratio than compression ratio. It is believed that a combination of complexity, cost, mechanical size and losses prevents this concept from being in production engines today.

A simpler way to achieve over-expansion with the conventional crank mechanism is to use inlet valve closing timings as presented by Ralph Miller [23]. There are two strategies, either early inlet valve closing (EIVC) or late inlet valve closing (LIVC). These valve timing strategies reduce the effective compression ratio, while the effective expansion ratio is maintained. A drawback with these strategies is the reduction in effective engine displacement, which affects the power density. The engine has the displacement of a large engine but can only produce power similar to a smaller displacement engine. This is the opposite of what is desired with engine downsizing.

Another possibility to extract more expansion work is to add an extra turbine to the exhaust flow. This turbine is directly connected through a gearing system to the engine's

crankshaft and is called turbo-compound technology. Figure 2.6 presents an layout of this concept. The idea is to expand the leftover exhaust energy to also power the engine crankshaft, not just the turbo compressor. The extra work output can improve overall efficiency, but it turns out that this only works in a limited operating range. Outside of this range the turbine becomes a flow restriction and causes higher back pressure which reduces engine efficiency.

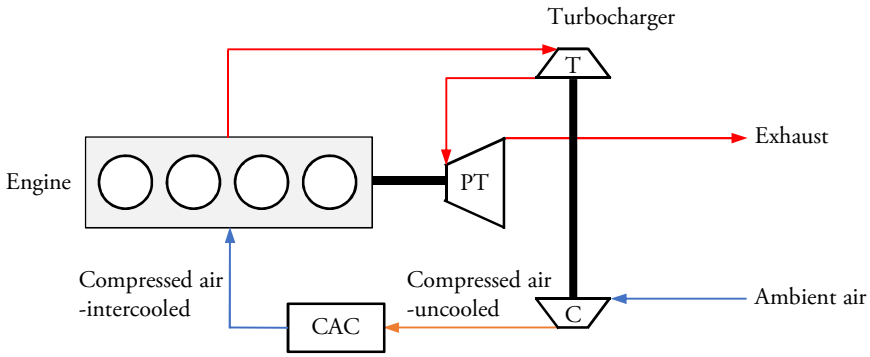

Figure 2.6: Overview of the turbo-compound concept. The turbo-compound turbine (PT), located downstream of the conventional turbine (T) to extract more work from the exhaust gas. The work is then transfered to the engine through a transmission system.

2.5 Split-cycle engines

Split cycle engines (also known as compound engines) have been studied since the 19^{th} century. The definition of split-cycle may vary, but for this thesis is a split-cycle defined as an engine cycle where the compression and expansion strokes are performed in different cylinders.

The split-cycle concept layout enables a potential for improved thermodynamic efficiency. Several various concepts have been invented, but very few actually made it into the prototype phase, and none made it into series production. These facts suggests that there are practical challenges regarding air flow restrictions, thermal management issues, late combustion phasing and mechanical issues with the crossover valve actuation mechanism [24]. An overview of the most relevant concepts is presented in this section.

2.5.1 Diesel series XIV engine

In 1897, Rudolf Diesel build a split-cycle engine with the target of achieving a very high efficiency [25]. This engine consists of two conventional combustion cylinders

with an added larger expansion cylinder connected to both the combustion cylinders. Unfortunately, the combustion cylinder's exhaust valves required a lot of cooling which completely compromised the efficiency. Compared to other contemporary engines of the time the fuel consumption was twice as high and Diesel later discarded the project.

2.5.2 Brayton gas engine cycle

Even though the Brayton cycle is today most commonly associated with contemporary gas turbines the original Brayton cycle consisted of a piston compressor and expander [25]. The combustion occurred at constant pressure in a volume between the cylinders. This version falls into the definition of a split-cycle. A great advantage is that it operates on a two-stroke cycle, which means it produces work output every crankshaft rotation which increases the power density. This was important during the early years of the combustion engine era when the engines were massive in relation to their power output.

The operating principle for modern gas turbines are the same, although the piston compressor and expander were replaced with turbo-machines. It is believed that the change to turbo-machines was due to power density.

2.5.3 Scuderi

The Scuderi split-cycle concept [26, 27, 28, 29] was being patented for the first time in 2003 and since then generated over 200 patents. It is the simplest form of split-cycle with a compression and a expansion cylinder. The authors claim that the main advantage with this concept is the reduced NO_x emissions, faster combustion due to increased charge motion and the ability to use as an air hybrid. The Scuderi concept has nevertheless not been able to demonstrate particularly high efficiency values. A study from 2012 [28] reported that the lowest brake specific fuel consumption of 236.8 g/kWh was reached. Assuming a fuel lower heating value of 44 MJ/kg the resulting brake efficiency is around 34.5 %. Even though it might be a good number relative to other spark-ignition engines it is still 10 percentage points worse than contemporary four-stroke diesel engines.

2.5.4 Isoengine

This split-cycle concept was first presented by Coney et. al in 2004 [30]. The concept has two cylinders, a compression and a combustion cylinder. Injection of water enables the compression to be isothermal. After the compression the water is separated while the compressed air is sent through a recuperator. The intention of this device is to use wasted exhaust heat to reheat the compressed air prior to induction into the combustion

cylinder. The net outcome of the isothermal compression and recuperation processes is that less energy is used to compress the air, while the potential for work extraction in the combustion cylinder increases with recuperation since the specific volume increases. The simulation results claimed that with diesel fuel the overall efficiency was close to 60 %.

The Isoengine was intended to be used for power generation purposes. A similar concept is the CryoPower engine [31] that has the same work principle as the Isoengine, with the main difference that it is intended to be used as a power source in heavy-duty vehicles. Because of this the water injection during the compression is replaced by liquid nitrogen (LN_2) injection instead. LN_2 can be produced on board which avoids the difficulties of handling a water system [32]. An experimental study of the combustion cylinder was presented in 2017 [33]. Two engine speeds were evaluated (800 and 1200 rpm) and it is observed that the air mass flow rate decreased at higher engine speed, although the induction time in terms of crank angle was increased. This is an indication that there might be an engine speed limitation with this concept [24]. However, cycle simulations based on the experimental data suggests that brake efficiency close to 60 % can be achieved.

2.5.5 Compact Compression Ignition

The Compact Compression Ignition (CCI) concept was first described in 1999 [34, 35]. It consists of three different cylinders: intake, combustion and exhaust. The cylinders have different cylinder displacements in order to achieve over-expansion. The first generation of this engine also had the combustion cylinder in an opposed piston configuration, claiming reduced heat transfer surface areas. It is also claimed that the surface area is reduced even further because of the low compression ratio in the combustion cylinder. The gas transfer between the cylinders occurs through cross over channels as the Scuderi concept. The inventors of this concept claim that the advantage with this concept is its compactness compared to naturally aspirated (NA) engines. They also claim that the efficiency will be higher due to the reduced heat transfer surface area but no number was mentioned.

It can be observed that in a 2^{nd} generation of this concept the layout with opposed piston has been abandoned. Instead, a boxer layout is now considered with engine banks of three cylinders containing each of the different pistons. Now it is claimed that a BTE of 52 % can be achieved, with less noise, vibrations and in a much more compact format compared to a conventional engine [36].

2.5.6 General Motors compound engine

General motors (GM) are also looking into the split-cycle concept. They have a patent on a split-cycle layout with 3 different cylinders [37]. This split-cycle concept consists of a compressor cylinder, one or more power cylinders and an expander cylinder. The compressor and expander operates on a two-stroke cycle while the power cylinder operates on a conventional four-stroke cycle. The claimed advantages are that different displacements can be used to achieve better thermodynamic efficiency. Also the option of using a recuperator heating the inlet charge of the power cylinder can be used to gain thermodynamic efficiency as a waste heat recovery device. It can also be used as a charge air cooler to reduce the tendencies for knock in a spark-ignition combustion case. Moreover, an additional advantage is that a catalyst can be installed on the exit of the power cylinder to complete the combustion of unburned fuel. This resembles very much one of the concepts studied in this thesis. Unfortunately, there are no studies published about this concept. But at the SAE High Efficiency IC Engine Symposium (Detroit, April 2018) a variant with a supercharger instead of a piston compressor was presented. With lean burn spark-ignition a brake thermal efficiency of 40.4 % could be achieved.

2.6 Summary of literature review

The current trend of four-stroke engine development is towards downsizing where the intention is to let the engine operate at higher load levels where the efficiency is higher. To maintain the same power output it is required that more work is done in the turbocharger. The drawback is that the turbocharger loses efficiency when the pressure ratios becomes too high, especially on the expansion side. The net effect could be that gas exchange efficiency is adversely affected. An additional drawback is that the turbocharger turbine can only supply power to the turbocharger compressor, not to the engine crankshaft.

Previous studies suggest that operating the engine highly diluted (high bulk gas to fuel-ratio) can enable higher thermodynamic efficiencies to be achieved. The higher bulk gas fraction maintains a lower temperature, which both reduces the heat transfer loss and maintains a lower specific heat capacity. However, this also requires higher inlet pressures and the turbocharger is once again the limiting factor. A potential gain in thermodynamic efficiency is lost by poor gas exchange efficiency. The same conclusions can be made about low temperature combustion concepts. They require a high inert gas concentration to enable a long ignition-delay to allow more time for fuel and air to premix prior to combustion. At high load it is therefore required to have high inlet pressure and once again the turbocharger is the limiting factor.

Exhaust loss can be reduced through an over-expanded cycle. Over-expansion can be achieved in several ways, with the most simple is to use early or late inlet valve closing strategies, so called ”Miller”-timing. But the drawback with this strategy is reduced power density due to reduced effective displacement. Another drawback is the worse mechanical efficiency, because the engine still has a geometrical large displacement but the power output is comparable to a smaller one. Solutions with additional turbine stages (turbo-compound) can also reduce the exhaust loss by extracting more work from the exhaust energy, but this can only be in a relatively narrow window. Outside of this window the turbo-compound turbine instead becomes a throttling loss.

The split-cycle engine concepts are possible solutions to improve the thermodynamic efficiency due to several potential advantages. One is that the compression and expansion ratios can be decoupled from each other without reducing the effective displacement. Another is that the compression and expansion processes can be optimized for their respective processes. It is desired that the compression process is as close to isothermal conditions as possible because the required work input decreases. The expansion process on the other hand is desired to be as close to an isentropic process as possible, because this will maximize the work output.

Several split-cycle concepts have been studied before. The major reason is the potential for thermodynamic efficiency improvements, but there are other advantages claimed as well. The Scuderi concept has not presented high efficiency levels, but claims to have an advantage regarding faster combustion, reduced NO_x emissions and the possibility to be part of an air hybrid solution. Except for high efficiency the CCI engine is also claimed to increase power density compared to naturally aspirated engines. The concept promising the highest efficiency is the Isoengine/CryoPower-concepts where 60 % brake efficiency is suggested by simulations. But there are still challenges relating to the gas exchange process.

One observation is that no split-cycle engines are in serial production at the moment. This suggests that there are practical challenges relating to thermal issues and choked gas flow. In the case of the Diesel series XIV engine the limiting factor was overheated exhaust valves. But this was the end of the 19^{th} century and the technological advances since then should be quite considerable, enabling similar concepts to work better today. And the increased CO_2 reduction requirements increases the motivation for this kind of engine concepts.

Chapter 3

The Double Compression-Expansion Engine concept

The shortcomings of downsizing and the limitations of turbocharger systems discussed in the previous chapter is a motivation to investigate other engine concepts. The concept studied in this thesis is an engine concept where the turbo machine (turbocharger) is replaced by a piston machine. The added piston machine is also connected to the crankshaft, enabling it to transfer energy to and from it. This concept has been labeled the ”Double Compression-Expansion Engine” (DCEE) because the compression and expansion strokes are performed twice in a complete engine cycle.

The main advantage of the piston machine compared to the turbo machine is the ability to work more efficiently at high pressure ratios. A higher inlet pressure can be achieved which increases the load capability and enables a further engine downsizing. The increased inlet pressure also means that the in-cylinder pressure increases but this is compensated with a reduced compression ratio. As was the case with the conventional four-stroke engine the resulting decrease in effective expansion ratio leads to increased exhaust energy loss. But since the piston machine can expand more efficiently at high pressure ratios this does not pose the same issue.

This thesis presents studies and investigations of two different DCEE concepts. The first version has two different cylinders and is labeled the ”4-4” concept. It is called so because each of the two cylinders operates on a four-stroke cycle. The second version is labeled the ”2-4-2” version. It has 3 different cylinders, where 2 of them operate on a two-stroke cycle and the last cylinder operates on a four-stroke cycle.

A more in-depth description is presented in the following sections.

3.1 The 4-4 concept

This version of DCEE consists of two cylinders, a low pressure (LP) and a high pressure (HP) cylinder, which are presented in Figure 3.1. The displacement of the LP cylinder is considerably larger than the HP cylinder. In the flow path from the LP cylinder into the HP cylinder there is a volume (low pressure tank, LP tank) that enables an isobaric transfer of compressed gas. A charge air cooler (CAC) reduces the compressed gas temperature. Both cylinders are connected via connecting rods to the engine's crankshaft. This layout has similarities to the conventional turbocharged four stroke engine, where the HP cylinder operates according to the conventional four stroke cycle. The main difference is that the conventional turbocharger (turbo machine) has been replaced with the LP cylinder (piston machine).

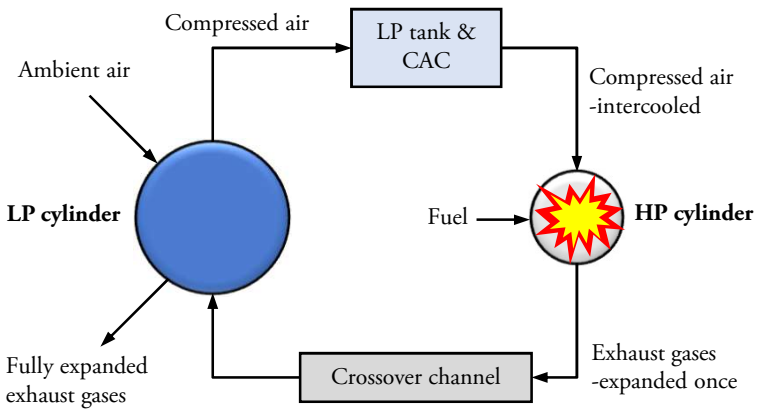

Figure 3.1: The 4-4 version of the DCEE concept.

3.1.1 LP cylinder

The LP cylinder operates over the following four strokes which are completed over two crankshaft revolutions. The pressure volume diagram in Figure 3.2 presents the pressure and volume during the different strokes:

1 → 2. Induction of ambient air from top dead center (TDC) to bottom dead center (BDC).

2 → 3. Compression for around half of the stroke and then a valve to the LP tank opens.

3 → 4. Transfer of compressed air into the LP tank.

4 → 5. Recompression of residual air to match pressure at TDC.

5 → 6. Induction of hot, combusted gas from the HP cylinder and perform the second expansion stroke. This happens simultaneously with the HP cylinder's exhaust stroke (**5 → 6**).

6 → 1. Expelling expanded exhaust gas into ambient.

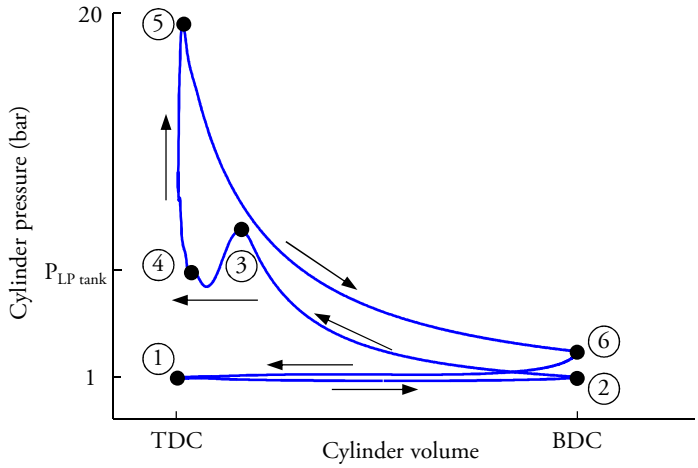

Figure 3.2: Pressure-volume diagram for the LP cylinder. The numbered circles presents the different points of the process in the LP cylinder.

3.1.2 HP cylinder

The HP cylinder also operates on a four-stroke cycle which is very similar to the conventional four-stroke combustion engine. However there is a major difference that will be presented in the actual process. The pressure-volume diagram in Figure 3.3 presents the entire HP cylinder process, while Figure 3.4 presents the same diagram with focus on the gas exchange loop.

1 → 2. Induction of compressed air from LP tank, from piston TDC to BDC.

2 → 3. Second compression stage from BDC to TDC. Close to TDC the fuel is injected and combustion is initiated.

3 → 4. Combustion where the temperature and pressure increases.

4 → 5. First expansion stage, from TDC to BDC.

5 → 6. Outlet stroke, where the piston pushes the combusted gas into the LP cylinder through the crossover channel. This occurs simultaneously with the third stroke in the LP cylinder **5 → 6** in LP cylinder. Since the displacement of the LP cylinder is larger this stroke effectively becomes the second expansion stage.

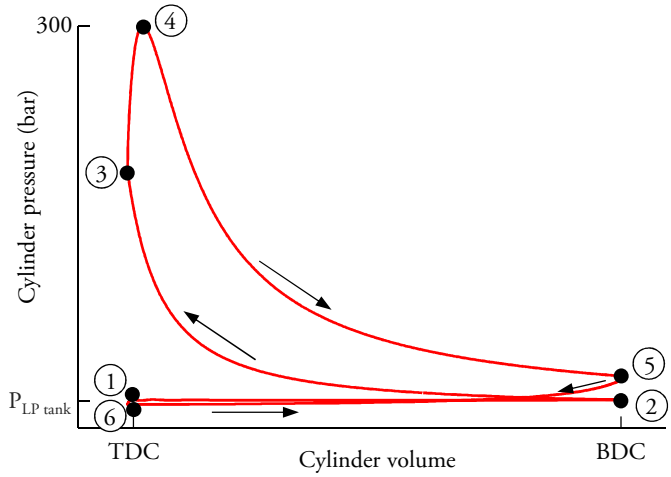

Figure 3.3: Pressure-volume diagram for the HP cylinder.

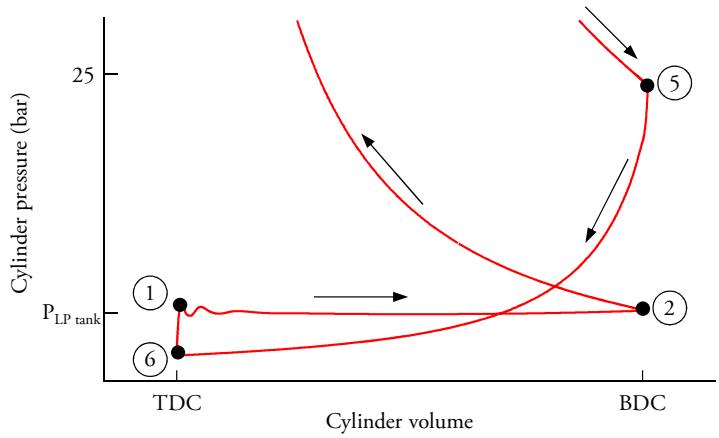

Figure 3.4: Gas exchange loop of the HP cylinder.

Figure 3.5 and Figure 3.6 present the pressure trace for both cylinders during the cycle. This concept requires that the HP and LP cylinders are synchronized to perform the second expansion stage (processes **5** → **6** for both cylinders).

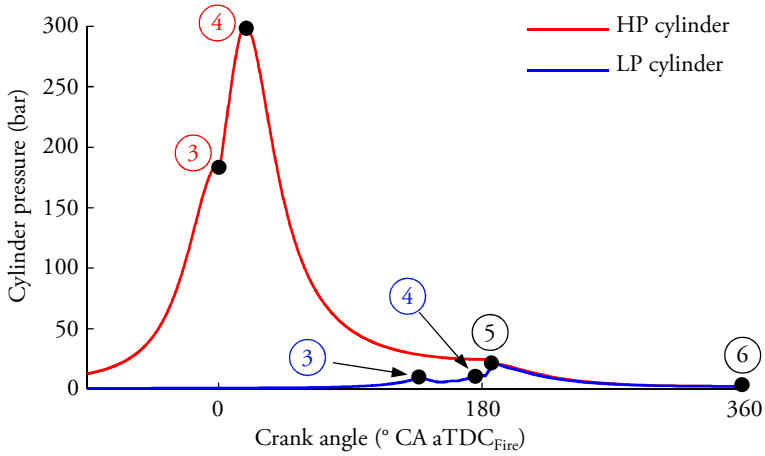

Figure 3.5: Pressure traces for the LP and HP cylinder. The x-axis refers to the HP cylinder crank angle position. Observe how the LP and HP cylinder pressure becomes similar between 180 and 360 °CA aTDC$_{Fire}$.

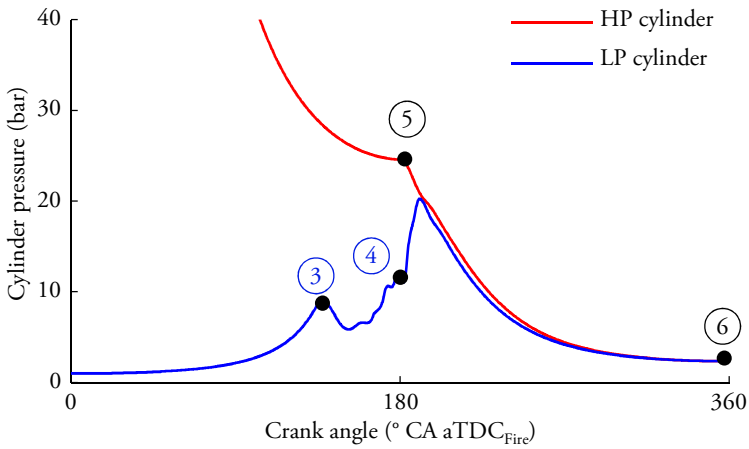

Figure 3.6: Zoomed in pressure traces for the LP and HP cylinder. The x-axis refers to the HP cylinder crank angle position.

3.2 The 2-4-2 concept

Because the compression and expansion processes in the 4-4 concept occur in the same cylinders, complete over-expansion is not achieved. Another drawback is the choked air flow in the LP cylinder head. It has to handle 4 different air paths and the effective flow area is only half of a conventional engine.

These issues are solved in the second version of the DCEE concept where the LP cylinder has been replaced with dedicated compression and expansion cylinders. Instead of

having one cylinder alternating between doing a compression and expansion these two cylinders are each performing one of these tasks.

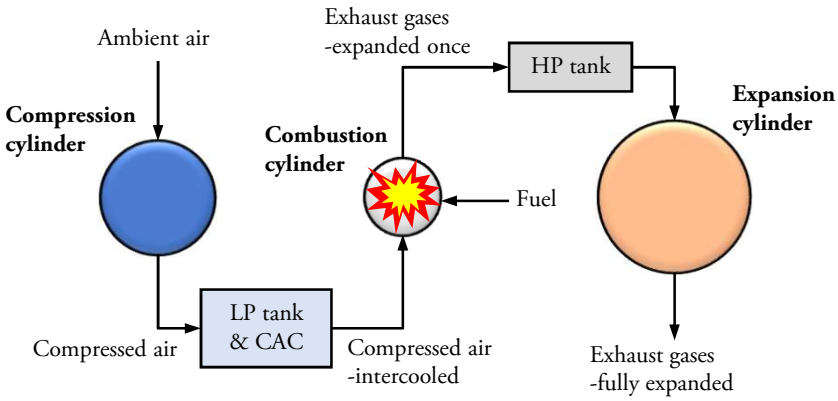

Figure 3.7: The 2-4-2 version of the DCEE concept.

Figure 3.7 presents the DCEE 2-4-2 version. There are three different cylinders, a compression cylinder, a combustion cylinder (which are very similar to the HP cylinder in the 4-4 layout) and an expansion cylinder. The combustion cylinder has the smallest displacement, the compression cylinder is the 2^{nd} largest and the expansion cylinder is largest. Except for the intermediate tanks is this concept very similar to the patent filed by GM [37].

Basically, this concept is similar to the 4-4 layout, with the main difference being the strokes previously performed in the LP cylinder are now performed in the compression and expansion cylinders. Another difference is that this layout has two intermediate tanks adjacent to the combustion cylinder. The LP tank is located on the inlet side of the combustion cylinder while the high pressure tank (HP tank) is placed on the exhaust side. As was the case for the 4-4 concept, the tanks enable isobaric gas transfer between the cylinders because of their large volume relative to the cylinder displacement.

Another advantage of this layout is that it does not constrain the selection of phasing between the 3 pistons in the cylinders. It therefore enables a phasing choice that can aid engine balancing to reduce vibrations.

3.2.1 Compression cylinder

The compression cylinder operates on a two-stroke cycle completed over 1 crankshaft revolution. The process in the compression cylinder is presented in Figure 3.8 and described below:

1 → 2. Induction of ambient air from TDC to BDC through an open inlet valve.

2 → 3. Compression of the inducted ambient air. An outlet valve opens at the end of compression.

3 → 4. The compressed air is transferred into the LP tank through the open outlet valve. The piston reaches TDC where the outlet valve closes.

4 → 1. A re-expansion occurs to equalize the in-cylinder pressure to ambient pressure. At the end of the re-expansion the inlet valve opens and a new cycle can begin.

The pressure-volume diagram for the compression cylinder is presented in Figure 3.8.

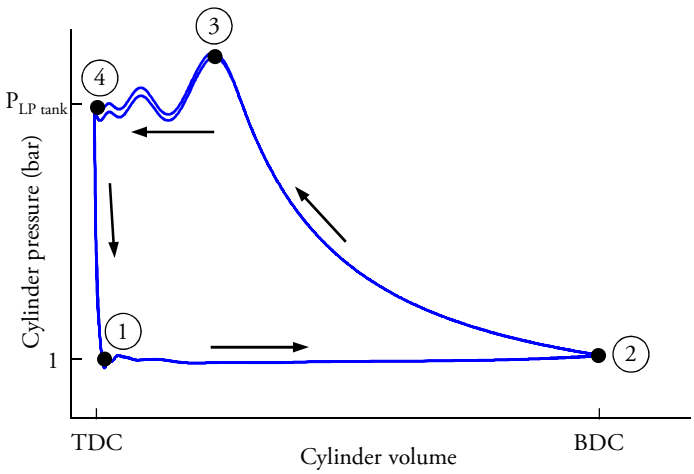

Figure 3.8: Pressure-volume diagram for the compression cylinder.

3.2.2 Combustion cylinder

The combustion cylinder operates on a four-stroke cycle completed over 2 crankshaft revolutions. In general it follows the conventional four-stroke cycle, but with some differences. Figure 3.9 presents the PV-diagram and the combustion cylinder cycle is described below:

1 → 2. Induction of compressed air from the LP tank through the open inlet valve.

2 → 3. Inlet valve closes and 2^{nd} compression stage begins.

3 → 4. At the end of the 2^{nd} compressions stage fuel is injected into the cylinder and combustion is initiated.

4 → 5. Combustion ends and expansion proceeds until piston reaches BDC.

5 → 6. Exhaust blow down when the exhaust valve opens close to BDC. The higher in-cylinder pressure than the adjacent HP tank pressure causes the partly expanded gases to expand (unrestrained).

6 → 7. Exhaust gas is pushed into the HP tank by the piston movement from BDC to TDC.

7 → 1. Gas exchange where the exhaust valve closes while the inlet valve opens and a new cycle can be started again.

The pressure-volume diagram for the combustion cylinder is presented in Figure 3.9.

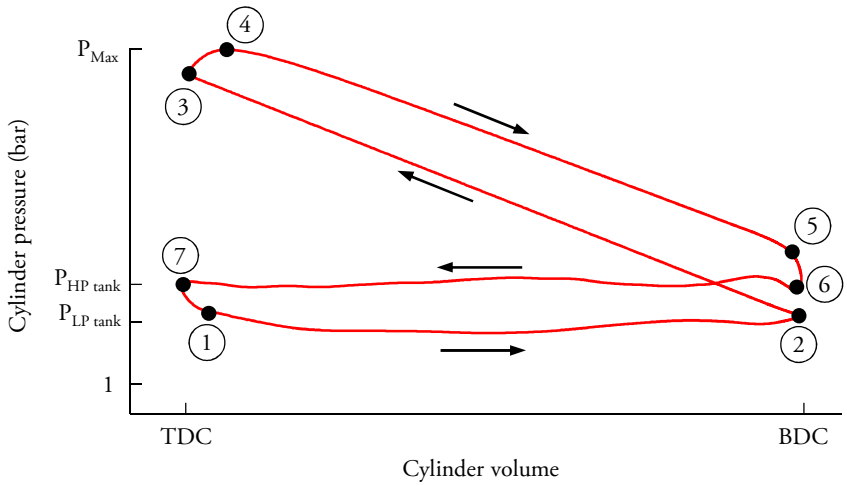

Figure 3.9: Pressure-volume diagram for the combustion cylinder. Observe that logarithmic scaling has been used.

3.2.3 Expansion cylinder

Like the compression cylinder, the expansion cylinder operates on a two-stroke cycle, completed over 1 crankshaft revolution. Figure 3.10 presents the PV-diagram and the cycle is described below:

1 → 2. Expansion cylinder's inlet valve is open and gas from the HP tank is inducted into the cylinder. At around one third of the stroke the inlet valve closes. The swept volume from TDC until the inlet valve closes is defined as the "induction volume".

2 → 3. Expansion until the gas has reached ambient pressure. Expansion cylinder exhaust valve opens close to BDC.

3 → 4. The completely expanded gas is now expelled into the exhaust manifold through the open exhaust valve. Close to TDC the exhaust valve closes.

4 → 1. A short re-compression is performed to bring the in-cylinder pressure to the same level as the HP tank. A new cycle can begin.

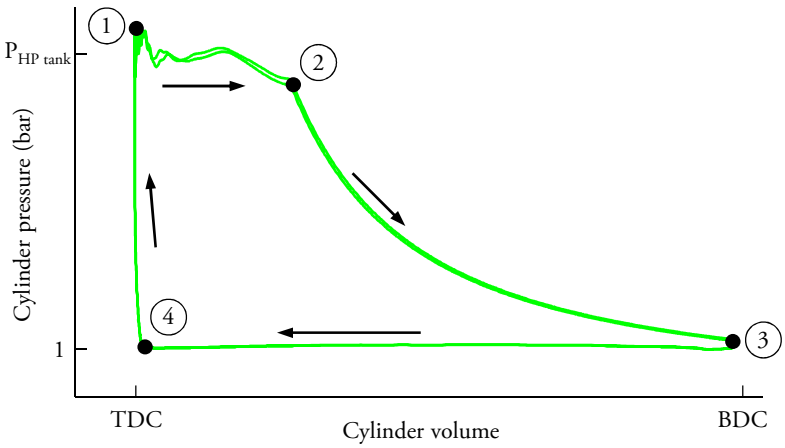

Figure 3.10: Pressure-volume diagram for the expansion cylinder.

3.2.4 Potential advantages & drawbacks

The advantage with the 2-4-2 DCEE layout compared to the 4-4 concept is that it enables independent selection of cylinder displacement for the compression and expansion cylinders. This enables an over-expanded cycle because the displacement of the compression and expansion cylinders determine the compression and expansion ratios respectively. Another advantage enabled with this layout is the possibility to design the compression and expansion cylinders with different thermal philosophies. In general it is desired that the compression process occurs as close to isothermal conditions as possible. This reduces the energy required to compress the ambient air. The expansion cylinder on the other hand should be insulated to preserve as much heat as possible for the expansion process. The expansion work output increases since the mean pressure during the expansion process becomes higher when less heat is lost. A potential problem could be the constant thermal load on the expansion cylinder. In a conventional engine the alternating hot and cool cycles maintain the temperature at manageable levels. But with the expansion cylinder being only exposed to hot exhaust gases the thermal load can be a potential challenge to overcome.

The issues of limited valve area and choked flows in the 4-4 concept is also reduced. Each cylinder head in the 2-4-2 layout only needs to handle 2 different flows, while the cylinder head in the LP cylinder of the 4-4 concept has to handle 4 different flows. The effective valve area is therefore doubled and lower flow loss over the valves is expected.

A possible drawback with the DCEE concept compared to the conventional four-stroke cycle is the potential increased flow losses because of the increased number of gas exchange events. The gas is inducted multiple times in the DCEE cycle (only once in a conventional four-stroke cycle). Another possible drawback is the additional spatial volume required compared to a conventional engine concept. The LP, compression and expansion cylinders are expected to output much lower mean effective pressures compared to the conventional four-stroke cycle. Clever engine architecture can be a solution to be able to maintain a competitive power density.

Chapter 4

Experimental engine rig

The experiments were performed on a heavy duty Volvo D13 compression-ignition engine. Main modifications are the conversion into single cylinder operation with combustion only in cylinder 6, reduced compression ratio to 11.5:1 and the removal of the original turbocharger. Engine motoring and braking is enabled by connecting the engine crankshaft to an ABB M3BP-355SMC-4 electric motor. Figure 4.1 presents a schematic layout of the engine rig while Table 4.1 provides the engine specifications.

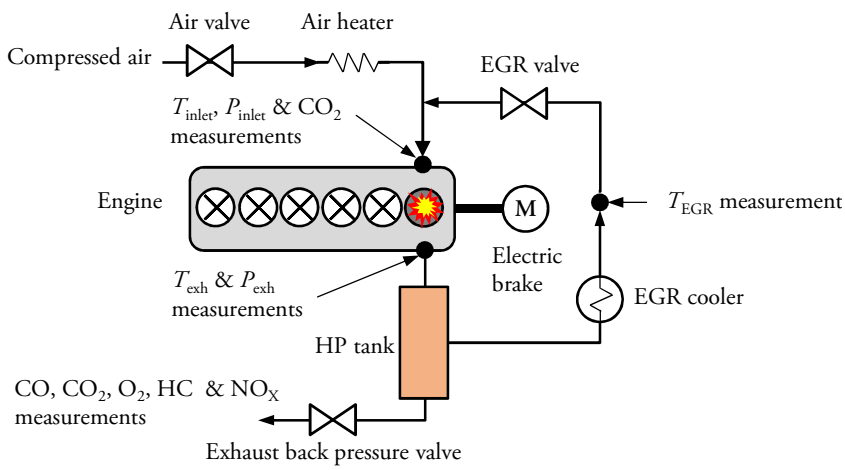

Figure 4.1: Layout of the test rig. Note the locations for temperature, pressure and emissions measurements.

Table 4.1: Data over the experimental test rig.

Engine parameter	Value
Bore x stroke	131 x 158 mm
Displacement	2.13 dm^3
Connecting rod length	265 mm
Compression ratio	11.5:1
Fuel type, lower heating value (Q_{LHV})	Diesel, 43.15 MJ/kg
Fuel system	Common rail, direct injection
Inlet valve opening timing	-45 °CA $aTDC_{GE}$
Inlet valve closing timing	236 °CA $aTDC_{GE}$
Exhaust valve opening timing	-236 °CA $aTDC_{GE}$
Exhaust valve closing timing	21 °CA $aTDC_{GE}$

Fuel injection system

The experimental engine is equipped with a common-rail direct injection fuel system. Common-rail pressure is built up by a fuel plunger located inside the injector. Camshaft lobes push the plunger which pushes fuel into the rail. An outlet meter valve controls the amount of fuel transferred into the common-rail which determines the common-rail pressure. Data for the fuel injector is presented in Table 4.2.

Table 4.2: Data for the fuel injector used in the experimental test rig.

Fuel injector data	Value
Number of holes	7
Umbrella spray angle	145°
Nozzle flow number	3 L/min

Gas exchange system

Because the engine is converted into single cylinder operation the original turbocharger could not be used. Instead, compressed air is provided from an external compressor. An electric air valve is used to control the engine's inlet manifold pressure. Three parallel mounted Leister heaters with a power of 15 kW each heat the inlet air.

The exhaust manifold has a built in tank with a volume of 30 dm^3. The intention is to simulate the HP tank in the DCEE 2-4-2 concept. Exhaust back pressure ($P_{exhaust}$) is controlled with a poppet valve. The engine uses a high pressure EGR-system where the inert gas is fed from the HP tank into the inlet manifold again. An EGR cooler and valve are used to cool and control the EGR_{rate} (definition in section 4.3.3).

4.1 Measurement equipment

A set of pressure sensors, thermocouples and other measurement equipment are used to monitor the engine. This equipment is split into a low frequency system and a high frequency system which are described in the following subsections.

4.1.1 Low frequency data

Temperatures in the inlet manifold, exhaust manifold, after the EGR-cooler and coolant exit were measured with type K thermocouples (exact locations are presented in Figure 4.1). These thermocouples are specified to have a largest error of either ± 1.5 or $0.004 \cdot |T|$ (temperatures in Celsius). Inlet manifold and exhaust back pressures were measured with Keller PAA-23SY with a pressure range of 0-20 bar. An AVL AMAi60-emissions system measures the molar concentrations of CO, CO_2, O_2, UHC and after the back pressure valve. Also the CO_2 concentration in the inlet manifold was measured to determine the EGR_{rate}. The AVL AMAi60-system was calibrated with zero and span gases every day engine experiments were conducted.

A scale is used to determine the fuel flow. The scale measures the remaining fuel in a container with a temporal resolution of 0.2 seconds. For every engine operating point fuel measurement over 60 seconds are recorded when stationary conditions have been reached. The fuel flow is then calculated with a linear regression model.

4.1.2 High frequency data

A Leine-Linde encoder monitors the crankshaft's angular position and speed, with a resolution of 0.2 °CA. It also provides two TDC signals which enables a separation of gas exchange and combustion TDC. An analog 0-5 V sensor monitors the fuel rail pressure. In-cylinder pressure is measured with a Kistler 7061-C piezo-electric pressure transducer. The pressure is sampled with the same frequency as the crank angle encoder. A current clamp connected to the injector power cable records the injector needle lift signal.

4.2 Data acquisition and engine control system

The engine control and data acquisition system consists of a "target" and a "host" computer. National Instruments LabVIEW real-time module and a PCIe-7842R FPGA card is installed on the target computer. This setup enables collection of high frequency data (crank angle resolved) but also provides engine control. Engine control signals input

into the host computer are received by the target computer and sent to the relevant actuators. The low frequency signals are collected with an Agilent 34972A logger. This data is then saved in the host computer. The fuel injection settings and common rail pressure is controlled by National Instruments FPGA and Drivven DI modules. A well tuned PI-controller maintains a set common rail pressure. A feed-forward loop with a PID-controller regulates power to the air heater to maintain a desired set inlet temperature (T_{inlet}). Inlet pressure (P_{inlet}), exhaust back pressure ($P_{exhaust}$) and EGR-valve position is set manually. Figure 4.2 presents the data acquisition and control system layout.

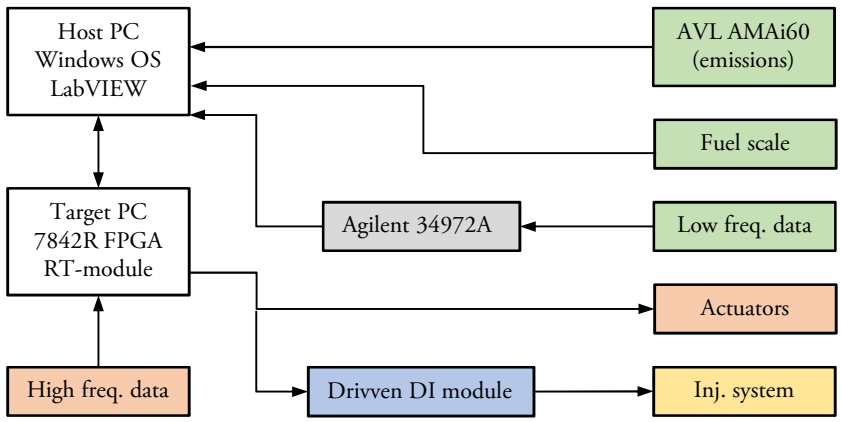

Figure 4.2: Overview of the data acquisition and engine control system.

4.3 Post processing of experimental data

For each operating point, pressure data for 300 engine cycles are recorded and saved. An average pressure trace is calculated from these cycles. The in-cylinder piezo-electric sensor provides an excellent linearity, but can only provide a relative pressure signal. A pegging process is required to obtain absolute pressure data. This was done by letting the in-cylinder pressure trace match the measured absolute pressure in the inlet manifold at the end of the inlet stroke (between 180 and 190 °CA bTDC$_{Fire}$).

During post processing a crank angle offset was introduced. The objective is to place the motored peak cylinder pressure at 0.5 °CA bTDC$_{Fire}$. This is also defined as the ”TDC-loss angle”, as presented in Figure 4.3. This value is important because the calculated mean effective pressures are very sensitive to the TDC-loss angle. From experience from other engine test rigs the selected value of 0.5 °CA bTDC$_{Fire}$ is a good estimation.

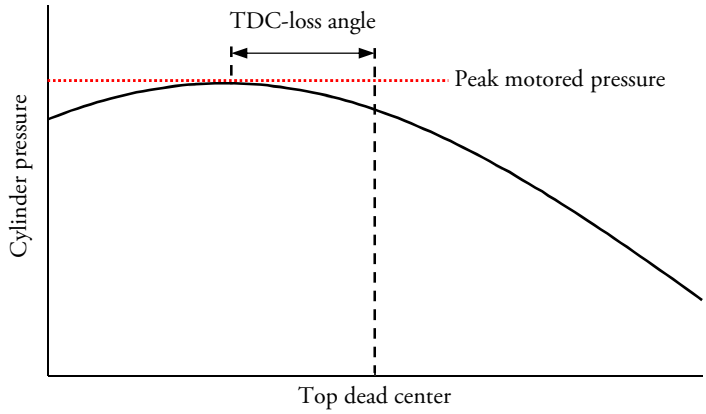

Figure 4.3: Definition of TDC-loss angle.

4.3.1 Heat release calculation

The heat release rate is derived from the measured and averaged cylinder pressure trace and the calculated volume trace with the following equation, derived in [38]:

$$\frac{\partial Q}{\partial \theta} = \frac{\gamma}{\gamma - 1} P \frac{\partial V}{\partial \theta} + \frac{V}{\gamma - 1} V \frac{\partial P}{\partial \theta} \tag{4.1}$$

where Q is the released heat energy, γ is the specific heat ratio c_p/c_v, P is the pressure and V is the volume. A constant γ-value of 1.33 was used in the calculations. Since the main focus of this analysis is on the thermodynamic cycle and not the combustion process it was determined that a apparent heat release calculation is good enough. Determining the actual heat release rate requires estimation of heat loss which is a more time consuming process.

4.3.2 Determination of air/fuel-ratio

The λ-value is defined as:

$$\lambda = \frac{(A/F)_{actual}}{(A/F)_{stoichiometric}} \tag{4.2}$$

where $(A/F)_{actual}$ is the actual air-to-fuel-ratio while $(A/F)_{stoichiometric}$ is the air-to-fuel ratio for a stoichiometric mixture.

λ-value was calculated based on the measured exhaust composition and the equations (4.67) and (4.68) provided from [38].

4.3.3 EGR

The EGR_{rate} is defined as:

$$EGR_{rate} = \frac{xCO_2^{inlet}}{xCO_2^{exhaust}} \tag{4.3}$$

where xCO_2^{inlet} is the measured inlet molar fraction and xCO_2^{inlet} is the exhaust molar fraction.

4.4 Definitions and calculations of mean effective pressure and efficiency

The energy conversion process from the fuel's chemical energy into mechanical work output is presented by the Sankey-diagram in Figure 4.4. The different energies are divided by the cylinder displacement and therefore become mean effective pressure, *MEP*.

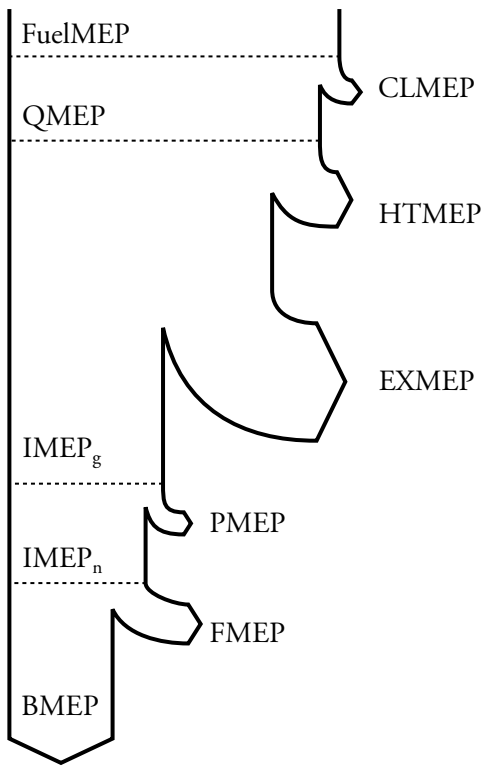

Figure 4.4: Sankey-diagram presenting the process of converting fuel energy into engine brake work.

FuelMEP is defined as:

$$FuelMEP = \frac{m_f \cdot Q_{LHV}}{V_d} \tag{4.4}$$

where m_f is the injected fuel mass, Q_{LHV} is the fuel's lower heating value and V_d is the cylinder displacement. The combustion process converts the fuel into heat energy, *QMEP*. It is defined as:

$$QMEP = \frac{Q}{V_D} \tag{4.5}$$

where Q is the total heat energy released.

Gross indicated mean effective pressure ($IMEP_g$) is defined as:

$$IMEP_g = \int_{-180}^{180} PdV \tag{4.6}$$

and the net indicated mean effective pressure ($IMEP_n$) is defined as:

$$IMEP_n = \oint PdV \tag{4.7}$$

The overall brake work is expressed as brake mean effective pressure, *BMEP*:

$$BMEP = \frac{W_b}{V_d} \tag{4.8}$$

where W_b is the brake work.

Combustion loss (*CLMEP*) during the combustion process is defined as:

$$CLMEP = FuelMEP - QMEP \tag{4.9}$$

Heat transfer loss (*HTMEP*) is defined as:

$$HTMEP = \frac{Q_{ht}}{V_d} \tag{4.10}$$

where Q_{ht} is the heat transfer loss during the cycle.

Exhaust loss (*EXMEP*) is defined as:

$$EXMEP = \frac{Q_{exh}}{V_d} \tag{4.11}$$

where Q_{exh} is the exhaust loss.

Pumping loss (*PMEP*) is defined as:

$$PMEP = IMEP_g - IMEP_n \tag{4.12}$$

Friction loss (*FMEP*) is defined as:

$$FMEP = IMEP_n - BMEP \tag{4.13}$$

Part efficiencies

The four part efficiencies are defined with the following equations.

Combustion efficiency (η_C):

$$\eta_C = \frac{QMEP}{FuelMEP} = 1 - \frac{CLMEP}{FuelMEP} \tag{4.14}$$

Thermodynamic efficiency (η_T):

$$\eta_T = \frac{IMEP_g}{QMEP} = 1 - \frac{HTMEP + EXMEP}{QMEP} \tag{4.15}$$

Gas exchange efficiency (η_{GE}):

$$\eta_{GE} = \frac{IMEP_n}{IMEP_g} = 1 - \frac{PMEP}{IMEP_g} \tag{4.16}$$

Mechanical efficiency (η_M):

$$\eta_M = \frac{BMEP}{IMEP_n} = 1 - \frac{FMEP}{IMEP_n} \tag{4.17}$$

And the overall engine efficiency is defined as brake efficiency (η_B):

$$\eta_B = \eta_C \times \eta_T \times \eta_{GE} \times \eta_M = \frac{BMEP}{FuelMEP} \tag{4.18}$$

Chapter 5

DCEE 4-4 concept studies

The first DCEE concept to be studied is the 4-4 version, originally presented in Paper I and Paper II. These studies were performed when no experimental test rig was available and therefore consist of only simulation studies. The focus of these studies is to determine how the proposed DCEE 4-4 version performs efficiency-wise both with a conventional combustion concept and a more advanced combustion concept. Different load control strategies and the charge air cooler's impact on engine efficiency are also evaluated.

5.1 Simulation model

GT-power [39] was used to model the proposed DCEE 4-4 version. The model consists of a LP cylinder and a HP cylinder, presented in Figure 5.1. A LP tank with a volume of 30 dm^3 is located in the flow path from the LP cylinder to the HP cylinder. A cross over channel connects the exhaust side of the HP cylinder back to the LP cylinder. This channel was modeled as a cylindric pipe with a diameter of 45 mm and a length of 100 mm, which corresponds to a volume of 0.16 dm^3.

In-cylinder heat transfer loss was modeled with the WoschniGT model. A heat convection multiplier value of 1.0 was set for the LP cylinder. The heat convection multiplier in the HP cylinder is set depending on which combustion concept is assumed. This will be described further in Section 5.2. A solver is used to estimate the wall temperatures, which improves the heat transfer loss estimations.

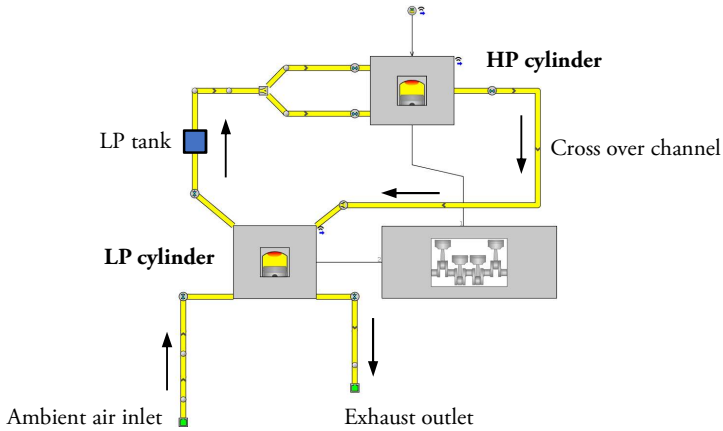

Figure 5.1: 4-4 simulation model.

Usually, the Chen-Flynn model [40] is used to estimate the *FMEP* which is calculated according to:

$$FMEP = FMEP_{const} + A \cdot PCP + B \cdot c_{p,m} + C \cdot c_{p,m}^2 \tag{5.1}$$

where $FMEP_{const}$ is the constant part of *FMEP*, A is the coefficient for peak cylinder pressure, B is the coefficient for mean piston speed, C is the coefficient for mean piston speed squared, $c_{p,m}$ is the mean piston speed and *PCP* is the peak cylinder pressure. The coefficients are selected based on experimental data. However, there is only data for cylinders with combustion and relatively high in-cylinder pressure. The LP cylinder operates at much lower peak pressures. In the simulations the highest peak pressure reached in the LP cylinder was 35 bar, which is an order of magnitude lower than the peak pressure obtained in the HP cylinder. For lower engine load cases the LP cylinder peak cylinder pressure could be as low as 15 bar.

However, some examples of *FMEP*-values in contemporary engines were found in the literature. An example is a naturally aspirated spark-ignition engine that has a motored *FMEP*-value of 0.28 bar at a mean piston speed of 5.8 m/s [41]. The peak cylinder pressure was not mentioned but it is assumed to be 80-100 bar. It can be compared to a force inducted engine where the reported peak pressure is 115 bar and a *FMEP* of 0.48 bar at similar mean piston speed (motored) [42]. For a medium duty compression-ignition engine the *FMEP* is reported to be 0.85 bar at comparable mean piston speeds and motored conditions [43]. *FMEP* increases to 1.25 bar at full load at the same engine speed. No peak cylinder pressure was reported, but it is assumed that the peak pressure is around 200 bar which is the general capability for contemporary heavy duty engines [44]. The mentioned engines and their respective *FMEP* are presented in Figure 5.2.

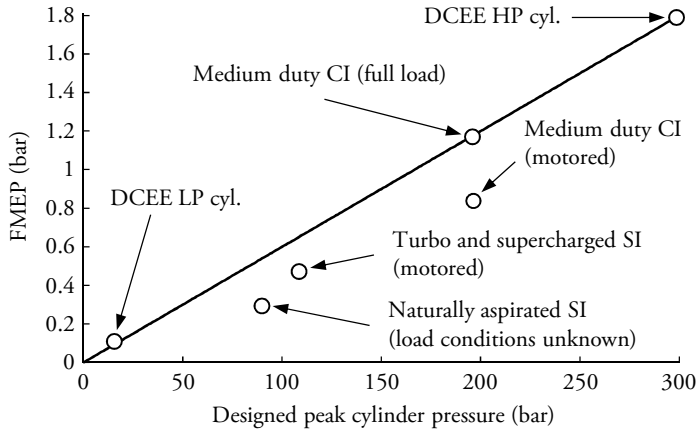

Figure 5.2: The *FMEP* model used in the simulations. *FMEP* values for different engines found in the literature are presented [41, 42, 43].

Since there is a trend relating *FMEP* with the peak cylinder pressure a more simplistic *FMEP*-model estimation was used. It assumes that the *FMEP* relates to the peak cylinder pressure by:

$$FMEP(bar) = PCP(bar) \cdot \frac{1.2}{200} \tag{5.2}$$

5.2 Simulation procedure

The simulation procedure is presented in two parts. The first part covers a study where two different combustion modes are evaluated. The second part presents studies of load control strategies for the proposed DCEE concept. Two different load control strategies and the impact from charge air cooling on engine efficiency are also evaluated.

5.2.1 Study of different combustion modes

Two combustion modes with the 4-4 concept are studied in this simulation. The first case assumes that the conventional compression-ignition concept is used with a low dilution case. This means that a high fuel quantity is injected and the air/fuel-ratio is low (λ = 1.2 and no EGR). The temperature during the combustion process becomes very high due to the low dilution. A charge air cooler located between the LP cylinder and the LP tank reduces the compressed air temperature to 350 K. This will decrease the bulk gas temperature during the combustion process and is expected to aid thermodynamic efficiency.

The second simulation case assumes a low temperature combustion (LTC) mode is used. Previous research studies of these combustion concepts suggest that the heat transfer loss is considerably reduced compared to the conventional combustion concept [14, 17, 18]. This was considered in the model by setting the heat transfer coefficient to 0.5 in the HP cylinder (1.0 in the conventional combustion case). However, this combustion concept requires highly diluted operation with either a high EGR_{rate} or lean operation. A typical combination used is a λ-value around 1.5 and 50 % EGR_{rate} according to [45].

Table 5.1: Engine geometry used for the simulation model.

Combustion mode	Conventional CI	LTC
λ	1.2	3.0
HP cylinder bore×stroke	95×100 mm	
HP cylinder displacement	0.71 dm^3	
HP cylinder CR	11.5:1	
LP cylinder bore×stroke	317×100 mm	249×100 mm
LP cylinder displacement	7.9 dm^3	4.9 dm^3
LP cylinder CR	100:1	
EGR_{rate}	No EGR	
Charge air cooling temperature	350 K	No CAC
Convection multiplier HP cylinder	1.0	0.5
Convection multiplier LP cylinder	1.0	

Because of the high dilution rate the load capability decreases compared to the first simulation case. As will be explained in Chapter 7 the advantage of charge air cooling at low engine loads is outweighed by the drawback. Because of this no charge air cooling of the compressed air is modeled in this case.

The HP cylinder has a displacement of 0.71 dm^3 and a geometrical compression ratio of 11.5:1. The compression cylinder displacement was adjusted to reach a compression pressure of 250 bar in the HP cylinder. Table 5.1 presents the engine geometries along with other engine settings. The combustion was modeled with a Wiebe function and its parameters were adjusted to maintain a peak firing pressure of 300 bar.

5.2.2 Study of load control strategies

The main target of this study was to determine which load control strategy provides the highest efficiency. As a starting point the simulation model and geometry from the case with low temperature combustion (presented in Table 5.1) was used but with some modifications. For this simulation it was assumed that a conventional combustion mode was used throughout the load range. This means that the heat convection multiplier in the HP cylinder was set to 1.0 instead of 0.5. The engine speed was also increased slightly from 1900 rpm to 2000 rpm.

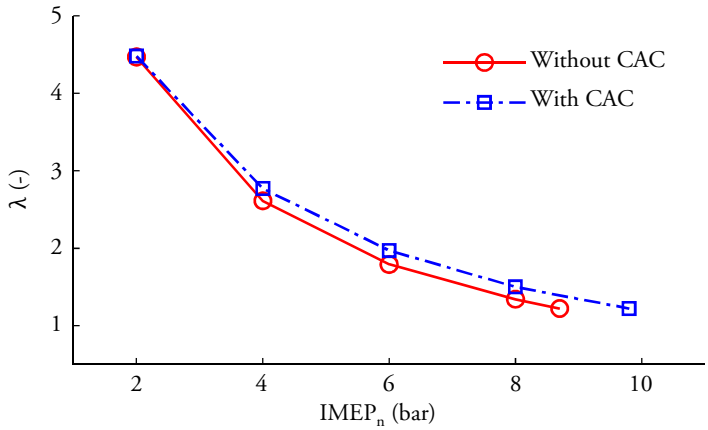

Figure 5.3: λ-value during the load sweep when only fuel injection quantity is changed.

Two engine load control strategies were studied. The first load control strategy is to only vary the injected fuel quantity. This means that the λ-value changes with load, as presented in Figure 5.3. The second load control strategy is to vary the air flow together with the fuel flow. The air flow is varied such that the λ-value is maintained constant regardless of engine load. By varying the closing timing of the LP cylinder's inlet valve (from ambient) the air flow into the engine can be controlled. Two strategies exist, early and late inlet valve closing. Both strategies reduces the effective swept volume during the inlet stroke. The main difference between the strategies is that the inducted gas becomes warmer with an early closing timing. Because of this drawback the late inlet valve closing strategy was selected to control load. The λ-value was maintained at 1.2 during the simulations.

The engine load levels evaluated are from 2 bar $IMEP_n$ and up until the load obtained with a λ-value of 1.2 (in 2 bar increments). The mean effective pressure for the entire 4-4 DCEE is defined as:

$$MEP_{engine} = \frac{MEP_{LP} \cdot V_{d,LP} + MEP_{HP} \cdot V_{d,HP}}{V_{d,engine}} \tag{5.3}$$

where MEP_{LP} and $V_{d,LP}$ is the mean effective pressure and cylinder displacement for the LP cylinder while MEP_{HP} and $V_{d,HP}$ represents the same values for the HP cylinder and $V_{d,engine}$ is the total engine displacement.

In the results part, the load control strategy where only fuel quantity is varied is labeled as the "Lambda" control case, because the λ-value depends on engine load. The case where a delayed LP cylinder inlet valve closing timing is used is refereed as the "Miller"-control strategy.

5.3 Results

The results from the studies of the proposed 4-4 DCEE concept are divided into two parts. The first part covers the results with different combustion modes while the second part presents the load control strategy results.

5.3.1 Conventional & low temperature combustion

A combination of high inlet pressure (8 bar), charge air cooling and low dilution (λ = 1.2 and no EGR) results in a extremely high *BMEP*-level in the HP cylinder with the conventional combustion mode. On the other hand, the obtained *BMEP*-level in the LP cylinder is much more modest. Because of the low *BMEP* obtained in the LP cylinder the overall *BMEP* is also quite modest. For the LTC case the high dilution requirement limits load capability. However, in comparison with contemporary four-stroke force inducted engines the obtained HP cylinder *BMEP*-level is relatively high, thanks to a high inlet pressure. The $IMEP_n$, *FMEP* and *BMEP* levels obtained from the simulations are presented in Table 5.2.

Table 5.2: Simulated mean effective pressures.

Combustion mode	Conventional CI	LTC
λ	1.2	3.0
LP cylinder $IMEP_n$	2.78 bar	0.33 bar
HP cylinder $IMEP_n$	76.3 bar	31.7 bar
Total engine $IMEP_n$	8.8 bar	4.3 bar
LP cylinder *FMEP*	0.21 bar	0.09 bar
HP cylinder *FMEP*	1.80 bar	1.80 bar
Total engine *FMEP*	0.34 bar	0.31 bar
LP cylinder *BMEP*	2.57 bar	0.23 bar
HP cylinder *BMEP*	74.5 bar	29.9 bar
Total engine *BMEP*	8.5 bar	4.0 bar

The resulting part efficiencies are presented in the Table 5.3. Both models achieve a high thermodynamic efficiency, thanks to a high overall expansion ratio (from 300 bar to 2 bar). Another possible contributor is the reduced wall surface area to volume-ratio in the HP cylinder due to low compression ratio (explained in the appendix). The case with low temperature combustion also has the benefit of reduced heat transfer loss, which results in the extremely high thermodynamic efficiency. Because of the higher load capability, the conventional combustion case has higher gas exchange and mechanical efficiencies since these relative losses decreases with load increase. Figure 5.4 presents the energy distribution for both the studied combustion cases.

Table 5.3: The resultant part and brake efficiencies from the simulations. Combustion efficiency was assumed to be 100 %.

Combustion mode	Conventional CI	LTC
λ	1.2	3.0
Thermodynamic efficiency	57.7 %	61.9 %
Gas exchange efficiency	98.2 %	97.5 %
Mechanical efficiency	96.1 %	92.8 %
Brake efficiency	54.5 %	56.0 %

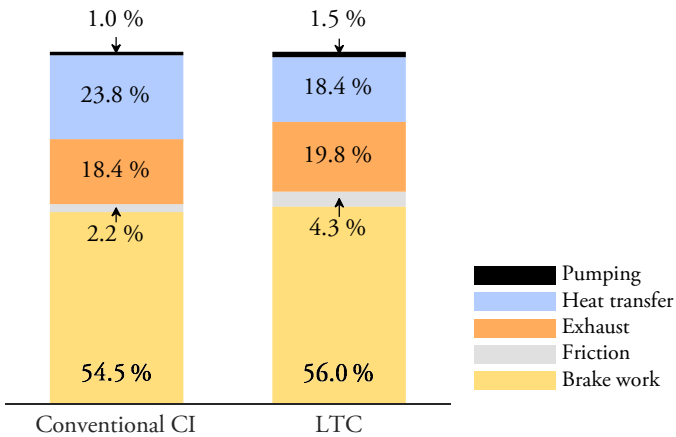

Figure 5.4: Energy distribution for the different combustion modes in the 4-4 concept.

5.3.2 Load control strategy

Figure 5.5 presents the thermodynamic efficiencies for the 4 different load control cases. A lambda controlled load strategy without charge air cooler is the most efficient strategy at low engine loads. As explained before the drawbacks with charge air cooling outweighs the advantages at low loads. The Miller load control strategy cases suffer from low dilution causing high temperature, specific heat capacity and heat transfer loss. At higher loads the advantages with charge air cooling become more apparent and from 8 bar $IMEP_n$ and above the model with charge air cooler has higher thermodynamic efficiency. Another advantage is the increased load capability because the mass flow of air increases with a charge air cooler.

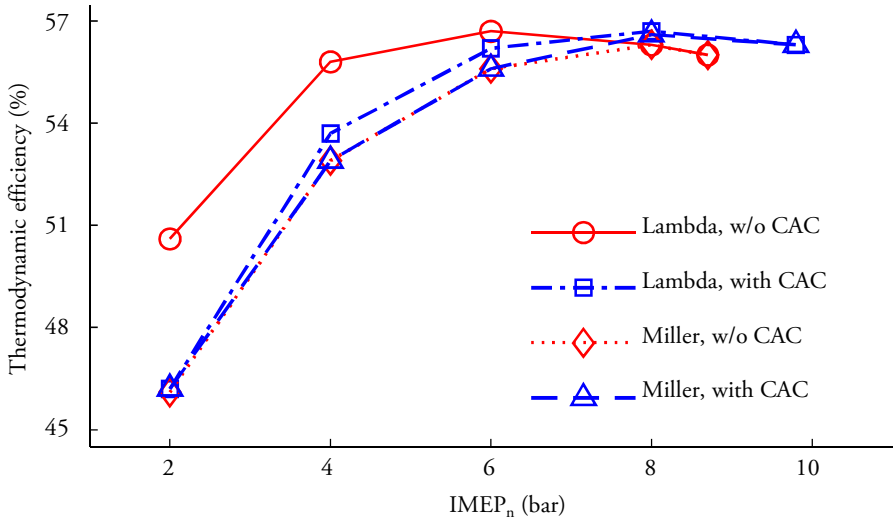

Figure 5.5: Thermodynamic efficiency comparison between different load control strategies over a load sweep.

The Miller load control strategy has a considerably higher mechanical efficiency at lower engine loads, as presented in Figure 5.6. The main reason is the reduced inlet pressure which also reduces peak cylinder pressures in both LP and HP cylinders. As the friction loss is assumed to be dependent on peak cylinder pressure (Equation (5.2)) the resulting friction loss also decreases. At higher engine loads the required air flow increases which also increases the peak cylinder pressure. This causes the mechanical efficiency to converge at higher engine loads.

Table 5.4: Comparison of brake efficiency between different load control strategies. The highest brake efficiency at each load level is indicated with green text font.

Control strategy / $IMEP_n$ (bar)	2.0	4.0	6.0	8.0	Max load
Lambda, without CAC	38.0 %	*48.1 %*	*51.3 %*	52.0 %	51.8 %
Lambda, with CAC	35.5 %	46.7 %	51.0 %	52.5 %	52.7 %
Miller, without CAC	39.1 %	47.8 %	50.9 %	52.1 %	51.8 %
Miller, with CAC	*39.2 %*	47.8 %	51.2 %	*52.7 %*	*52.7 %*
Best combination	*39.2 %*	*48.1 %*	*51.3 %*	*52.7 %*	*52.7 %*

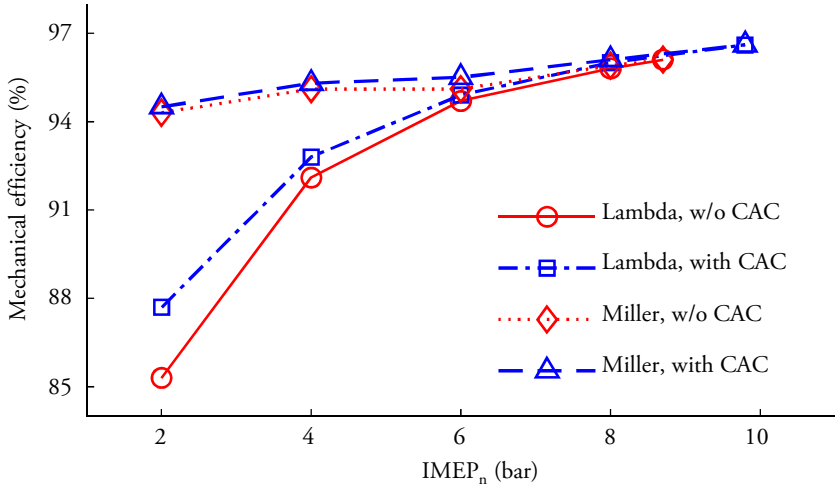

Figure 5.6: Mechanical efficiency comparison between different load control strategies over a load sweep.

The resulting brake efficiency for all load cases (Figure 5.7) becomes quite similar although major differences in thermodynamic and mechanical efficiency could be observed. The highest brake efficiency at low loads is obtained with a Miller control strategy, while at high loads intercooling should be used to maximize brake efficiency. Table 5.4 presents the optimal brake efficiency over a load range if different load control strategies are considered.

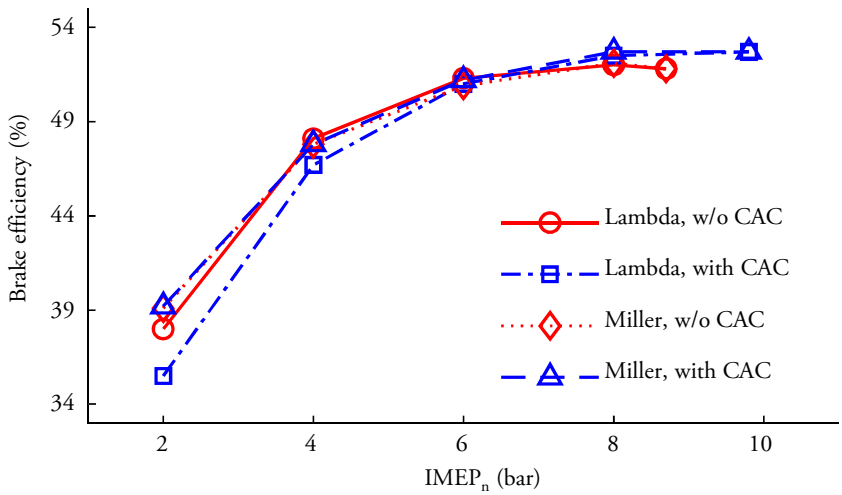

Figure 5.7: Brake efficiency comparison between different load control strategies over a load sweep.

5.4 DCEE 4-4 studies summary

A simulation study of the proposed 4-4 DCEE concept has been presented in this chapter. With the assumption of 8 bar inlet pressure, 300 bar peak cylinder pressure and low temperature combustion mode the brake efficiency can reach 56.0 %. With a conventional compression-ignition combustion concept the brake efficiency reached 54.5 %, with the advantage of a much higher load capability. This load case uses a charge air cooler to reduce the charge temperature which reduces the heat transfer loss and improves the gas properties. Since there is no requirement on high dilution the load capability of this concept is also much higher.

In a following study the focus was on the part load efficiency of the DCEE-concept. Two different load control strategies were evaluated. The first strategy (Lambda) only controls the fuel flow when the load is changed while the second strategy (Miller) also controls the air flow through late inlet valve closing timing. It was discovered that they had their respective advantages and drawbacks. The Lambda load control strategy has the higher thermodynamic efficiency, because of the higher dilution with this strategy. However, due to higher cylinder pressures the friction loss is higher which also reduces the mechanical efficiency. For the lowest evaluated engine load the brake efficiency becomes highest when the Lambda controlled strategy without charge air cooling is used. The charge air cooler deteriorates the efficiency at low load because of the reduction in expansion work. At mid- and high loads the advantages of charge air cooling become more apparent and improves the system brake efficiency.

It was also observed that the LP cylinder head became a source for gas exchange loss because it needs to handle 4 different gas flow paths. The effective valve flow area is only half of the one in a conventional four-stroke engine. Another drawback with this concept is that the compression and expansion stages takes place in the same cylinders, thereby providing no over-expansion. It also requires that the HP- and LP cylinders are synchronized to make the cycle work, eliminating the opportunity to use the phasing between the cylinders as a measure to balance the engine in terms of noise, vibration and harshness (NVH).

Chapter 6

Study of inlet temperature effects

The studies regarding inlet temperature effects on the thermodynamic efficiency are presented in this chapter and based on the study in Paper III. The motivation behind this study was to understand what advantages charge air cooling can provide for the DCEE concept. These studies are also useful for a conventional four-stroke engine. It is often reported that the thermodynamic efficiency improves with a lower inlet temperature [46, 47]. But most commonly it is explained with reduced heat transfer. However, there are other factors involved as well, such as the specific heat capacity of the working medium. The aim of this study is to determine how large the contribution of each of these factors are on the thermodynamic efficiency. The tools used for this study are both engine experiments and simulations in GT-power.

6.1 Theory

The gross indicated efficiency is determined by the combustion, heat transfer and exhaust losses. But the working medium and its properties also has an effect. This section will briefly explain the factors affecting the thermodynamic efficiency.

For a complete combustion case, the fuel and air are converted into carbon-dioxide (CO_2) and water (H_2O). However, in real combustion processes there are always losses due to incomplete combustion. UHC and CO are examples of species formed due to incomplete combustion. These species contain energy that was not released as thermal energy during the combustion process.

General heat transfer is modeled as:

$$\dot{q} = h_c(T_g - T_w) \tag{6.1}$$

where $\dot{q}$ is the heat flux, h_c is the heat transfer coefficient and $T_g - T_w$ is the temperature difference between the gas and the wall surface. If the temperature difference between the gas and the wall is kept low, the heat flux will decrease. By cooling the charge air the bulk gas temperature is reduced which also reduces the heat transfer loss.

The exhaust loss is defined as the residual heat energy escaping with the exhaust gases. This loss is largely determined by the effective expansion ratio, which is controlled by the geometrical expansion ratio and combustion phasing.

The specific heat capacities of a gas is defined as:

$$c_v = \left(\frac{\partial u}{\partial T}\right)_v \tag{6.2}$$

$$c_p = \left(\frac{\partial h}{\partial T}\right)_p \tag{6.3}$$

where c_v is the specific heat capacity at constant volume while c_p is the specific heat at constant pressure. For an ideal gas, c_p and c_v are related to each other as:

$$R_{spec} \equiv \frac{R_{universal}}{M} = c_p - c_v \tag{6.4}$$

where R_{spec} is the specific gas constant, $R_{universal}$ is the universal gas constant and M is the molar mass of the specific species.

The specific heat ratio (γ) is defined as:

$$\gamma = \frac{c_p}{c_v} \tag{6.5}$$

The values of c_p and c_v depend on temperature and pressure which is presented in Figure 6.1. At temperatures above 230 °C the specific heat capacities increase monotonically even at a pressure of 500 bar.

The specific heat capacity has an important effect on the engine cycle. For an idealized Otto cycle (isochoric heat addition) the pressure increase during the heat addition event can be expressed as:

$$\triangle P = \frac{R_{spec} \cdot Q_{in}}{V \cdot c_v} \tag{6.6}$$

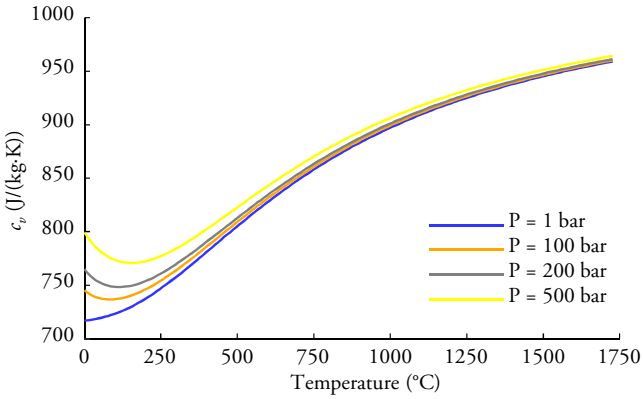

Figure 6.1: Specific heat capacity (c_v) as function of temperature and pressure for atmospheric air from [48].

where $\triangle P$ is the pressure increase over the heat addition process, Q_{in} is the heat energy added from the combustion process and V is the volume.

Equation (6.6) indicates that $\triangle P$ is inversely proportional to the specific heat capacity for an isochoric process, c_v:

$$\triangle P \propto \frac{1}{c_v} \tag{6.7}$$

This means that the pressure increase achieved during the heat addition process is larger when c_v is low. Figure 6.2 presents the impact of specific heat capacity on idealized engine cycles with isochoric heat addition. The case with low specific heat capacity achieves a higher compression pressure. But a more important observation is that the pressure increase from the heat addition process is higher with a low c_v value although a similar amount of heat was added. The higher pressure increase means that the expansion starts from a higher pressure and more expansion work is extracted from the cycle, resulting in a higher thermodynamic efficiency.

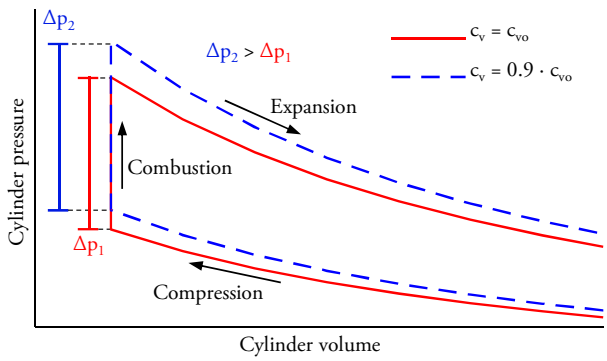

Figure 6.2: Specific heat capacity impacts on the pressure-volume diagrams for idealized engine cycles.

6.2 Experimental procedure

The engine experiments were conducted with 2 different fueling rates (expressed as *FuelMEP*). The fueling rate was changed through different injection durations, 700 µs for the low fueling cases (labeled as A cases) and 1170 µs for the high fueling cases (labeled as B cases). An injection pressure of 1500 bar and an injection timing of -5 °CA aTDC$_{Fire}$ were used in all cases.

Table 6.1: Engine settings for the different operating points.

Case	A1	A2	B1	B2
T_{inlet} (°C)	35	80	35	70
T_{inject} (µs)	700		1170	
FuelMEP (bar)	19.4		34.7	
P_{inlet} (bar)	3.0		3.0	
$P_{exhaust}$ (bar)	5.5		5.5	
P_{inject} (bar)	1500		1500	
SOI (°CA aTDC$_{Fire}$)	-5		-5	
EGR_{rate} (%)	39.5	40.1	45.9	45.8
Engine speed (rpm)	1200		1200	

For each of the fueling cases, two different inlet temperature settings were evaluated making it 4 operating points in total. Inlet pressure was kept at 3 bar while exhaust back pressure was kept at 5.5 bar. With low fueling rate the EGR_{rate} was 40 % and for the high fueling rate the EGR_{rate} was 46 %. The 4 different operating points are presented in Table 6.1.

6.3 Experimental results

The ignition delay is longer with lower inlet temperature as observed in the apparent rate of heat release plots (aRoHR) presented in Figure 6.3. The longer ignition delay allows the fuel and air to premix for a longer time prior to auto-ignition. This results in a faster heat release. The difference in heat release profile is very clear with the low fueling rate.

The peak cylinder pressure (presented in Figure 6.4) increases with low inlet temperature. A part of that is attributed to the higher compression pressure, but the pressure increase during the combustion process is a more significant contributor. Because the expansion process begins with a higher pressure the boundary work extracted from the expansion process is increased, hence $IMEP_g$ increases.

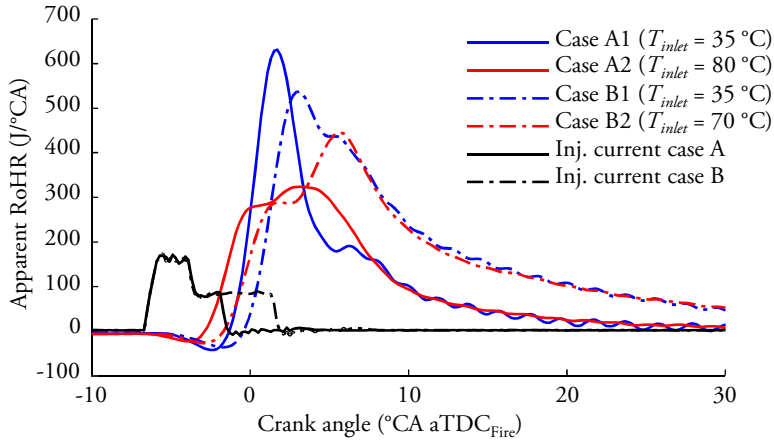

Figure 6.3: Rate of heat release rates between the 4 experimental cases.

With a low fueling rate (19.4 bar *FuelMEP*), $IMEP_g$ increases with 2.1 % when the inlet temperature is reduced by 45 °C. At the high fueling rate a 4.4 % increase in $IMEP_g$ is observed when inlet temperature is reduced by 35 °C. Details about the experimental results are presented in Table 6.2.

There are several possible effects that together contribute to the differences in cylinder pressure and work output as discussed in section 6.1. An example is the combustion efficiency which was very similar at the low fueling rate. At high fueling rate the combustion efficiency for high inlet temperature suffers from low oxygen availability due to lower gas density. However, the possible effects from heat transfer, gas properties and effective expansion ratio cannot be quantified with only the experimental data. A simulation tool is used to determine the impact from these parameters.

Table 6.2: Results from engine experiments.

Case	A1	A2	B1	B2
T_{inlet} (°C)	35	80	35	70
T_{inject} (µs)	700		1170	
Measured λ (-)	2.77	2.38	1.34	1.22
$IMEP_g$ (bar)	9.23	9.04	16.07	15.39
$IMEP_g$ increase compared to high inlet temp (bar)	+0.19	0	+0.68	0
Measured *FuelMEP* (bar)	19.4		34.7	
Combustion efficiency (%)	99.8	99.8	99.7	99.0
Thermodynamic efficiency (%)	47.7	46.7	46.5	44.9
GIE (%)	47.6	46.6	46.3	44.4
Relative *GIE* increase compared to high inlet temp (%)	+2.1	-	+4.4	-

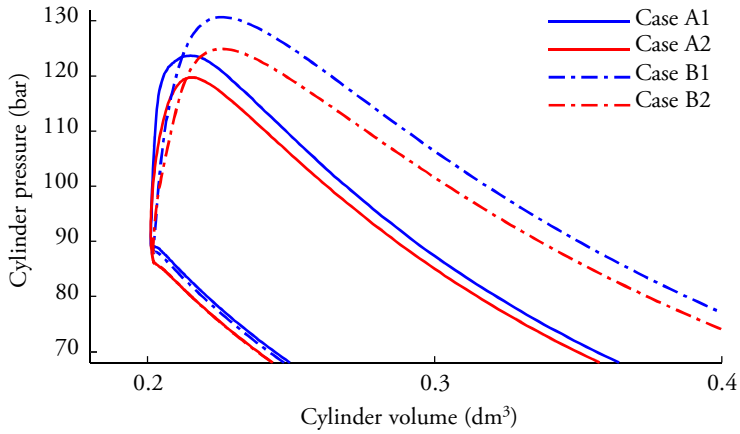

Figure 6.4: Pressure-volume diagram comparison for the different experimental cases.

6.4 Simulation model & procedure

To be able to quantify the effects of the different factors, a 1D-simulation model replicating the experimental test rig was created in GT-power [39]. Figure 6.5 presents the simulation layout. The simulation model was given the same geometry as the experimental test rig. One difference was that the compression ratio needed to be 11.7:1 instead of the experimental test rig's 11.5:1 to match the results. The model is calibrated against the four performed experimental cases A1, A2, B1 and B2. Table 6.3 presents the metrics considered important to match with the simulation model.

Table 6.3: Boundary conditions from engine experiments important to match for the simulation model.

Case	A1	A2	B1	B2
$T_{exhaust}$ (°C)	334	388	517	575
$IMEP_g$ (bar)	9.23	9.04	16.07	15.39
GIE (%)	47.6	46.6	46.3	44.4

Heat transfer was modeled with the WoschniGT model in conjunction with a wall temperature solver. The specific heat capacity of the working medium is calculated with NASA-NIST tables [49].

After the simulation model has been calibrated to the experimental cases, the high inlet temperature cases (A2 and B2) were the starting points of the simulation studies. The main target of these studies is to decouple the effects from specific heat capacity, rate of heat release profile and heat transfer.

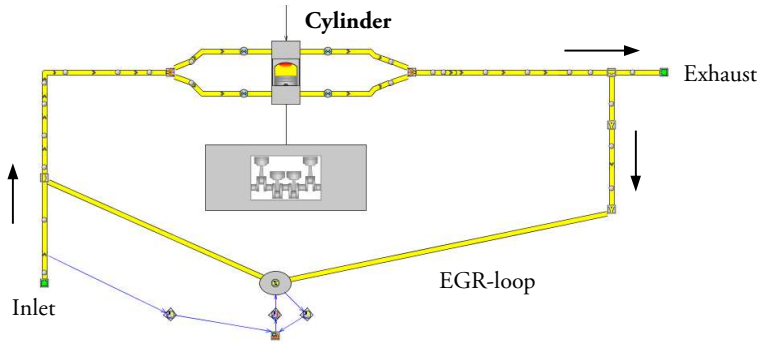

Figure 6.5: 1D-simulation model for the study of inlet temperature effects.

6.4.1 Simulation 1 — Contributions from specific heat capacity

Starting with the A2 and B2 cases, inlet temperature was reduced to 35 °C in this simulation. The reduction in temperature decreases the specific heat capacity as presented in Figure 6.1. But a secondary effect is also that the heat transfer is reduced due to lower bulk gas temperatures. In order to counter this the heat convective multiplier was increased to maintain the same heat rejection loss rate during the expansion stroke.

6.4.2 Simulation 2 — Contributions from rate of heat release profile

To determine the effects due to the change in heat release profile alone the rate of heat release profile was changed. The inlet temperature and the average heat transfer rate during the expansion were maintained.

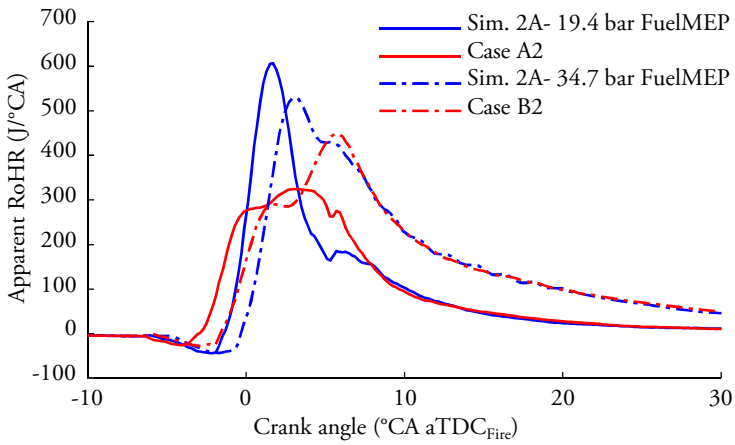

Figure 6.6: The RoHR-profiles used in the simulation 2 models compared to the experimental cases.

6.4.3 Simulation 3 — Contributions from heat transfer

The heat loss rate during the expansion stroke was adjusted to match the one obtained from the high inlet temperature case. Inlet temperature and rate of heat release profile were maintained.

Table 6.4 presents a summary over the simulation cases.

Table 6.4: Simulation cases studied. Letter "H" means that the setting from the high inlet temperature case (A2 or B2) was used while letter "L" means that the setting from the inlet temperature case (A1 or B1) was used.

Simulation case	Sim 1	Sim 2	Sim 3
T_{inlet}	**L**	H	H
RoHR-profile	H	**L**	H
Heat transfer	H	H	**L**

6.5 Simulation results

The results of the simulation studies are presented here and summarized in Figure 6.7.

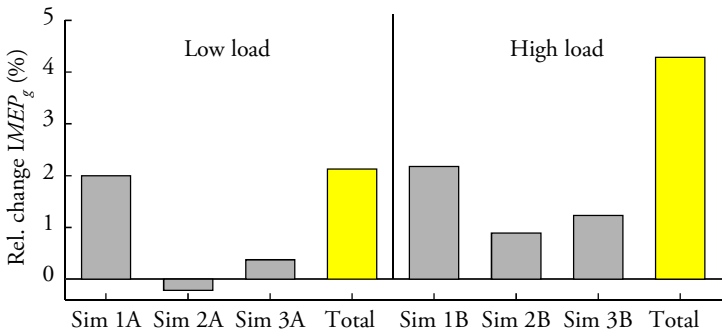

Figure 6.7: The relative change in $IMEP_g$ for the different simulation cases.

6.5.1 Simulation 1 results — Contributions from lower specific heat capacity

The reduced inlet temperature reduces the specific heat capacity as presented in Figure 6.8. As was discussed in the theory section, the pressure increase during the combustion process is greater with low values of c_v. This is visible in the PV-diagrams presented in Figure 6.9. The increase in pressure results in increased $IMEP_g$ values. The relative improvement in $IMEP_g$ and GIE is 2.0 % compared to case A2. It means that the decreased specific heat capacity contributes to almost 93 % of the overall change observed from

the engine experiments. At the higher fueling case $IMEP_g$ increased with 2.2 %, which is almost 51 % of the overall increase in $IMEP_g$ observed from the engine experiments. The detailed results are presented in Table 6.5.

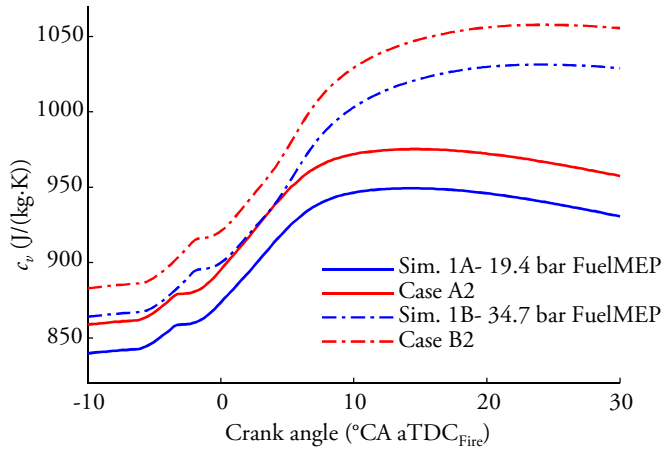

Figure 6.8: Specific heat capacity (c_v) during the combustion process from the simulations.

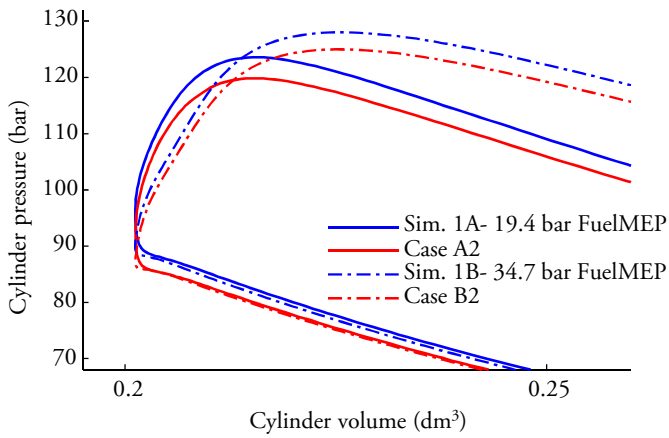

Figure 6.9: PV-diagram comparison simulation 1.

Table 6.5: Resulting change in work output and efficiency due to inlet temperature change with all other parameters kept constant.

Case	A2	Sim 1A	A1	B2	Sim 1B	B1
FuelMEP (bar)		19.4			34.7	
$IMEP_g$ (bar)	9.03	9.21	9.23	15.41	15.74	16.07
$IMEP_g$ change (bar)	-	+0.18	+0.19	-	+0.34	+0.66
GIE (%)	46.6	47.5	47.6	44.4	45.4	46.3
Rel. impro. *GIE* (%)	-	+2.0	+2.1	-	+2.2	+4.4
Fract. of total incr. (%)	-	92.9	-	-	50.7	-

6.5.2 Simulation 2 results — Contributions from rate of heat release profile

The effects of a change in rate of heat release (RoHR) profile is presented in Figure 6.10. The change in RoHR-profile contributes to very minor differences in $IMEP_g$. At low fueling rate the $IMEP_g$ decreases very slightly (0.2 %). At high fueling rate the $IMEP_g$ increases by 0.9 %, however it must be noted that the combustion efficiency is included in these numbers (0.7 % contribution). Deducting this effect the net contribution from the RoHR-profile remains at +0.2 %, which is quite small compared to the overall change of 4.4 %. The contribution to the overall change in $IMEP_g$ and *GIE* is -10 % for the low fueling case while it is 21 % for the high fueling case. Table 6.6 presents the detailed results.

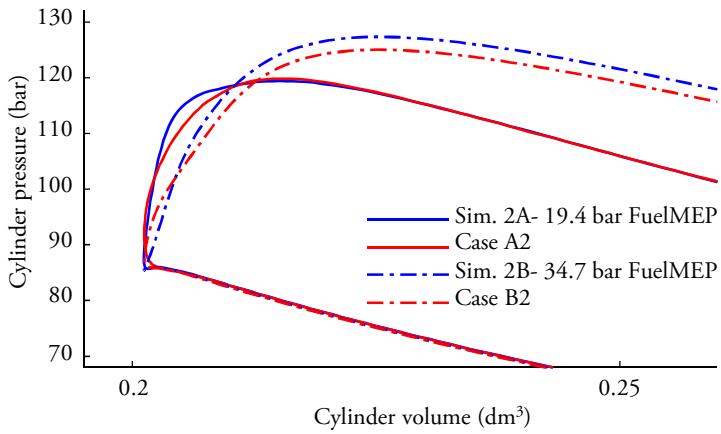

Figure 6.10: PV-diagram comparison from simulation 2.

Table 6.6: Resulting change in work output and efficiency due to change of heat release profile with all other parameters kept constant.

Case	A2	Sim 2A	A1	B2	Sim 2B	B1
FuelMEP (bar)		19.4			34.7	
$IMEP_g$ (bar)	9.03	9.01	9.23	15.41	15.54	16.07
$IMEP_g$ change (bar)	-	-0.02	+0.19	-	+0.14	+0.66
GIE (%)	46.6	46.5	47.6	44.4	44.8	46.3
Rel. impro. *GIE* (%)	-	-0.2	+2.1	-	+0.9	+4.4
Fract. of total incr. (%)	-	-10.1	-	-	20.6	-

6.5.3 Simulation 3 results — Contributions from heat transfer

At low fueling rate the decrease in average heat transfer rate during the expansion stroke was only 0.6 kW. The reduction in heat transfer rendered an increase in $IMEP_g$ of 0.04 bar, which is a relative increase of 0.4 %. The contribution to the overall increase is 17 %.

At high fueling rate the average heat transfer rate decreased by 4.4 kW. That caused $IMEP_g$ to improve by 0.19 bar, which is an improvement of 1.1 % and an contribution of 29 % to the overall improvement. The results are presented in Table 6.7

Table 6.7: Resulting change in work output and efficiency due to inlet temperature change with all other parameters kept constant.

Case	A2	Sim 3A	A1	B2	Sim 3B	B1
FuelMEP (bar)		19.4			34.7	
Average HTR expansion (kW)	25.4	24.8	24.8	31.1	26.7	26.7
$IMEP_g$ (bar)	9.03	9.07	9.23	15.41	15.60	16.07
$IMEP_g$ change (bar)	-	+0.04	+0.19	-	+0.19	+0.66
GIE (%)	46.6	46.8	47.6	44.4	44.9	46.3
Rel. impro. *GIE* (%)	-	0.4	+2.1	-	+1.2	+4.4
Fract. of total incr. (%)	-	17.2	-	-	28.7	-

6.6 Study of inlet temperature effects summary

This chapter has presented studies focused on the inlet temperature effects on the gross indicated efficiency. Significant improvements in gross indicated efficiency when the inlet temperature is reduced are observed from engine experiments, 2.1 % at low load (9 bar $IMEP_g$) and 4.4 % at high load (15 bar $IMEP_g$). There were observations of changes in combustion efficiency, heat release profile and combustion phasing. Moreover

it is expected that gas properties and heat transfer loss changed as well. But only the contribution from the combustion efficiency is possible to quantify of these effects.

To be able to quantify the possible effects a simulation model was created in GT-power which was calibrated to the experimental data. Three different simulations were performed where the contributions from gas properties, heat transfer and combustion phasing were evaluated. The results suggest that the largest contributor is the improved gas properties, enabling a higher pressure increase over the combustion process. The increased pressure leads to higher mean pressure during the expansion stroke which increases the expansion work output and efficiency. At low load this effect contributes with 2.0 % increase in $IMEP_g$, while the increase in $IMEP_g$ is 2.2 % at high load. Moreover, at high load additional effects from reduced heat transfer and improved combustion efficiency contribute to the 4.4 % increase in $IMEP_g$.

Chapter 7

DCEE 2-4-2 concept studies

This chapter presents the studies of the proposed 2-4-2 concept, originally presented in Paper IV. Engine experiments in conjunction with simulations tool were used to obtain full system efficiency results. The first part of the studies is with results replicating the ones achieved in the experimental rig. The second part explores pathways to improve the efficiency further.

It should be noted that for this and the following chapter are the mean effective pressures normalized with only the combustion cylinder's displacement. The purpose is to provide mean effective pressure values that is easy to compare to the conventional four-stroke cycle.

7.1 Experimental procedure

The experimental test rig was operated at 5 nominal fueling rates (*FuelMEP*) and 3 inlet pressure levels. A threshold on the λ-value (>1.2) was set to maintain a good combustion efficiency and avoid excessive soot emissions. The λ-limit means that high fueling rate with low inlet pressure could not be operated. The 15 potential cases became 10. Figure 7.1 visualizes the operating points while Table 7.1 describes them in detail.

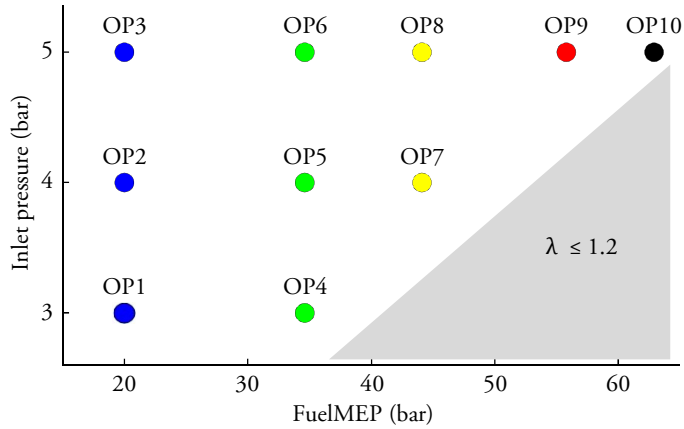

Figure 7.1: The 10 different operating points concerning fueling rate (*FuelMEP*) and inlet pressure. The gray triangle indicates areas where $\lambda \leq 1.2$ and hence not operated.

All operating points were conducted with an engine speed of 1200 rpm and inlet temperature of 70 °C. An EGR_{rate} around 40 % was maintained, intended to limit NO_x emissions. These emissions were kept below 5 g/kWh (gross indicated specific emissions). Start of injection (*SOI*) timing was adjusted so that neither the peak cylinder pressure nor the maximum pressure rise rate (MPRR) exceeded 210 bar and 12 bar/°CA respectively. Exhaust back pressure was kept around twice the inlet pressure. However, for the 5 bar inlet pressure cases the exhaust back pressure would have been 10 bar, which could cause issues. The thermal loads can potentially be too high for the exhaust valve and cause it to fail prematurely. Another potential problem is increased back flow of residual gas into the inlet manifold during the valve overlap period. The exhaust back pressure was therefore limited to 8 bar.

Table 7.1: Engine settings for the different operating points.

Operating point (OP)	1	2	3	4	5	6	7	8	9	10
P_{inlet} (bar)	3	4	5	3	4	5	4	5	5	5
Nom. *FuelMEP* (bar)		20			34			44	56	63
T_{inlet} (°C)		70			70			70	70	70
SOI (°CA aTDC$_{Fire}$)	-5	-4	-2	-5	-4	-2	-2	-2	-2	-1
CA_{50} (°CA aTDC$_{Fire}$)	4.7	5.1	6.7	9.3	8.7	9.3	11.5	9.7	10.7	13.3
T_{inj} (µs)		700			1170			1300	1500	1750
P_{inj} (bar)		1500			1500			1900	2200	2100
$P_{exhaust}$ (bar)	5.5	8.2	8.0	5.5	8.1	8.1	7.9	8.1	8.0	8.0
λ (-)	2.31	2.92	3.85	1.27	1.56	2.20	1.28	1.67	1.36	1.24
EGR_{rate} (%)	39	41	40	37	42	39	37	39	36	35
Engine speed (rpm)		1200			1200			1200	1200	1200

7.2 Simulation model & procedure

The experimental test rig can only evaluate the combustion cylinder part in the proposed DCEE 2-4-2 concept. To obtain brake efficiency estimations for the entire DCEE 2-4-2 system the obtained experimental data needs to be completed with simulation studies.

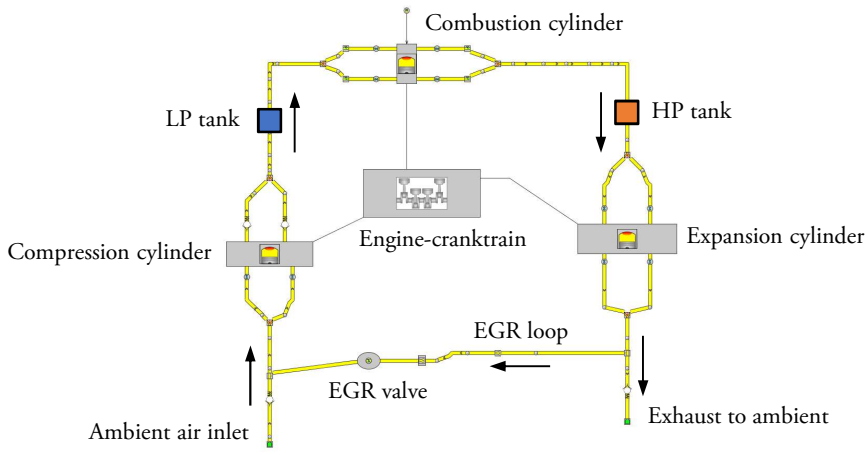

Figure 7.2: Simulation model of the proposed DCEE 2-4-2 concept. The intermediate tanks adjacent to the combustion cylinder are also presented.

The simulation model consists of a compression, a combustion and an expansion cylinder as presented in Figure 7.2. The LP and HP-tanks have been modeled with a volume of 32 dm^3. Upstream of the LP tank a charge air cooler is used to cool the compressed air to 70 °C. The model also uses a low pressure EGR-loop, where the exhaust gases downstream of the expansion cylinder is fed back into the inlet manifold of the compression cylinder. An option could be to use a high-pressure EGR-loop as used in the experimental test rig. But a major drawback is that the mass flow is directed away from the expansion cylinder, limiting its work output and engine efficiency. A back pressure of 1.09 bar for the expansion cylinder was used to enable the EGR-loop to function properly while the inlet ambient pressure was set to 1.00 bar.

Figure 7.3 presents the losses that have been considered in the simulations and are presented in the following sections.

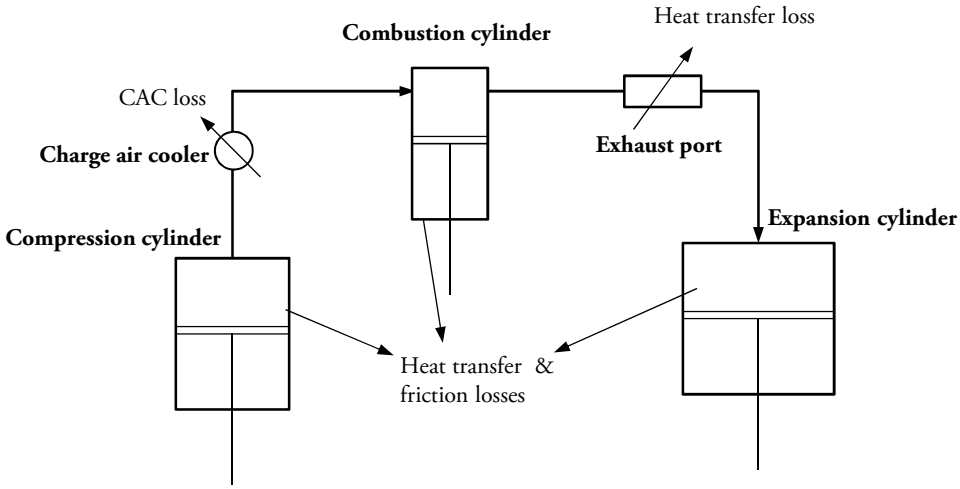

Figure 7.3: Simulation model of the proposed DCEE 2-4-2 concept. The intermediate tanks adjacent to the combustion cylinder are also presented.

7.2.1 Heat transfer modeling

The in-cylinder heat transfer was modeled with the WoschniGT model as described in [38]. The combustion and expansion cylinders applies a solver to calculate the wall temperature during the cycle. A fixed wall temperature for the compression cylinder was used to reduce simulation time. This is an acceptable approximation because the heat transfer in the compression cylinder is low anyway (exposed to only cold gas). The heat convection multiplier was set to 1.0 for the compression and expansion cylinders while the multiplier for the combustion cylinder was adjusted to match the metrics obtained from engine experiments.

The simulations also assumed that the HP tank and the piping are perfectly insulated and no heat is lost. Heat loss in the combustion cylinder's exhaust ports was modeled with a wall temperature solver and a heat transfer multiplier of 1.0 was selected. The heat lost in the charge air cooler has also been accounted for. The reduced gas temperature reduces heat loss and specific heat capacity, which will improve the thermodynamic efficiency. However, it also reduces the potential expansion work output from the expansion cylinder which also can deteriorate the overall cycle efficiency.

7.2.2 Friction model

The friction model used is the same as the one used in the simulation studies over the 4-4 model and presented in Figure 5.2 and Equation (5.2).

7.2.3 Simulation procedure

The first step in the procedure is to calibrate the model so that the boundary conditions obtained from the 10 experimental operating points are matched. Important metrics that needs to be matched are: $IMEP_g$, λ-value, inlet temperature, inlet pressure, exhaust temperature and exhaust back pressure. The metrics were matched by adjusting the heat transfer coefficient in the combustion cylinder and select appropriate compression and expansion cylinder displacements (described below).

The rate of heat release profiles obtained from the engine experiments were directly input into the simulation model (presented in Figure 7.6).

The geometry of the combustion cylinder is the same as the test rig but the compression and expansion cylinders vary with operating point. The compression cylinder displacement was selected to achieve the airflow and λ-value obtained from the experiments. Expansion cylinder displacement was selected to obtain an end of expansion pressure of 1.2 bar, as illustrated in Figure 7.4.

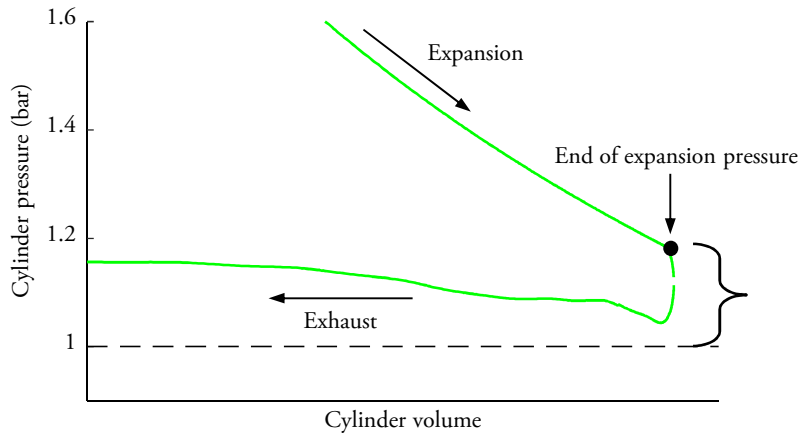

Figure 7.4: The expansion cylinder pressure at the end of 2^{nd} stage expansion.

Table 7.2 presents the cylinder displacements required for the different operating points.

Table 7.2: Cylinder displacements for the different operating points used in the simulations.

Operating point (OP)	1	2	3	4	5	6	7	8	9	10
Compression cyl. (dm^3)	2.4	3.2	4.2	2.4	3.1	4.1	3.0	4.0	4.1	3.9
Combustion cyl. (dm^3)		2.1			2.1			2.1	2.1	2.1
Expansion cyl. (dm^3)	3.0	3.2	3.8	4.0	4.2	4.7	4.2	5.2	6.0	6.3
Total displacement (dm^3)	7.5	8.5	10.0	8.5	9.3	10.9	9.3	11.4	12.2	12.4

It was also investigated how the heat loss in the combustion cylinder's exhaust ports affect the system efficiency. The calibrated simulation model was modified by turning off the heat loss in the exhaust ports of the combustion cylinder.

7.3 Experimental results

The obtained pressure traces for all 10 operating points are presented in Figure 7.5. As expected, the peak cylinder pressure increases with inlet pressure and engine load. The only exception is the operating point 10 where a slower combustion rate due to lower injection pressure reduces the peak cylinder pressure. This is confirmed in the apparent rate of heat release plots presented in Figure 7.6. The peak rate of heat release is lower compared to operating point 9 even though the fueling rate is higher. All the rate of heat release profiles in general resemble the conventional compression-ignition combustion.

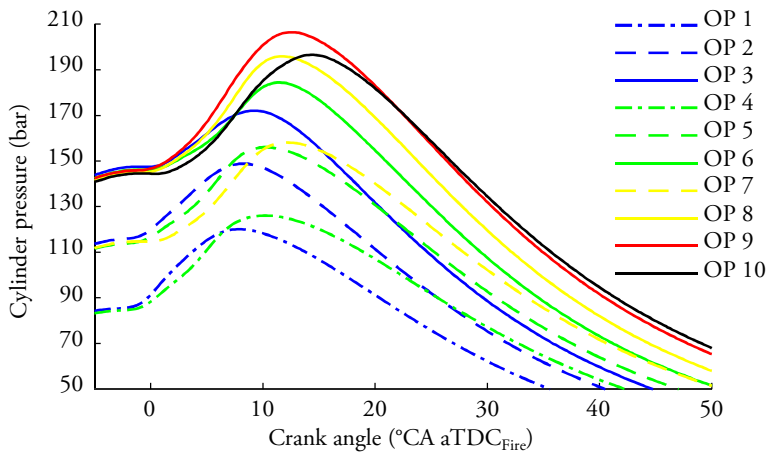

Figure 7.5: Pressure traces for the 10 experimental points. The pressure traces are averaged from 300 cycles and then filtered. Peak cylinder pressure was kept below 210 bar while the peak pressure rise rate is 12 bar/°CA.

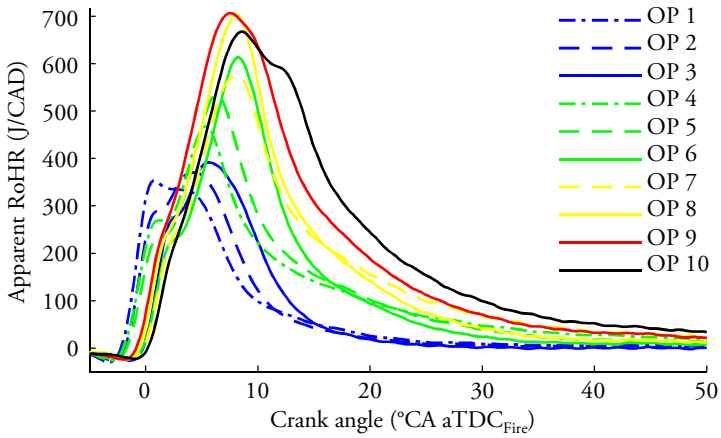

Figure 7.6: Apparent heat release rates for the 10 operating points.

A majority of the operating points achieved a combustion efficiency above 99.8 %. The cases where the combustion efficiency was lower had a λ-value below 1.3. Even though the combustion efficiency deteriorated it is still very high (99.1 % as worst). The resulting combustion efficiencies are presented in Figure 7.7.

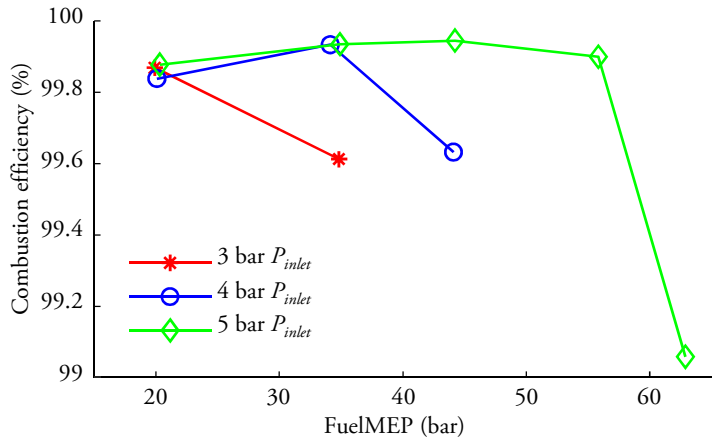

Figure 7.7: Calculated combustion efficiency based on measured emissions. Cases with η_C below 99.8 % are operated with $\lambda < 1.30$.

The resulting *GIE* are presented in Figure 7.8. The majority of the operating points achieves a *GIE* between 46.3 % and 47.6 %. The operating points with a *GIE* below 46 % have in common that the λ is below 1.3 and suffered from slightly worse combustion efficiency. Another explanation is that the overall dilution level is lower with these cases which could cause increased heat transfer loss and worse thermodynamic gas

properties. Moreover, the highest fueling operating point (OP 10) also suffers from later combustion phasing which reduces the effective expansion ratio and *GIE* decreases to below 44.0 %. The detailed results from the experiments are presented in Table 7.3.

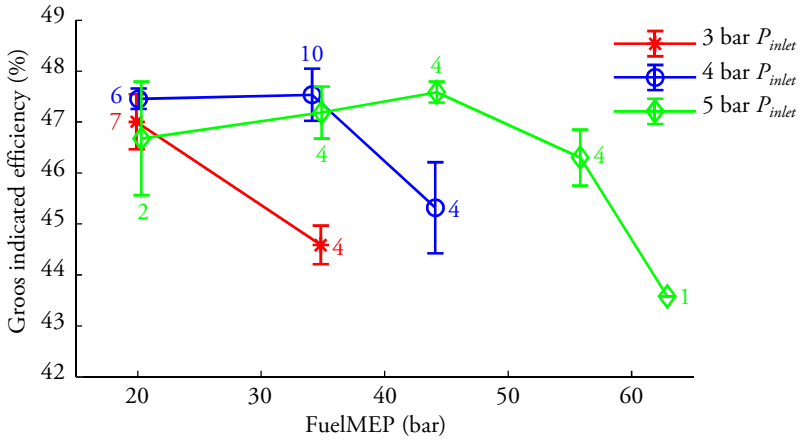

Figure 7.8: Gross indicated efficiency for the 10 operating points. The error bars indicates one standard deviation from the mean value and the adjacent number how many times the operating point was operated in total.

Table 7.3: Results from engine experiments.

Operating point (OP)	1	2	3	4	5	6	7	8	9	10
P_{inlet} (bar)	3.0	4.0	5.0	3.0	4.0	5.0	4.0	5.0	5.0	5.0
Nom. *FuelMEP* (bar)		20			34			44	56	63
Fuel flow, $\dot{m}_f$ (g/s)	0.98	0.99	1.00	1.72	1.68	1.72	2.18	2.18	2.76	3.10
Inj. fuel mass, (mg/cycle)	98	99	100	172	168	172	218	218	276	310
CA_{50} (°CA aTDC$_{Fire}$)	4.7	5.1	6.7	9.3	8.7	9.3	11.5	9.7	10.7	13.3
$T_{exhaust}$ (°C)	393	346	292	605	525	417	638	503	580	663
Measured *FuelMEP* (bar)	19.9	20.1	20.3	34.8	34.1	34.9	44.1	44.2	55.8	62.9
λ (-)	2.31	2.92	3.85	1.27	1.56	2.20	1.28	1.67	1.36	1.24
η_C (%)	99.9	99.8	99.9	99.6	99.9	99.9	99.6	99.9	99.9	99.1
$IMEP_g$ (bar)	9.4	9.5	9.5	15.5	16.2	16.5	20.0	21.0	25.9	27.4
$IMEP_n$ (bar)	6.5	4.8	5.8	12.7	11.7	12.6	15.5	17.0	22.1	23.3
GIE (%)	47.0	47.5	46.7	44.6	47.5	47.2	45.3	47.6	46.3	43.6

7.4 Simulation results

Figure 7.9 presents the obtained simulated system efficiencies for the 2-4-2 concept. The highest brake efficiency obtained is 51.0 % and is obtained at 56 bar *FuelMEP* and 5 bar inlet pressure (OP 9). At the highest load the *GIE* decreases by 2.6 percentage points,

which causes the system brake efficiency to decrease with 1.1 percentage points. The energy distribution for these two cases are presented in Figure 7.10.

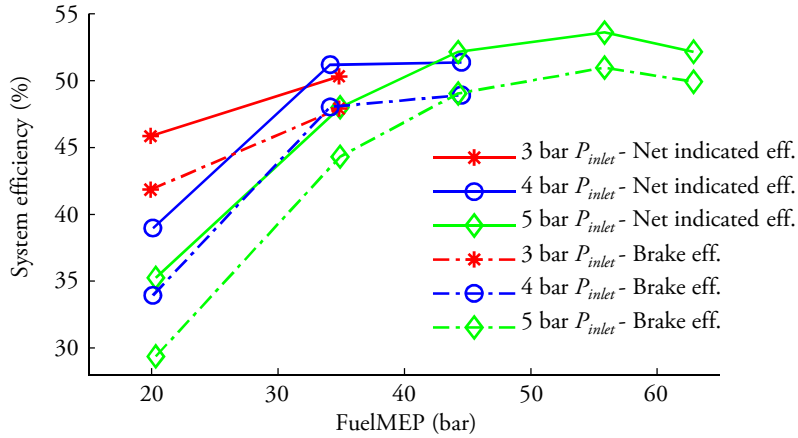

Figure 7.9: System net indicated efficiency and brake efficiency as function of fueling rate (*FuelMEP*) and combustion cylinder inlet pressure.

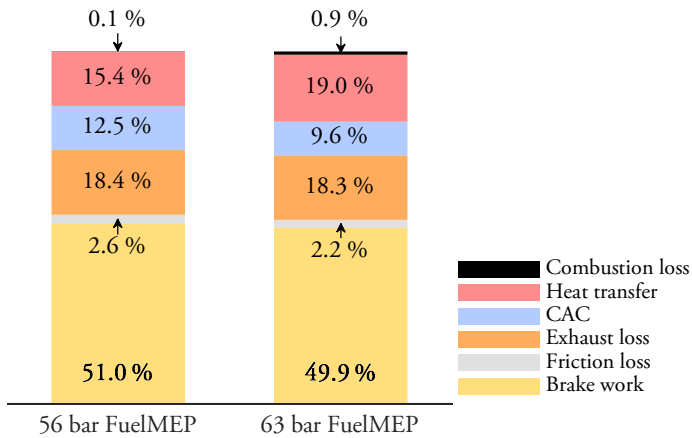

Figure 7.10: Energy distribution for operating points 9 (left) and 10 (right).

In general, the engine efficiency decreases with lower engine loads. The explanations are probably similar to the conventional four stroke engines where higher relative friction and gas exchange losses limit the system brake efficiency. The selection of combustion cylinder inlet pressure is also an important parameter. At lowest load (20 bar *FuelMEP*) the system brake efficiency can be either 41.8 % (3 bar inlet pressure) or 29.4 % (5 bar inlet pressure). The 5 bar inlet pressure case suffers from high losses in the charge air cooler. What happens is that a significant amount of energy is used to compress ambient

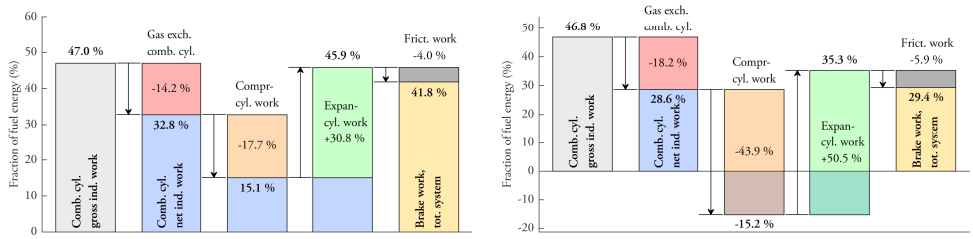

Figure 7.11: Work distribution comparison between 3 bar inlet pressure (left figure) and 5 bar inlet pressure (right figure) at *FuelMEP* = 20 bar.

air which increases its temperature and pressure. The warm compressed gas is then cooled in a charge air cooler which takes away its ability to perform expansion work. The severity of this loss increases with increased inlet pressure. The work and energy distribution comparisons are presented in Figure 7.11 and Figure 7.12 respectively.

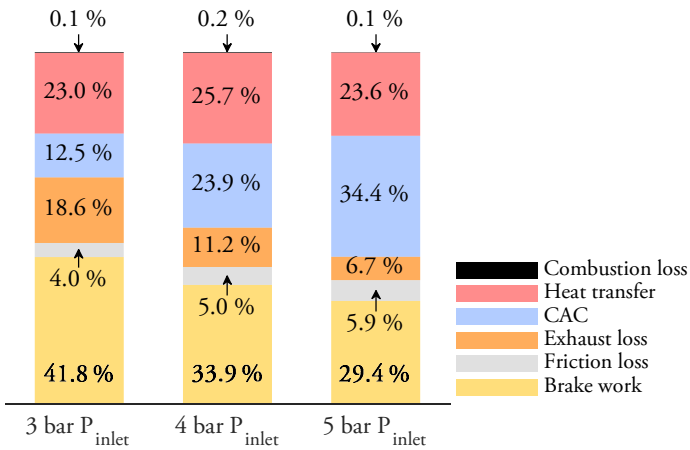

Figure 7.12: The energy distribution for the full DCEE system at nominal *FuelMEP* = 20 bar (OP1, OP2 and OP3).

The simulation results are presented in Table 7.4.

Table 7.4: System efficiency results.

Operating point (OP)	1	2	3	4	5	6	7	8	9	10
P_{inlet} (bar)	3.0	4.0	5.0	3.0	4.0	5.0	4.0	5.0	5.0	5.0
Nom. *FuelMEP* (bar)		20			34			44	56	63
Comb. cyl *GIE* (%)	47.0	47.5	46.7	44.6	47.5	47.2	45.3	47.6	46.3	43.6
System net ind. eff. (%)	45.8	38.9	35.3	50.3	51.2	48.0	51.4	52.2	53.6	52.2
System brake eff. (%)	41.8	33.9	29.4	47.9	48.0	44.3	48.9	49.1	51.0	49.9

With insulated exhaust ports the exhaust temperature increases, as presented in Figure 7.13. For example is the temperature increase 30 °C for operating point 9. The work output from the expansion cylinder increases which improves the overall system efficiency. A comparison of system net indicated efficiency with and without insulation in the exhaust ports is presented in Figure 7.14. The case with highest system brake efficiency (OP9) sees a efficiency improvement of 1.8 percentage points due to the decreased heat transfer loss. The work distribution is presented in Figure 7.15.

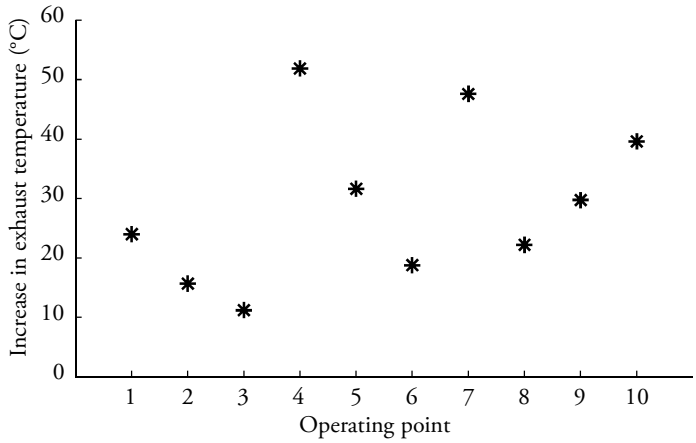

Figure 7.13: Combustion cylinder exhaust temperature increase due to insulated exhaust ports.

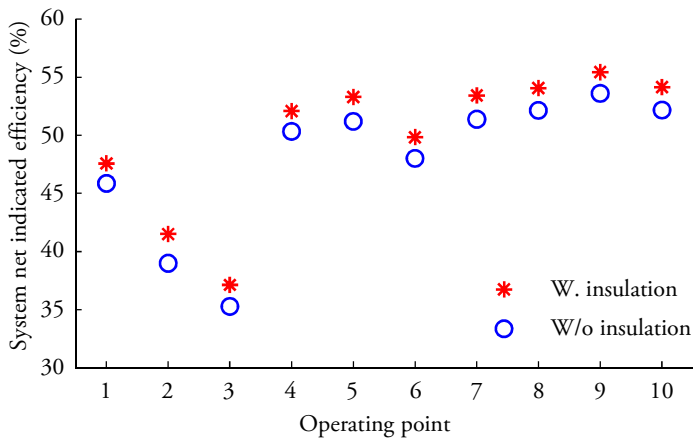

Figure 7.14: Comparison of system net indicated efficiency with and without exhaust port insulation.

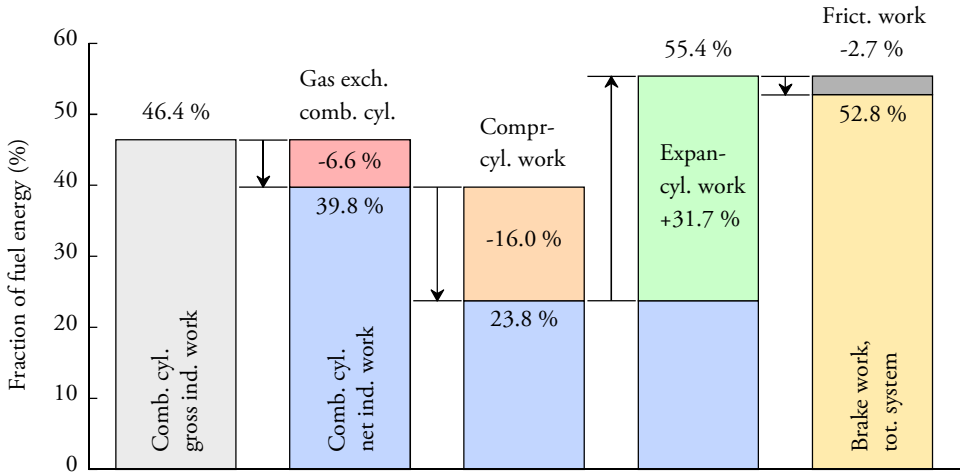

Figure 7.15: Work distribution for operating point 9 with insulated exhaust ports.

7.5 DCEE 2-4-2 concept studies summary

The study of the proposed DCEE 2-4-2 concept has been presented in this chapter. Compared to the 4-4 concept, this DCEE version has the advantages of reducing flow losses due to larger available valve area in the cylinder heads, providing over-expansion and enabling free selection of phasing between the cylinders.

These studies include both experimental and simulation studies. 10 different points were operated in the experimental engine, at 5 different fueling rates (20-63 bar *FuelMEP*) and 3 different inlet pressures (3-5 bar). Measured gross indicated efficiency is around 47 % for the majority of the operating points, but there were three operating points where this efficiency was 45.3 % or lower. They have in common that they were operated with λ-values below 1.30 with worse combustion efficiency. But the reduction in gross indicated efficiency can only partly explain the decreased efficiency. Higher heat and exhaust losses are also expected contributions but as mentioned in the previous chapter cannot be assessed with only experimental data.

To establish full DCEE system brake efficiency a simulation model in GT-power was created. The data obtained from the experiments were used as calibration data and boundary conditions in the simulation mode. The simulations suggest that at the lowest load point the operation with excessively high inlet pressure i devastating for system brake efficiency. At the lowest load (20 bar *FuelMEP*) the system brake efficiency is 41.8 % at an inlet pressure setting of 3 bar, while the system brake efficiency decreases to 29.4 % with 5 bar inlet pressure. The explanation is the increased energy dissipated in the charge

air cooler with a higher inlet pressure. The work consumed to compress the charge is lost while the advantages of high dilution are relatively small at this load point.

The highest system brake efficiency was achieved in operating point 9, operated at 56 bar *FuelMEP* and 5 bar combustion cylinder inlet pressure. A system brake efficiency of 51.0 % was achieved in this operating point. With the addition of insulated combustion cylinder exhaust ports the combustion cylinder's exhaust temperature increased by 30 °C. The higher temperature increases the work output from the expansion cylinder and the system brake efficiency increases to 52.8 %. This operating point became the reference point for the optimizing studies presented in the following chapter.

Chapter 8

Optimizing DCEE for higher efficiency

The simulations based on the experimental data of the DCEE 2-4-2 concept indicates that the highest system brake efficiency of 51.0 % can be achieved in operating point 9. Insulating the combustion cylinder's exhaust ports improved the system brake efficiency to 52.8 % in this particular operating point. This operating point became the baseline for further simulation studies aimed at improving the DCEE system brake efficiency. The 5 different areas that have been evaluated are:

1. Valve lift profile with reduced valve overlap.
2. Pressure level in the HP tank.
3. Cold compression cylinder walls.
4. Combustion cylinder inlet temperature.
5. Combustion phasing.

8.1 Camshaft with reduced valve overlap

The experimental test rig uses a camshaft that is designed for a conventional four-stroke cycle. To maximize the volumetric efficiency the period when both inlet and exhaust valves are open simultaneously (defined as the valve overlap) is relatively long. This period enables time for in- and outflows to occur when the piston is changing direction at

TDC_{GE}. Since an engine normally operates with inlet pressure and exhaust back pressure that are almost similar, there is no problem with back flow during the valve overlap period. But the DCEE concept operates with a much higher exhaust back pressure relative to the inlet pressure. It is therefore expected that back flow from the exhaust into the inlet manifold is happening during the gas exchange process when both the inlet and exhaust valves are open.

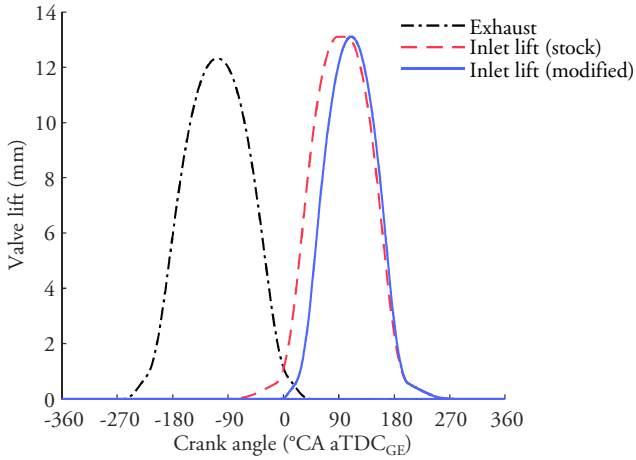

Figure 8.1: Comparison of the original inlet valve lift profile to the modified with later inlet valve opening.

To reduce the back flow, a camshaft with a reduced valve overlap period has been studied. The main difference is that the modified camshaft has a later inlet valve opening timing, resulting in a valve overlap period of 13 °CA instead of 66 °CA. Inlet valve maximum lift and closing timing is maintained. The valve lift profile is presented in Figure 8.1 and Table 8.1 presents the valve opening and closing timings.

Table 8.1: Comparison of valve timings between stock and modified camshaft.

Camshaft	Stock	Modified
Inlet valve opening (°CA aTDC$_{GE}$)	-45	8
Inlet valve closing (°CA aTDC$_{GE}$)	236	234
Exhaust valve opening (°CA aTDC$_{GE}$)	-236	
Exhaust valve closing (°CA aTDC$_{GE}$)	21	
Valve overlap (°CA)	66	13

8.2 Pressure in the HP tank

The reference case was operated at 5 bar inlet pressure. At the end of the expansion process the in-cylinder pressure is around 13 bar when the exhaust valves opens (EVO), as indicated in Figure 8.2. But the back pressure is only 8 bar which is also the pressure in the HP tank. This means that there will be an unrestrained expansion from the higher in-cylinder pressure to the HP tank. The unrestrained expansion is eliminated if the pressure in the HP tank is increased to 13 bar.

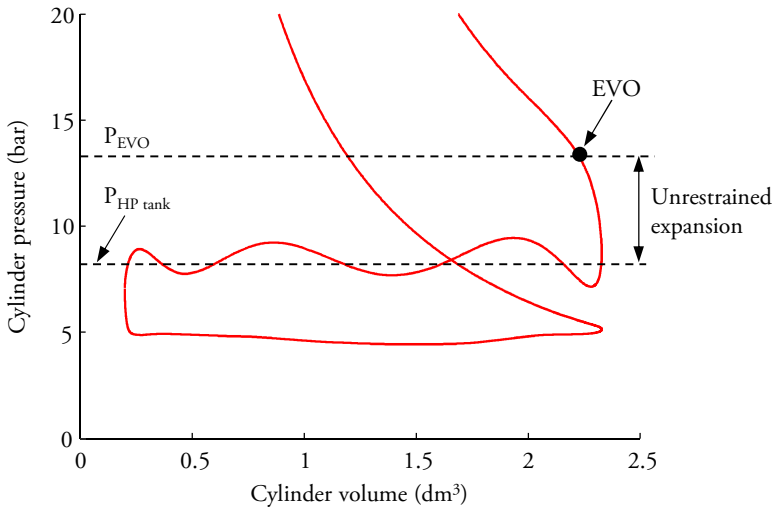

Figure 8.2: PV-diagram illustrating the pressure when the exhaust valve opens in the combustion cylinder (reference case). It also presents the pressure during the exhaust stroke where the combusted gases are pushed into the HP tank.

The pressure level in the HP tank is controlled by the closing timing of the expansion cylinder's inlet valve. This will change the expansion cylinder's induction volume and also the HP tank pressure. The question is at what pressure the HP tank should be operated to obtain the highest efficiency.

The unrestrained expansion process can be modeled in two different ways. One model is to assume it to be completely isentropic such that the following relation between pressure (P) and volume (V) holds:

$$PV^{\gamma} = C \tag{8.1}$$

where γ is the specific heat ratio.

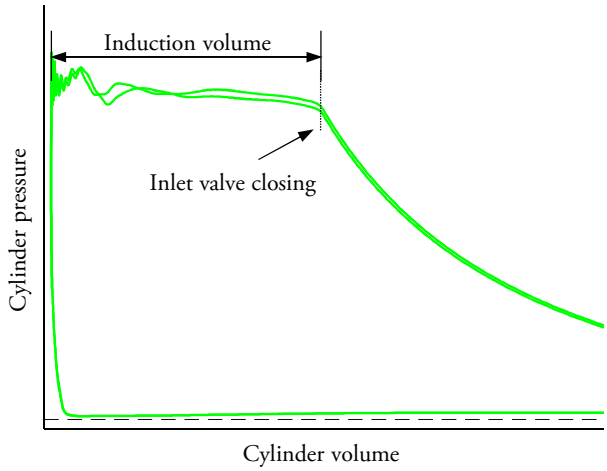

Figure 8.3: Illustration of the expansion cylinder induction volume.

A second options is to model the unrestrained expansion as a free expansion, also known as Joule expansion [50] which implies the following relation between pressure and volume:

$$PV = C \tag{8.2}$$

The resulting difference between these two models during an expansion process is presented in Figure 8.4. For a given volumetric expansion ratio, the Joule expansion maintains a higher pressure. It could also be interpreted that for a given pressure ratio, the Joule model can obtain a higher volumetric expansion ratio.

The method to determine the resulting brake efficiency was based solely on idealized calculations. As a starting point the work distribution for operating point 9 is used, presented in Figure 7.15. The summarized work output from the combustion cylinder $IMEP_g$ (46.4 % of fuel energy), compression cylinder $IMEP_n$ (-16.0 % of fuel energy) and total engine friction $FMEP$ (2.7 % of fuel energy) amounts to 27.7 % of the fuel energy. Then the work from the gas exchange loop in the combustion cylinder and net indicated work from the expansion cylinder is added to calculate the system brake efficiency.

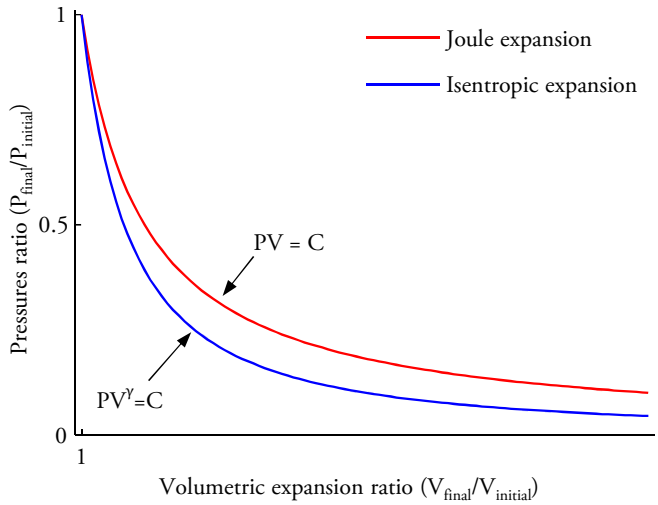

Figure 8.4: A comparison between the pressures during isentropic or Joule expansion. For a given expansion ratio, the pressure remains higher with the Joule expansion model.

8.3 Cold compression cylinder walls

A conventional engine is designed to lose as little heat as possible during the combustion and expansion processes. One of the measures taken is to maintain the engine coolant at an elevated temperature, which also keeps the cylinder wall surfaces at a higher temperature. However, for a compression process it is instead desired that heat is rejected during the compression process. This will reduce the work required to perform the compression. Another advantage is the lower inlet temperature to the DCEE combustion cylinder which improves its thermodynamic efficiency as explained in Chapter 6.

The most desirable case is when the heat rejection is high enough to maintain the starting temperature during the entire compression process, labeled as isothermal compression. However, isothermal compression needs time to reach thermal equilibrium, requiring the process to be slow. But at an engine speed of 1200 rpm the cycle time is only 100 ms, which means the compression process is completed in 25 ms (assuming constant engine speed throughout the cycle). Reducing the engine speed can increase the heat rejected but the power density decreases also. The difficulties of obtaining isothermal compression explains why the Isoengine injected either water or liquid nitrogen during the compression process [30, 31, 32].

Although isothermal compression cannot be achieved without injection of foreign species, a simple measure to increase the heat rejection is to reduce the coolant temperature in the compression cylinder. The approach for this simulation study is to assume that the coolant in the compression cylinder is kept at 25 °C (instead of 82 °C in the reference

case). An expected outcome of this change is that more heat is rejected from the gas during the compression process, therefore decreasing the compression work. A side effect with the reduced coolant temperature is the increased volumetric efficiency due to higher gas density. The compression cylinder displacement was slightly reduced to maintain the same air flow and λ-value as the reference case. The changes are presented in Table 8.2.

Table 8.2: Boundary conditions for the compression cylinder and its displacement.

Case	Reference	Cold comp. cyl.
Cylinder liner and head wall temperature	82 °C	25 °C
Compression cylinder displacement	4.1 dm^3	4.0 dm^3

8.4 Combustion cylinder inlet temperature

As was studied in Chapter 6 a lower inlet temperature to the combustion cylinder will increase its gross indicated efficiency due to mainly lower specific heat capacity and reduced heat transfer loss. However, it is not certain that the improved gross indicated efficiency also improves the overall DCEE system efficiency. Cooling the charged air also reduces its ability to perform expansion work because the specific volume and pressure decreases.

A study where the inlet temperature of the combustion cylinder was evaluated at 40 °C and 100 °C (70 °C in the reference case) was performed, and the three different cases are presented in Table 8.3.

Table 8.3: Temperature levels for the combustion cylinder inlet temperature study.

Case	Reference	Low temp	High temp
T_{inlet}	70 °C	40 °C	100 °C

8.5 Combustion phasing

The reference case was operated with a combustion phasing (defined as CA_{50}) of 10.7 °CA aTDC$_{Fire}$. It is expected that an advanced combustion phasing will improve the combustion cylinder's gross indicated efficiency, but the heat loss and peak cylinder pressure is expected to increase as well. The risk is that the increased heat loss reduces the energy available for expansion and reduces the expansion cylinder work output. To determine the possible impacts and optimal combustion phasing a simulation study was performed where the combustion phasing was swept between 4.7-22.7 °CA aTDC$_{Fire}$.

An effect of sweeping the combustion phasing is that the effective expansion ratio is changed. For the reference case an end of expansion pressure of 1.2 bar in the expansion cylinder was reached. When the combustion phasing is advanced this pressure is reduced slightly, because the effective expansion ratio increased. The opposite happens with a retarded combustion phasing. A second simulation case was evaluated where the expansion cylinder displacement was adjusted so that a pressure of 1.2 bar at end of expansion is maintained. This means that the expansion cylinder displacement was reduced for cases with advanced combustion and increased for cases with retarded combustion. It turned out that the slight differences in pressure at the end of expansion didn't change the system efficiency considerably and were omitted from presentation for clarity reasons.

8.6 Results

The results from the simulation study of the five different areas are presented below.

8.6.1 Camshaft with reduced valve overlap

When the valve overlap is reduced, the back flow through the inlet valve decreases as presented in Figure 8.5. The back flow of gas occurs at gas exchange TDC, where the higher exhaust back pressure pushes the gas from the exhaust manifold into the inlet manifold.

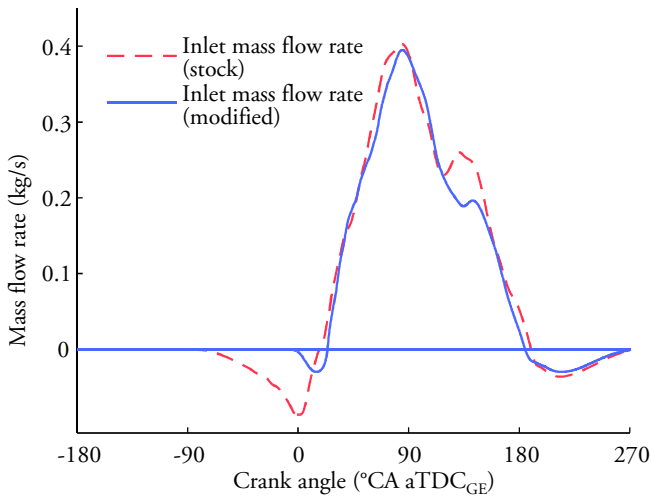

Figure 8.5: Mass flow through the inlet valve. Mass flow below zero indicates flow from the cylinder into the inlet manifold.

As a result of the reduced residual gas quantity trapped inside the cylinder, the in-cylinder temperature is decreased which improves the gas properties while heat loss is reduced. The combustion cylinder gross indicated efficiency improved by 0.2 percentage points. More noticeable is the increase in expansion cylinder work output from 31.7 % to 32.1 % of the fuel energy. A probable explanation is the improved gas properties which maintains a higher pressure throughout the expansion stroke. A conclusion of the results is presented in Table 8.4.

Table 8.4: Comparison of valve timings and brake efficiency for the full DCEE system.

Inlet valve lift profile	Stock	Modified
Valve overlap	66 °CA	13 °CA
GIE (combustion cylinder)	46.4 %	46.6 %
Expans. cyl. work (relative to fuel energy)	31.7 %	32.1 %
Brake efficiency	52.8 %	53.4 %

8.6.2 Pressure in the HP tank

The difference between a Joule or isentropic expansion modeling of the unrestrained expansion is presented in Figure 8.6 and Figure 8.7 respectively. The most noticeable difference is the increased induction volume obtained with a Joule expansion. This means the expansion can proceed over a larger volume before the pressure has reached close to ambient pressure. More expansion work output can be extracted from the cycle because of this.

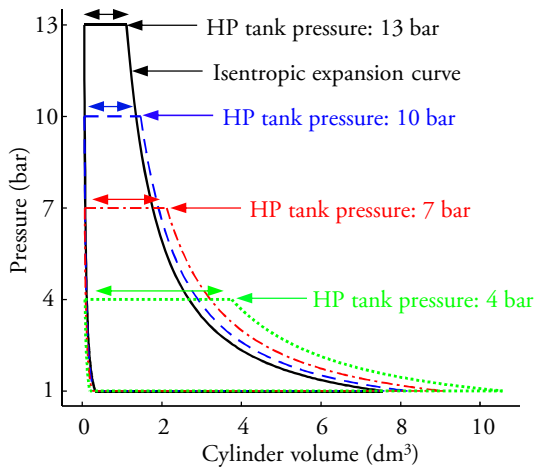

Figure 8.6: Resulting expansion cylinder PV-diagram at different HP tank pressures, assuming Joule expansion. Note that the induction volume increases relative to the isentropic expansion curve with decreasing HP tank pressures. Horizontal arrows indicates the induction volume.

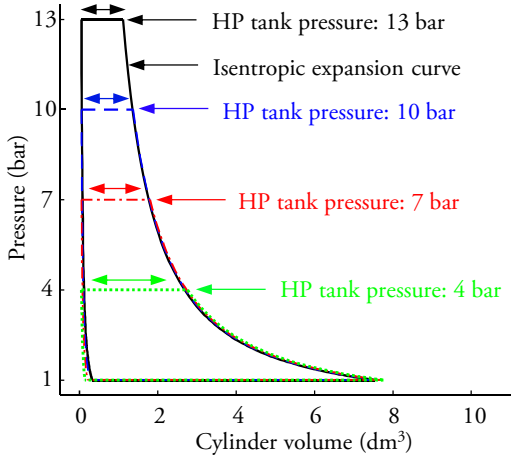

Figure 8.7: Resulting expansion cylinder PV-diagram at different HP tank pressures, assuming isentropic expansion. As expected, the induction volumes matches those from the isentropic expansion curve. Horizontal arrows indicates the induction volume.

Figure 8.8 presents the resulting theoretical system brake efficiency for a sweep of HP tank pressure. For the isentropic case the highest brake efficiency is achieved when the HP tank pressure matches the pressure at exhaust valve opening. However, when the Joule model is assumed, the highest efficiency is obtained with a HP tank pressure around 7 bar because the sum of combustion cylinder gas exchange and expansion cylinder work output is greatest at this pressure level.

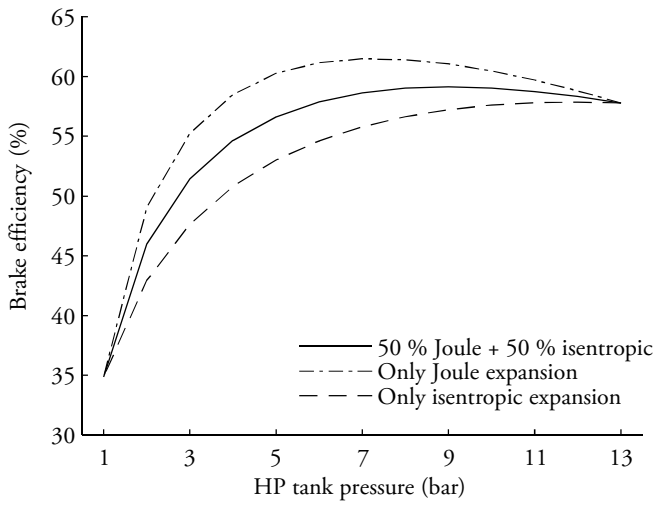

Figure 8.8: Theoretical brake efficiency as function of HP tank pressure with different assumptions of the unrestrained expansion.

The most realistic assumption should be that the unrestrained expansion is neither exclusively Joule nor exclusively isentropic. If a 50-50 mixed mode assumption is made the solid line in Figure 8.8 is formed. It indicates that the highest theoretical brake efficiency occurs around 9 bar HP tank pressure. But the brake efficiency is relatively insensitive to changes in pressure between 7 bar and 13 bar HP tank pressures. Since the experiments were already operated at 8 bar inlet pressure this result indicates there is no large potential for improved system brake efficiency with an increased HP tank pressure. Another potential effect is the increased residual gas fraction due to higher HP tank pressure. As discussed earlier the residual gas has higher temperature causing deteriorated thermodynamic efficiency. Also the heat loss and thermal load on the exhaust valve is expected to increase which also compromises efficiency and reliability of the components.

8.6.3 Cold compression cylinder

The work consumed during the compression process decreases when a compression cylinder with cold walls is used. For the reference case the compression cylinder consumed 16.0 % of the fuel energy, with cooler walls it decreased to 15.7 %. As a result of the reduced compression cylinder energy consumption the system brake efficiency improves by the same amount. The results are concluded in Figure 8.9 and in Table 8.5.

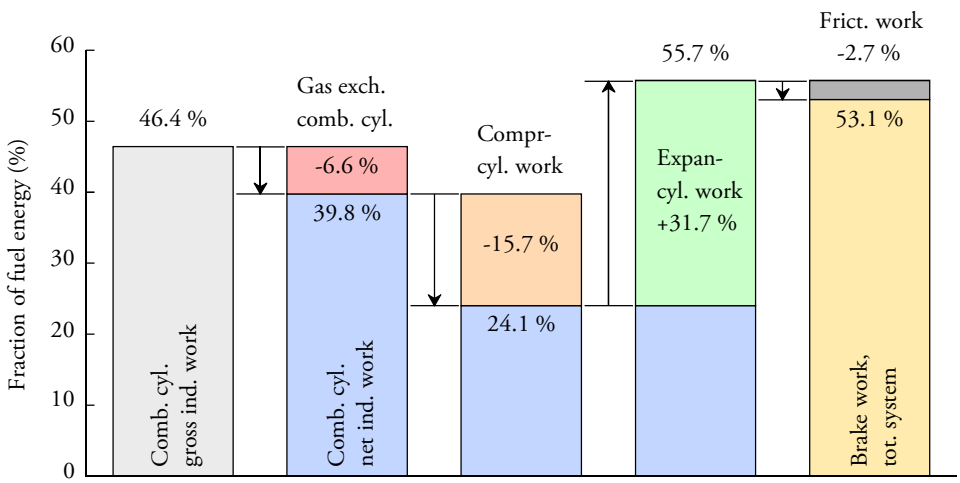

Figure 8.9: Work distribution for the full DCEE system with reduced coolant temperature in the compression cylinder.

Table 8.5: Comparison of the wall temperature effect on the compression cylinder work requirement and system brake efficiency.

Case	Reference	Cold comp. cyl.
Cylinder liner and head wall temperature	82 °C	25 °C
Compr. cyl. work (as fraction of fuel energy)	16.0 %	15.7 %
Brake efficiency	52.8 %	53.1 %

8.6.4 Combustion cylinder inlet temperature

As expected, a lower inlet temperature (40 °C) improves the combustion cylinder gross indicated efficiency due to the reasons discussed in Chapter 6. However, more energy is wasted in the charge air cooler which reduces the work output from the expansion cylinder as well and the resulting system net indicated and brake efficiencies are similar to the reference case. An advantage is that the peak cylinder pressure decreased from 210 bar to 204 bar. Increasing the inlet temperature to 100 °C results in a reduced combustion cylinder gross indicated efficiency. But as less energy is dissipated in the charge air cooler more energy becomes available for the expansion process in the expansion cylinder. As in the low temperature case both these effects are equal and the resulting system net indicated efficiency becomes similar to the reference case. However, due to the slightly higher peak cylinder pressure the mechanical losses increased slightly which made the system brake efficiency 0.1 percentage points lower compared to the reference case. The results are concluded in Table 8.6.

Table 8.6: Comparison of inlet temperature effect on DCEE system efficiency.

Case	Reference	Low T_{inlet}	High T_{inlet}
T_{inlet}	70 °C	40 °C	100 °C
Resulting peak cylinder pressure	210 bar	204 bar	214 bar
System net indicated efficiency	55.4 %	55.4 %	55.4 %
Friction work (% of fuel energy)	2.6 %	2.6 %	2.7 %
Brake efficiency	52.8 %	52.8 %	52.7 %

8.6.5 Combustion phasing

The peak cylinder pressure and combustion cylinder gross indicated efficiency increase when the combustion phasing is advanced, as indicated in Figure 8.10. Advancing the combustion phasing by 3 °CA from the reference case improves *GIE* by 0.6 percentage points. Peak cylinder pressure increases 16 bar relative to the reference case. Advancing another 3 °CA results in a further *GIE* improvement of 0.3 percentage points with a peak cylinder pressure of 240 bar (210 bar for the reference case). Unfortunately, the increase

in *GIE* is not fully transferred into improved system level efficiency. For the 3 °CA combustion advance case the system net indicated efficiency improved by 0.3 percentage points, as indicated in Figure 8.11. It seems like the gain in combustion cylinder gross indicated work output is partly countered by decreased expansion cylinder work output. If the higher friction loss (due to higher peak cylinder pressure) are considered the system brake efficiency improves by less than 0.1 percentage points. For the case with another 3 °CA combustion phasing advance the system net indicated efficiency does not improve. The gain in combustion cylinder *GIE* is completely countered by a decrease in expansion cylinder work output. But increased peak cylinder pressure causes higher friction loss which decreases the system brake efficiency back to the same level as the reference case. No major gain in system brake efficiency can thus be expected with an earlier combustion phasing. It might instead be more troublesome since higher peak cylinder pressure can compromise the structural integrity of the engine.

If the combustion phasing on the other hand is retarded, the opposite trends are observed. The combustion cylinder's *GIE* decreases by 1.6 percentage point when the phasing is delayed by 6 °CA. The impact on the system level becomes much less, the system net indicated efficiency decreased by 1.0 percentage point and the system brake efficiency is only 0.7 percentage points worse than the reference case. But the advantage is the 35 bar lower peak cylinder pressure. This is a significant advantage for the engine's structural integrity. Moreover the NO_x emissions are expected to decrease as well. Further combustion phasing delay reduces peak cylinder even more, but at this stage the impact on system brake efficiency becomes quite large (1.7 percentage points deficit compared to the reference case).

In conclusion, it is observed that the combustion phasing still affects the system level efficiency, but seems to be less influential in comparison to the case of the conventional four-stroke engine.

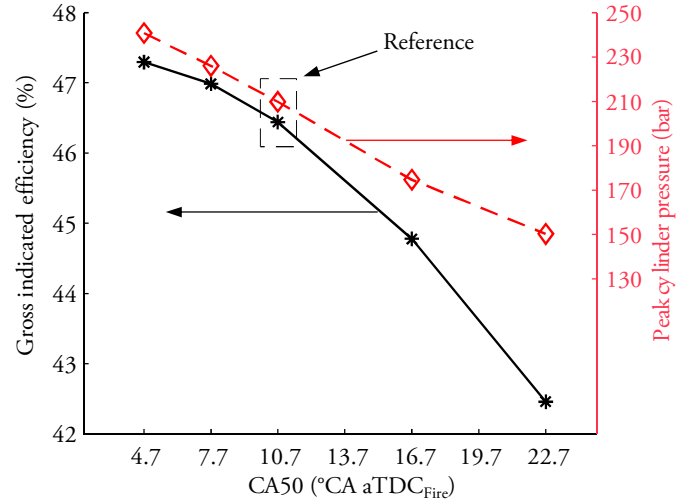

Figure 8.10: Simulated combustion cylinder η_G and peak cylinder pressure as function of CA_{50}.

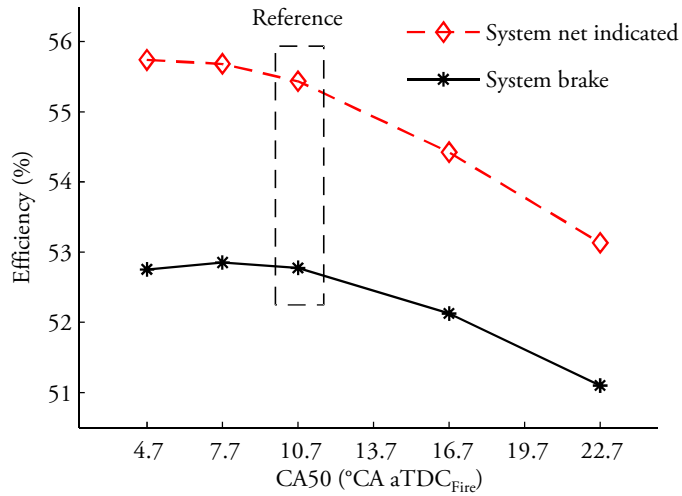

Figure 8.11: Simulated brake efficiency as function of CA_{50} with maintained cylinder geometry. The results for the case with changed expander cylinder geometry are very similar and therefore not plotted for clarity reasons.

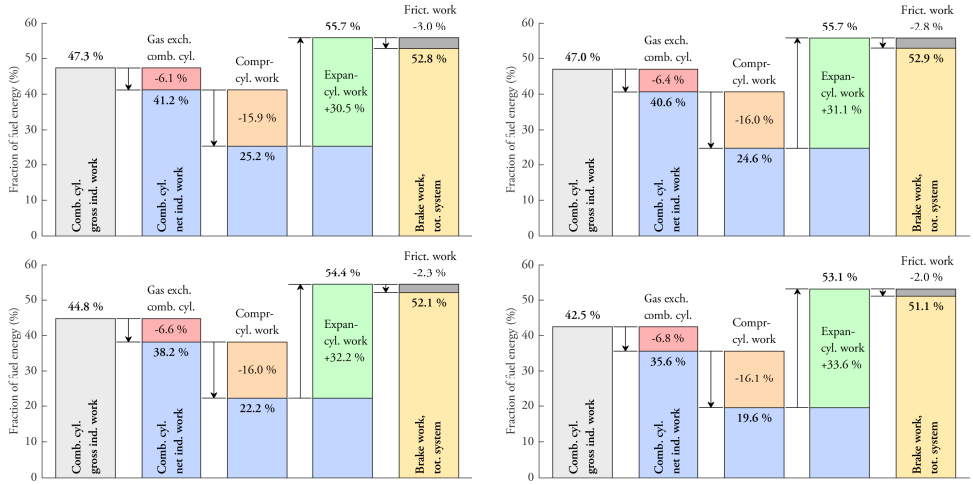

Figure 8.12: Work distribution comparison for combustion phasing sweep. Top left is for the CA_{50} = 4.7 °CA aTDC$_{Fire}$ case, top right is for the CA_{50} = 7.7 °CA aTDC$_{Fire}$ case, bottom left is for the CA_{50} = 16.7 °CA aTDC$_{Fire}$ case and bottom right is for the CA_{50} = 22.7 °CA aTDC$_{Fire}$ case.

The work difference for the combustion phasing sweeps are presented in Figure 8.12. The work distribution for the reference case can be found in Figure 7.15.

8.7 DCEE optimizing for higher efficiency summary

This chapter has presented simulation studies aimed at improving the system brake efficiency of the DCEE 2-4-2 concept and also provide knowledge regarding other potential effects. Operating point 9 from the previous study with insulated exhaust ports was used as the reference case. 5 different subsystems were selected for more thorough investigations.

Only two of the evaluated subsystems showed system brake efficiency improvement potential. By delaying the combustion cylinder's inlet valve opening the valve overlap period is reduced from 66 °CA to 13 °CA. Less exhaust gas is flowing into the inlet manifold and the residual gas fraction is reduced. This results in a lower charge temperature which in turn reduces the heat transfer loss and improves gas properties. The overall impact from these effects is an improved system brake efficiency of 0.6 percentage points. Using a cold compression cylinder is the second area where improved efficiency can be seen. Reducing the combustion cylinder's coolant temperature to 25 °C the heat rejected during the compression stroke increases, which reduces the required compression work with 0.3 % of the fuel energy. This means the system brake efficiency improves with 0.3 percentage points.

The studies of the three other areas didn't suggest any potential for further system brake efficiency improvements. However, the studies indicate that some of these can be used as a degree of freedom to control the process. One example is the inlet temperature, where a temperature change of $\pm$ 30 °C showed no change in system brake efficiency. Since there is no efficiency penalty, the inlet temperature can for example be used to control the combustion process with more advanced combustion concepts. The inlet temperature could also be used to maintain an optional exhaust after-treatment system at its optimal temperature window.

The second parameter that didn't show any system brake efficiency gains is the combustion phasing. Advancing the combustion phasing by 3 °CA improved the gross indicated efficiency by 0.6 percentage points, but due to higher heat loss and less expansion cylinder work output the system brake efficiency only improved by 0.08 percentage points. At the same time the peak cylinder pressure increases with 16 bar and it is also expected that the NO_x emissions increase.

The effects from reducing the unrestrained expansion also did not promise any further system brake efficiency improvements. Theoretical studies reveal that small gains can be expected when the HP tank pressure is increased from 8 bar to 9 bar. But these studies did not consider the increased residual gas fraction, which causes higher temperature and heat loss. With this effect considered it is therefore not expected that the system brake efficiency can improve.

In conclusion these simulation studies resulted in a total achievable system brake efficiency of 53.7 %. Additionally the measured NO_x emissions are 90 ppm, which corresponds to 0.3 g/kWh brake specific emissions. This value is below the current Euro VI legislation requirement of 0.4 g/kWh.

Chapter 9

Summary

This thesis has presented studies of the Double Compression-Expansion Engine concept. The main focus has been on evaluating the system brake efficiency of this concept and finding pathways for further efficiency improvements.

The studies led to evaluations of two different concept alternatives. Simulation studies of the first concept, labeled the 4-4 version, evaluated both a conventional compression-ignition concept and a more advanced low temperature combustion concept. Previous studies of the LTC concept suggest a major decrease in heat loss, which was the main motivator to evaluate the LTC concept with the DCEE concept. The combination of LTC and DCEE showed that a system brake efficiency of 56.0 % could be reached, thanks to high thermodynamic efficiency. However, this was with the assumption that the inlet pressure to the combustion (HP) cylinder is 8 bar and a peak firing pressure of 300 bar. It was later decided that the following studies of the DCEE concept should be evaluated with the conventional compression-ignition concept because it is much easier to control.

Later, a study evaluating different load control strategies was conducted. Due to the assumption of conventional compression-ignition with higher heat transfer loss the brake efficiency decreased to 52.7 % at the best load point. The first load control strategy is labeled as the ”Lambda”-strategy, because only the fuel amount is changed with load. The λ-value will therefore change with load. The second strategy is labeled the ”Miller”-strategy, because late inlet valve closing on the LP cylinder is used to change the air flow as well. The differences between these two load control strategies are observed for the lower load regimes. With the ”Lambda”-strategy a higher thermodynamic efficiency is obtained because of the higher dilution. However, this strategy results in high friction loss because the peak cylinder pressure becomes high due to high inlet pressure.

The issue with high friction loss can be solved by restricting inlet pressure with the Miller load control strategy. Air flow is limited by closing the LP cylinder inlet valve late, well into the compression stroke. In this strategy the target was to maintain a constant λ-value of 1.2. The reduced peak cylinder pressure improved the mechanical efficiency, but the drawback is the low dilution rate and poor thermodynamic efficiency. Overall, the brake efficiency at low load is highest with the Miller load control strategy.

The evaluated strategies form the extreme borders of load control, where the Miller strategy maintains a completely fixed λ-value while the Lambda strategy allows for the greatest fluctuation in λ-value throughout the load range. An interesting study and suggested future work would be to try a combination of these strategies. This means that the λ-value is allowed to fluctuate with load, but the airflow is partly controlled as well. The load control studies also presented the drawbacks of using a charge air cooler at low engine loads. The advantage of low charge temperature is quite limited at low loads while the drawback of wasting energy that could have been used for expansion is greater. Using a charge air cooler at low load results in worse overall system efficiency. However, at mid loads and above charge air cooling results in higher overall efficiency.

A more general investigation into the effects of charge air cooling on the thermodynamic efficiency is also presented. Observations from engine experiments indicated a trend of improved gross indicated efficiency with lower inlet temperatures. At an engine load of 9 bar $IMEP_g$ the efficiency improved by 2.1 % when the inlet temperature was reduced from 80 °C to 35 °C. At 15 bar $IMEP_g$ the efficiency improved by 4.4 % with a inlet temperature change from 70 °C to 35 °C. It is suspected that the observed improvements are due to a combination of better gas properties, reduced heat transfer loss, better combustion efficiency and change in combustion phasing (affects the exhaust loss). But only the combustion efficiency can be quantified, and it can only partly explain the improved gross indicated efficiency. The contributions from gas properties, heat and exhaust loss cannot be quantified based on only the experimental data.

To be able to quantify the effects, a simulation model was created and then calibrated to the experimental data. The great advantage with the simulation tool is its ability to decouple the different effects. The results from this study indicates that improved gas properties is the major contributor to improved gross indicated efficiency with a lower inlet temperature. The lower specific heat capacity increases the pressure rise during the combustion event. Since the expansion occurs at a higher pressure the expansion work output increases. At the two engine loads evaluated the reduced specific heat capacities contribute with 93 % and 51 % for the 9 bar and 15 bar $IMEP_g$ cases respectively. The explanation why the contribution is larger at low loads is that the change in combustion efficiency and heat transfer loss was quite small at this load point, while at the higher load point the contribution from these effects increases. However, the reduced specific heat capacity is still the dominant effect.

Based on the findings of the 4-4 concept a second DCEE version was evaluated. The 4-4 concept suffers from flow loss due to flow area limitations in the LP cylinder head since 4 different gas flows need to be handled. Since the compression and expansion occur in same cylinders over-expansion cannot be achieved unless late or early inlet valve closing strategies are used. The lack of over-expansion and problems with flow loss are addressed with the 2-4-2 concept. The layout with 3 cylinders enables a sequential gas flow, where ambient air enters one cylinder and exhaust gas exits another, which was not the case with the 4-4 concept.

For the 2-4-2 concept studies an experimental test rig is available to provide data for the combustion cylinder. In total 10 operating points were evaluated in the experimental test rig. These were operated at different inlet pressures and fueling rates from 20 bar to 63 bar *FuelMEP*. Most of the cases obtained a gross indicated efficiency around 47 %, but in some cases it was lower due to decreased combustion efficiency (due to low λ), low dilution or non-optimal injection setting.

The measured data became boundary conditions for the simulation model to match. After the simulation model was calibrated full DCEE system evaluations could be performed. The highest system brake efficiency was obtained in operating point 9 where a system brake efficiency of 51.0 % could be achieved. It was also observed that excessive inlet pressure settings at low loads cause reduced system brake efficiency, explained by the additional work required to compress air to a higher pressure which is then dissipated in the charge air cooler. At the same time the advantage of greater dilution is limited at low engine loads.

In an effort to find pathways for further efficiency improvements of the DCEE concept several subsystems were studied more thoroughly. Operating point 9 from the 2-4-2 concept simulations were chosen as the reference case, because it had the highest brake efficiency of 51.0 % when calibrated to the experimental data. Assuming that the combustion cylinder's exhaust ports are insulated increases the exhaust temperature by 30 °C in this operating point. The added heat energy increases the expansion cylinder work output and the system brake efficiency increases to 52.8 %. Another area where improvements can be made is the optimized camshaft with reduced valve overlap resulting in another 0.6 percentage points gained. Using a cold compression cylinder contributes with another 0.3 percentage points, thanks to reduced compression cylinder work.

There were also several subsystems studied which resulted in that no system brake efficiency improvement can be expected. The first is the pressure in the HP tank. Theoretical investigations indicate that the HP tank pressure should be 9 bar to achieve the highest work output and efficiency for this operating point. The reference case was operated at 8 bar and the calculations suggests that 0.11 percentage points could be gained with a HP tank pressure of 9 bar. However, the calculations did not take into account

the drawbacks of increased heat transfer loss and residual gas fraction due to increased back pressure. It is expected that these drawbacks will outweigh the theoretical indicated work output gained with a higher pressure. Another area where no further gain can be expected is the combustion phasing. Advancing the combustion phasing by 3 °CA improves the combustion cylinder's gross indicated efficiency by 0.6 percentage points, but due to reduced expansion cylinder work output the net increase in system brake efficiency is only 0.08 percentage points. The small gain in efficiency came with a penalty of 16 bar higher peak cylinder pressure. It is expected that NO_x emissions increase as well, due to a higher local combustion temperature. Advancing the combustion phasing another 3 °CA saw a decrease in system brake efficiency with the penalty of a peak cylinder pressure approaching 240 bar. Also adjusting the combustion cylinder's inlet temperature revealed small changes in efficiency. In one way it is unfortunate because there is no possibility to improve efficiency. But it can also be used as an extra degree of freedom for controlling the combustion (especially for low temperature combustion concepts) or to ensure that the exhaust after-treatment system works in the optimal temperature window. This can be a very useful feature since there is no penalty in terms of engine efficiency.

In summary, optimizing the subsystems indicates a concept where a system brake efficiency of 53.7 % can be achieved. This is achieved with relatively modest inlet pressure of 5 bar and a peak cylinder pressure of 210 bar. Moreover, NO_x emissions was measured to 90 ppm, which results in brake specific NO_x emissions of only 0.30 g/kWh. This conforms to the Euro VI legislation which must be seen as an important advantage. No measurements of soot were done at this particular operating point, but with a λ-value of 1.36 it is expected that an after-treatment solution with a conventional diesel particulate filter is enough to conform to the Euro VI legislation.

Chapter 10

Future work

This thesis has shown results and investigations of the Double Compression-Expansion Engine concept. Both experimental and simulation studies have been conducted, but the experimental test rig covers only one part of the DCEE concept. It is suggested that an experimental test rig for the non-combustion cylinders is built for further studies. Together with the current test rig will this rig provide a full DCEE experimental rig to validate the results presented in this thesis. It will also provide more accurate information about *FMEP* values of the non-combusting cylinders.

The presented simulation studies indicates a trend for improved system brake efficiency with higher load. It is therefore an interesting study to operate the engine at even higher loads. But this will most likely require a higher inlet pressure which also causes higher peak cylinder pressures. A test rig with higher pressure capability is a requirement to achieve higher engine loads.

More experiments at the current load levels is also a suggested future work. The experiments were performed with an EGR_{rate} between 30 % and 40 %. It is expected that a lower EGR_{rate} can improve the efficiency, because air has better thermodynamic properties compared to EGR gas. But this will also cause higher NO_x emissions.

Another suggestion for future work is to look deeper into the combustion process. The experiments were conducted with only a single injection. There might be other injection strategies that are more optimal for this low compression ratio. Another interesting study is to look at novel combustion chamber designs, such as the ”Wave-piston” introduced by AB Volvo. Also, studying more advanced combustion concepts which has a potential for decreased heat transfer loss is of great interest. Since the DCEE 2-4-2 concept is over-expanded, preserved heat energy is of even greater value because more work output can be extracted.

Finally, looking further ahead for a possible production version and the aspects to make it work in a vehicle regarding noise and vibrations. The experience from the experiments with the HP tank is that the exhaust noise is lower compared to other engines. It is suspected that this is due to the high back pressure, where the pressured gradient when the exhaust valve opens is lower, reducing the noise. Other important aspects are power density and cost effectiveness of serial production of such a different engine concept.

Bibliography

[1] Intergovernmental Panel for Climate Change. *IPCC GLobal Warming of 1.5°C*. 2017.

[2] *CO2 Emissions from Fuel Combustion 2018*. OECD, oct 2018.

[3] Donald W Stanton. Systematic Development of Highly Efficient and Clean Engines to Meet Future Commercial Vehicle Greenhouse Gas Regulations. *SAE International Journal of Engines*, 6:1395–1480, 2013.

[4] Daniel Mohr, Timothy Shipp, and Xueting Lu. The Thermodynamic Design, Analysis and Test of Cummins' SuperTruck 2 50% Brake Thermal Efficiency Engine System. *SAE Technical Paper 2019-01-0247*, apr 2019.

[5] US Department of Energy. Energy Department Announces $137 Million Investment in Commercial and Passenger Vehicle Efficiency.

[6] Timothy Johnson and Ameya Joshi. Review of Vehicle Engine Efficiency and Emissions. *SAE Int. J. Engines 11(6):1307-1330*, 2018.

[7] Wayne Eckerle. Innovative Approaches to Improving Engine Efficiency. Directions in Engine-Efficiency and Emissions Research (DEER) conference, 2007.

[8] Jerald A Caton. A Comparison of Lean Operation and Exhaust Gas Recirculation: Thermodynamic Reasons for the Increases of Efficiency. *SAE Technical Paper 2013-01-0266*, 2013.

[9] Jerald A Caton. On the importance of specific heats as regards efficiency increases for highly dilute IC engines. *Energy Conversion and Management*, 79:146–160, 2014.

[10] Hung Nguyen-Schäfer. *Rotordynamics of Automotive Turbochargers, 2nd edition*. Springer International Publishing, 2015.

[11] Erik Svensson, Lianhao Yin, Per Tunestal, Marcus Thern, and Martin Tuner. Evaluation of Different Turbocharger Configurations for a Heavy-Duty Partially Premixed Combustion Engine. *SAE Int. J. Engines 10(5):2575-2595*, 2017.

[12] Magnus Christensen, Bengt Johansson, and Patrik Einewall. Homogeneous Charge Compression Ignition (HCCI) Using Isooctane, Ethanol and Natural Gas - A Comparison with Spark Ignition Operation. *SAE Technical Paper 972874*, 1997.

[13] Jari Hyvönen, Carl Wilhelmsson, and Bengt Johansson. The Effect of Displacement on Air-Diluted Multi-Cylinder HCCI Engine Performance. *SAE Technical Paper 2006-01-0205*, 2006.

[14] Vittorio Manente, Bengt Johansson, Per Tunestal, and William Cannella. Effects of Different Type of Gasoline Fuels on Heavy Duty Partially Premixed Combustion. *SAE International Journal of Engines*, 2:71–88, 2009.

[15] Vittorio Manente, Claes-Goeran Zander, Bengt Johansson, Per Tunestal, and William Cannella. An Advanced Internal Combustion Engine Concept for Low Emissions and High Efficiency from Idle to Max Load Using Gasoline Partially Premixed Combustion. *SAE Technical Paper 2010-01-2198*, 2010.

[16] Derek Splitter, Martin Wissink, Dan DelVescovo, and Rolf D Reitz. RCCI Engine Operation Towards 60% Thermal Efficiency. *SAE Technical Paper 2013-01-0279*, 2013.

[17] Helgi Fridriksson, Bengt Sunden, Shahrokh Hajireza, and Martin Tuner. CFD Investigation of Heat Transfer in a Diesel Engine with Diesel and PPC Combustion Modes. *SAE Technical Paper 2011-01-1838*, 2011.

[18] Martin Tuner, Bengt Johansson, Philip Keller, and Michael Becker. Loss Analysis of a HD-PPC Engine with Two-Stage Turbocharging Operating in the European Stationary Cycle. *SAE Technical Paper 2013-01-2700*, 2013.

[19] Maria Thirouard and Pierre Pacaud. Increasing Power Density in HSDI Engines as an Approach for Engine Downsizing. *SAE Int. J. Engines 3(2):56-71*, 2010.

[20] Mufaddel Dahodwala, Satyum Joshi, Hari Krishnamoorthy, Erik W Koehler, and Michael Franke. Evaluation of System Configurations for Downsizing a Heavy-Duty Diesel Engine for Non-Road Applications. *SAE Int. J. Engines 9(4):2272-2285*, 2016.

[21] Mori Ishii, Kiyohiro Shimokawa, Koichi Machida, and Hiroshi Nakajima. A Study on Improving Fuel Consumption of Heavy-Duty Diesel Engine Specifically Designed for Long-Haul Trucks on Highway. *SAE Technical Paper 2015-01-1256*, 2015.

[22] James Atkinson. Atkinson Gas Engine patent US367496A, 1887.

[23] Ralph Miller. Supercharged engine, patent US2817322A, 1957.

[24] Joshua Finneran, Colin P Garner, Michael Bassett, and Jonathan Hall. A review of split-cycle engines. *International Journal of Engine Research*, 2018.

[25] Lyle Cummins. *Diesel's Engine: From conception to 1918*. Carnot USA Books, 1993.

[26] Ford Phillips, Ian Gilbert, Jean-Pierre Pirault, and Marc Megel. Scuderi Split Cycle Research Engine: Overview, Architecture and Operation. *SAE Int. J. Engines 4(1):450-466*, 2011.

[27] Riccardo Meldolesi, George Bailey, Clive Lacy, Ian Gilbert, Jean-Pierre Pirault, and Anthony Perkins. Scuderi Split Cycle Fast Acting Valvetrain: Architecture and Development. *SAE Int. J. Engines 4(1):467-481*, 2011.

[28] Riccardo Meldolesi and Nicholas Badain. Scuderi Split Cycle Engine: Air Hybrid Vehicle Powertrain Simulation Study. *SAE Technical Paper 2012-01-1013*, 2012.

[29] David Branyon and Dean Simpson. Miller Cycle Application to the Scuderi Split Cycle Engine (by Downsizing the Compressor Cylinder). *SAE Technical Paper 2012-01-0419*, 2012.

[30] Mike W. Coney, Claus Linnemann, and H S Abdallah. A thermodynamic analysis of a novel high efficiency reciprocating internal combustion engine—the isoengine. *Energy*, 29(12):2585–2600, 2004.

[31] Guangyu Dong, Robert Morgan, and Morgan Heikal. A novel split cycle internal combustion engine with integral waste heat recovery. *Applied Energy*, 157:744–753, 2015.

[32] Guangyu Dong, Robert E Morgan, and Morgan R Heikal. Thermodynamic analysis and system design of a novel split cycle engine concept. *Energy*, 102:576–585, 2016.

[33] Robert E Morgan, Neville Jackson, Andrew Atkins, Guangyu Dong, Morgan Heikal, and Christopher Lenartowicz. The Recuperated Split Cycle - Experimental Combustion Data from a Single Cylinder Test Rig. *SAE International Journal of Engines*, 10:2596–2605, 2017.

[34] John M. Clarke. A New Compression Ignition Engine Concept for High Power Density. *Journal of Engineering for Gas Turbines and Power-transactions of The Asme - J ENG GAS TURB POWER-T ASME*, 121:211–217, 1999.

[35] John M. Clarke and Edward O'Malley. Analytical Comparison of a Turbocharged Conventional Diesel and a Naturally Aspirated Compact Compression Ignition Engine both Sized for a Highway Truck. *SAE Technical Paper 2013-01-1736*, 2013.

[36] Green Car Congress. Motiv Engines introduces 2nd-generation split-cycle concept; MkII Clarke-Brayton heavy-duty engine being designed for LNG, 2014.

[37] Russell P. Durrett and Venkatesh Gopalakrishnan. Internal combustion engine utilizing dual compression and dual expansion processes, patent US8371256B2, 2009.

[38] John B Heywood. *Internal combustion engine fundamentals*. McGraw-Hill Education, 1988.

[39] Gamma Technologies. GT-ISE v2016.

[40] Simon K Chen and Patrick F Flynn. Development of a Single Cylinder Compression Ignition Research Engine. *SAE Technical Paper 650733*, 1965.

[41] Frank Thomas Metzner, Norbert Becker, Wolfgang Demmelbauer-Ebner, Robert Müller, and Matthias W Bach. Der neue 6-l-W 12-Motor im Audi A8. *MTZ*, 65:254–266, 2004.

[42] Derek Crabb, Michael Fleiss, Jan-Erik Larsson, and Joop Somhorst. New Modular Engine Platform From Volvo. *MTZ*, 74(9):4–11, 2013.

[43] Andy Noble and Chris Such. Ways to reduce CO2 emissions from on-hiwghway, heavy duty diesel engines. In *Transport Research Arena*, Paris, 2014.

[44] Marc Megel, Barry Westmoreland, Guy Jones, Ford Phillips, Douglas Eberle, Mark Tussing, and NIgel Yeomans. Development of a Structurally Optimized Heavy Duty Diesel Cylinder Head Design Capable of 250 Bar Peak Cylinder Pressure Operation. *SAE International Journal of Engines*, 4:2736–2755, 2011.

[45] Vittorio Manente, Per Tunestal, Bengt Johansson, and William J Cannella. Effects of Ethanol and Different Type of Gasoline Fuels on Partially Premixed Combustion from Low to High Load. *SAE Technical Paper 2010-01-0871*, 2010.

[46] Shuli Wang, Kyle van der Waart, Bart Somers, and Philip de Goey. Experimental Study on the Potential of Higher Octane Number Fuels for Low Load Partially Premixed Combustion. *SAE Technical Paper 2017-01-0750*, 2017.

[47] Changle Li, Lianhao Yin, Sam Shamun, Martin Tuner, Bengt Johansson, Rickard Solsjo, and Xue-Song Bai. Transition from HCCI to PPC: the Sensitivity of Combustion Phasing to the Intake Temperature and the Injection Timing with and without EGR. *SAE Technical Paper 2016-01-0767*, 2016.

[48] Eric W Lemmon, Marcia L Huber, and Mark O McLinden. NIST Standard ReferenceDatabase 23: Reference Fluid Thermodynamic and Transport Properties - REFPROP. 9.0, 2010.

[49] Sanford Gordon Bonnie J. McBride Martin A. Reno. Coefficients for Calculating Thermodynamic and Transport Poroperties of Individual Species, 1993.

[50] Jacques-Olivier Goussard and Bernard Roulet. Free expansion for real gases. *American Journal of Physics*, 61:845–848, 1993.

Summary of papers

Paper I: Double Compression Expansion Engine Concepts: A Path to High Efficiency

N. Lam, M. Tunér, P. Tunestål, A. Andersson, S. Lundgren, B. Johansson
SAE Int. J. Engines 8(4):1562-1578, 2015, 2015-01-1260

This paper presents simulation studies over the proposed DCEE 4-4 cycle. Two different simulation cases was studied. The first uses a conventional compression-ignition process with a conventional heat transfer modeling. The second case studied the DCEE-concept in conjunction with a low temperature combustion mode. The aim of these studies is to obtain brake efficiency estimations for the DCEE 4-4 concept.

I created the simulation model, performed the simulations and wrote the paper. Bengt Johansson was my supervisor and provided technical suggestions and feedback and also proofreading. Arne Andersson, Staffan Lundgren, Martin Tunér and Per Tunestål supported by giving technical feedback and proofreading the paper. This paper was presented by me at SAE World Congress in Detroit, April 2015.

Paper II: Double Compression Expansion Engine Concepts: Efficiency Analysis over a Load Range

N. Lam, A. Andersson, P. Tunestål
SAE Technical Paper 2018-01-0886, 2018

This paper is a continuation of the studies performed in paper I. The main focus of this paper is to study how 2 different load control strategies can impact on the DCEE brake efficiency.

I created the simulation model, performed the simulations and wrote the paper. Per Tunestål helped with technical suggestions, gave feedback and proofread the paper. Arne Andersson

helped with proofreading. This paper was presented by me at SAE World Congress in Detroit, April 2018.

Paper III: Analyzing Factors Affecting Gross Indicated Efficiency When Inlet Temperature Is Changed

N. Lam, A. Andersson, P. Tunestål
SAE Technical Paper 2018-01-1780, 2018

This paper covers the more fundamental studies over the effects causing changed gross indicated efficiencies with inlet temperature. A combination of engine experiments and simulations were used to be able to quantify the different effects. This study was useful for the DCEE studies because it provided knowledge about the advantages with charge air cooling in the DCEE cycle.

I performed the engine experiments, post processed the data, calibrated the simulation model, performed the analysis and wrote the paper. Per Tunestål and Arne Andersson gave technical feedback and proofread the paper. This paper was presented by me at the SAE International Powertrain, Fuel and Lubricants meeting in Heidelberg, September 2018.

Paper IV: Simulation of system brake efficiency in a Double Compressions-Expansion Engine-concept (DCEE) based on experimental combustion data

N. Lam, A. Andersson, P. Tunestål
SAE Technical Paper 2019-01-0073, 2019

This paper covers the DCEE 2-4-2 concept studies. Engine experiments were performed to obtain data for the DCEE combustion cylinder while the simulations enabled system brake efficiency estimations. 10 different operating points from low fueling rate to high fueling rates were studied at several combustion cylinder inlet pressure conditions.

I performed the engine experiments, post processed the data, calibrated the simulation model, performed the analysis and wrote the paper. Per Tunestål and Arne Andersson gave technical feedback and proofread the paper. This paper was presented by me at the SAE International Powertrain, Fuel and Lubricants meeting in San Antonio, January 2019.

Paper v: Double Compression-Expansion Engine Concepts: Study of pathways for efficiency improvements

N. Lam, A. Andersson, P. Tunestål
Submitted to Applied Energy

This paper is a continuation of the studies performed in paper IV. 5 different subsystems in the proposed 2-4-2 DCEE concept were studied and investigated to evaluate if there is any potential for efficiency improvements.

I performed the engine experiments, post processed the data, created the simulation model, performed the simulations, analyzed the results and wrote the paper. Per Tunestål and Arne Andersson gave technical feedback and proofread the paper.

Appendix

Calculations of wall surface area to volume ratio

For a flat piston the total wall surface area is defined as:

$$A_{wall,tot} = A_{wall,piston} + A_{wall,cyl.head} + A_{wall,liner} = \frac{\pi B^2}{2} + \pi Bh \tag{1}$$

where B is the cylinder bore and h is the TDC height as defined in Figure 1. The volume at TDC is calculated as:

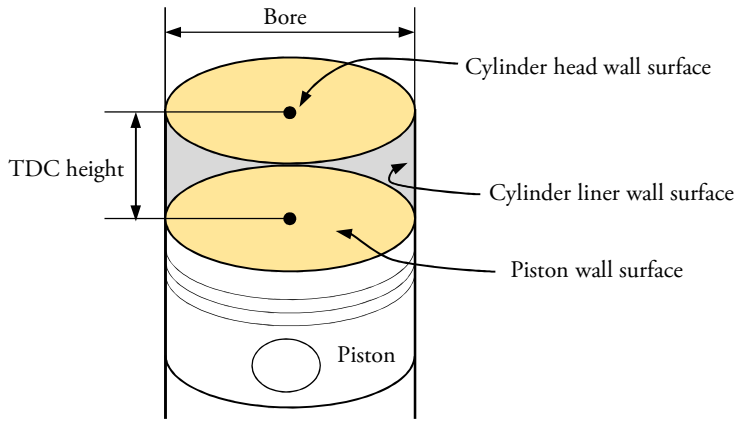

Figure 1: Definition of wall surface areas used in equation 1.

$$V_c = \frac{V_d}{CR-1} = \frac{\frac{\pi B^2 L}{4}}{CR-1} \tag{2}$$

where L is the stroke and CR is the compression ratio. The wall surface to volume-ratio then becomes:

$$\frac{A_{wall,tot}}{V_c} = \frac{\frac{\pi B^2}{2} + \pi Bh}{\frac{\frac{\pi B^2 L}{4}}{CR-1}} = \frac{2(CR-1)(B+2h)}{BL} = 2\frac{B(CR-1)+2L}{BL} \tag{3}$$

For the cylinder geometry used in the experimental test rig (bore = 131 mm and stroke = 158 mm) Figure 2 presents the total wall surface area to volume ratio. At compression ratio = 17:1 the ratio becomes 0.23 mm^2/mm^3 while it is 0.16 mm^2/mm^3 with CR = 11.5:1.

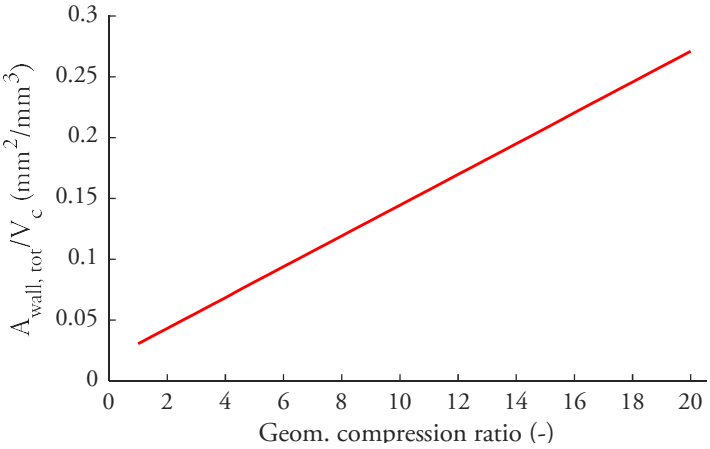

Figure 2: Calculated total wall surface area to volume ratio according to equation 3. Bore = 131 mm and stroke = 158 mm.

Notes

Notes

Notes

Notes

Notes

Notes

Notes